Gold-Mediated C–H Functionalisation

A thesis submitted for the degree of Doctor of Philosophy

Tanya Boorman

Queen Mary
University of London

Contents

Declaration……4

Acknowledgements……...5

List of Abbreviations…… 6

Abstract……8

Chapter One: Gold-Mediated C–H Functionalisation

1.1 Introduction……9

1.2 Aryl C–H Functionalisation…… 12

1.2.1 With Gold(III)…… 12

1.2.2 With Gold(I)……... 33

1.3 Alkyne C–H Functionalisation with Gold(I) and Gold(III)…… 38

1.4 Alkane C–H Functionalisation with Gold(I) and Gold(III)…… 49

1.5 Conclusions……57

Chapter Two: Gold(I) C–H Activation of Arenes

2.1 Introduction……58

2.2 Optimisation of the Reaction Conditions……61

2.3 Scope of the Reaction……..67

2.4 Mechanistic Proposal……... 72

2.5 Development of a Silver-Free C–H Activation Protocol……84

2.6 Conclusions……88

2.7 Experimental……... 90

2.7.1 General Comments…… 90

2.7.2 Experimental Procedures……90

2.7.3 Characterisation Data…….. 91

2.7.4 Kinetic Isotope Effect Experiment……. 105

2.7.5 Other Mechanistic Experiments……. 106

2.7.6 Crystallographic Data……107

Chapter Three: Gold-Mediated Double C–H Activation Cross-Coupling

3.1 Introduction……119

3.2 Optimisation of the Reaction……...122

3.3 Scope of the Reaction……..124
3.4 Mechanistic Proposal…….. 129
3.5 Gold-Mediated Decarboxylative Cross-Coupling…….. 135
3.6 Conclusions…….146
3.7 Experimental……... 148
3.7.1 General Comments……. 148
3.7.2 Experimental Procedures…… 148
3.7.3 Characterisation Data……. 150
3.7.4 Kinetic Isotope Effect Experients……...171
3.7.5 Other Mechanistic Experiments……. 174

References…….175

Declaration

I declare that the work presented in this thesis is my own and that no part of it has been submitted in support of an application for another degree or qualification of this or any other university or other institution of learning.

Those parts of this thesis having previously been published in the primary literature at the time of writing:

1. *Gold(I)-Mediated C–H Activation of Arenes*, P. Lu, T. C. Boorman, A. M. Z. Slawin and I. Larrosa, *J. Am. Chem. Soc.*, 2010, **132**, 5580–5581.

2. *Gold-Mediated C–H Functionalisation*, T. C. Boorman and I. Larrosa, *Chem. Soc. Rev.*, 2011, **40**, 1910-1925.

3. *Redox-Controlled Selectivity of C–H Activation in Oxidative Cross-Coupling of Arenes*, X. C. Cambeiro, T. C. Boorman, P. Lu and I. Larrosa *Angew. Chem. Int. Ed.*, 2013, **52**, 1781-1784.

Signature..... Date.....

Acknowledgements

First and foremost, I would like to thank Dr Igor Larrosa for his guidance, support and patience over the course of this project. He has been a continual source of motivation and inspiration, for which I am incredibly grateful.

I'd also like to thank members of the Larrosa group, both past and present. I couldn't have asked for better colleagues, advisors and friends to work alongside. Particular thanks must go to Dr Xacobe Cambeiro and Dr Pengfei Lu for their collaboration on these projects.

The members of my advisory panel, Professor Mike Watkinson and Dr Stephen Goldup, have been a great source of motivation and information. I'd like to thank them for their time, informative conversations and useful suggestions.

I'm grateful to members of the technical staff at Queen Mary for their advice and support. All crystallographic data was gratefully received from Dr Alexandra M. Z. Slawin, University of St. Andrews. High resolution mass spectrometry was performed by staff at the NMSSC, University of Swansea. I'd also like to acknowledge the EPSRC for funding this project.

Over the past few years, I have had the great fortune to be surrounded by a number of exceptionally kind and talented people. I couldn't begin to name every person, nor adequately express my gratitude, but I hope that they each understand how much their support and friendship is appreciated.

List of abbreviations

Ar	Aryl
DCE	1,2-Dichloroethane
DMA	N,N-Dimethylacetamide
DMF	N,N-Dimethylformamide
DMSO	Dimethylsulfoxide
DNBS	Di-N-butyl sulfate
dppf	1,1'-Bis(diphenylphosphino)ferrocene
EDG	Electron-donating group
Equiv	Equivalent
ESI	Electro-spray ionisation
EWG	Electron-withdrawing group
HRMS	High resolution mass spectrometry
IMes	1,3-Dimesityl-2,3-dihydro-1H-imidazole
IPr	1,3-Bis(2,6-diisopropylphenyl)-2,3-dihydro-1H-imidazole
IR	Infrared radiation
KIE	Kinetic isotope effect
L	Ligand
M	Molarity
MS	Molecular sieves
MW	Microwave
m/z	Mass-to-charge ratio
NBS	N-Bromosuccinimide
NIS	N-Iodosuccinimide
NMR	Nuclear magnetic resonance
$NaBAr_4$	Sodium tetrakis(3,5-bis(trifluoromethyl)phenyl)borate.
OTf	Trifluoromethansulfonate
PivOH	Pivalic acid
R	Generic substituent
RT	Room temperature
t	Time
T	Temperature

THF	Tetrahydrofuran
Ts	Tosyl
X	Charged ligand

Abstract

The transition metal–catalysed direct functionalisation of C–H bonds is an increasingly viable alternative to the multi–step strategies traditionally employed. The use of powerful and environmentally benign gold species in such transformations has highlighted their remarkable reactivity and led to a significant increase in their utilisation. This thesis provides an overview of our efforts to contribute to the rapidly expanding area of gold–catalysed C–H functionalisation. The introductory chapter will review existing methodologies, looking at transformations which rely on the ability of gold to perform C–H activation, as well as those exploiting its potent π-acidity.

The development of a gold(I) C–H activation of electron-deficient arenes will be described. Proceeding under very mild reaction conditions, the corresponding aryl gold(I) species are generated in excellent yields. The auration is highly regioselective, invariably activating the position with two *ortho*- electron-withdrawing groups. Our efforts to perform this auration in the absence of a silver source will then be discussed.

The unwavering fidelity of gold(I) to activation of electron-deficient arenes is counter to the established preference of gold(III) towards the activation of electron-rich arenes. We sought to exploit these contrasting modes of reactivity in the development of an oxidative gold(I)/gold(III) cross-coupling process. The scope and mechanism of this process will be discussed. An alternative method of generating aryl gold(I) species, relying on the capability of gold(I) to perform the decarboxylative activation of a number of benzoic acids, allowed us access to a wider substrate scope for the oxidative cross-coupling, than the C–H activation alone. This expansion of the scope will also be discussed in this final chapter.

Chapter One: Gold-mediated C–H Functionalisation

1.1 Introduction

Fundamentally, of course, organic molecules comprise the building blocks of living organisms but, on a more comprehensible scale, they are found in pharmaceuticals, agrochemicals, fuels, polymers, molecular switches and a vast number of other widely varied areas. Consequently, methods to synthesise these often complex molecules are in high–demand under both industrial and academic settings. Organic frameworks may be viewed as hydrocarbon skeletons intermittently supplemented with heteroatoms, most commonly oxygen, nitrogen, phosphorus, sulphur or a member of the halogens. Their construction usually entails multi–stage processes, involving the piecing together of fragments and addition of new functionalities at sites possessing suitably high chemical reactivity, which in practice means the presence of a multiple bond, halogen, heteroatom or metal to perform a functional group transformation or coupling. This requirement frequently means that synthetic strategies begin with starting materials bearing little resemblance to the target molecule.

Owing to high thermodynamic stability, and accordingly low chemical reactivity, carbon–hydrogen bonds are not considered as functional groups. That is to say that they are not deemed appropriately reactive to perform a functionalisation/functional group transformation directly. Instead the C–H bond is substituted for a more reactive functionality in a process which necessarily adds superfluous steps to the overall synthetic process. Were it possible to regard the C–H bond as a reactive centre, these additional steps could be eliminated and a far more streamlined synthetic strategy adopted, utilising starting materials with obvious structural similarity to the product. The abundance of C–H bonds in organic frameworks would therefore be an asset, synthetically, providing a multitude of sites for functionalisation.

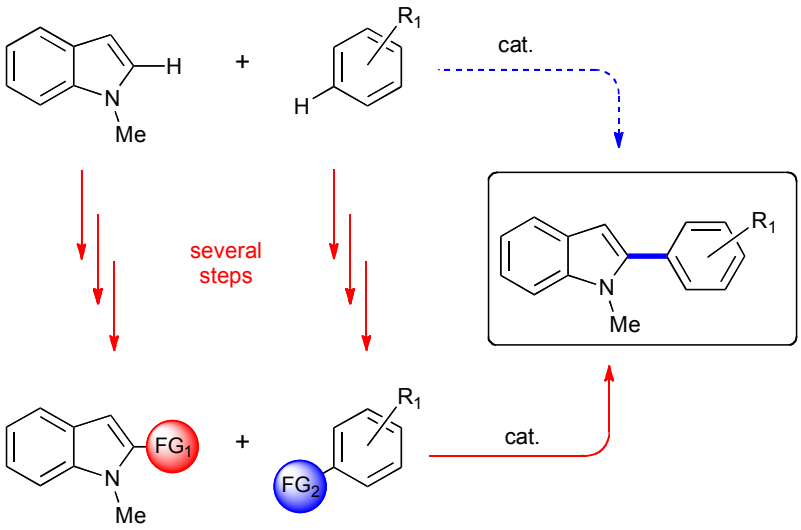

Scheme 1. Routes to diversification of the indole core. The red arrows represent the typically adopted approach and the blue arrows represent an alternative C–H functionalisation route.

This concept underlies the fields of C–H activation and C–H functionalisation and is illustrated in Scheme 1, where the red arrows represent the typically adopted approach to functionalisation, entailing installation of reactive functional groups and then addition of the fragments. The blue arrow represents what is clearly a much more straightforward approach, where the C–H bonds are directly functionalised. This route is substantially more time and cost effective and also more environmentally friendly, consuming less material and generating less waste, which is an important consideration in light of the ever growing trend towards "green chemistry".[1] These reactions are generally catalysed by transition metals and in such instances C–H activation may be defined as the reaction between a C–H bond and transition metal centre, as would typically be observed for the reactive C–X bond, resulting in the formation of a new C–M bond.[2] This process necessarily involves cleavage of the thermodynamically stable C–H bond and the development of methodologies capable of overcoming this energy barrier, while retaining selectivity, is an important and widespread ambition. C–H activation is commonly followed by functionalisation, the overall transformation therefore being a C–H functionalisation, involving a distinct C–H activation step.[3]

Although historically considered inert, the π-acidity of gold salts is well known and recent years have seen a substantial increase in the exploitation of this reactivity to effect a range of transformations.[4] The ability of gold(III) to perform C–H activation was also established several decades ago, however utilisation of this auration to achieve further functionalisation is a more recent realisation. This mode of reactivity has allowed gold to participate in a range of bond–forming reactions, including cross–coupling reactions, a notable addition considering the reluctance of gold to cycle between oxidation states.

The following pages will explore the role of gold catalysis in C–H functionalisation. The use of gold(I) and (III) in the C–H activation of arenes will be reviewed and the implications and potential for subsequent functionalisation examined. The gold–mediated activation of alkynes will then be analysed with a discussion of the reported methodologies. Finally the activation of C_{sp3}–H bonds will be addressed. This text is not intended to be a comprehensive review of the literature but rather an overview of progression in the field, aiming to provide the reader with an appreciation of advances and the potential in this fast–developing area.

1.2 Aryl C–H Functionalisation

1.2.1 With Gold(III)

The first C–H activation of arenes with Au(III) was reported by Kharasch and Isbell in 1931.[5] Their procedure allowed the auration of aromatics, such as benzene and toluene, at room temperature to produce a number of arylgold(III) compounds (Scheme 2). Following the initial C–H activation, the reaction proceeds to form diphenyl auric chloride, which subsequently decomposes to give benzene, chlorobenzene and gold(I) chloride. However, this process may be halted at the first C–H activation by addition of ether, alcohol or another oxygen–containing solvent, suggested to be a result of a stabilising interaction between oxygen and gold. The authors noted the ease with which this auration occurs and also the low stability of the resulting organogold compounds. A subsequent publication, by Kharasch and Beck,[6] detailed the extension of this procedure to the auration of aromatic nitriles. Further studies indicated that the reaction proceeds through an electrophilic aromatic substitution process. Although there were concerns raised over the reproducibility of the procedure, its use subsequently allowed the isolation and characterisation of a number of arylgold(III) compounds by Liddle and Parkin,[7] who employed various stabilising ligands to achieve the isolation, and De Graaf *et al.*,[8] who did not use ligands but did require, the environmentally harmful, carbon tetrachloride as a solvent.

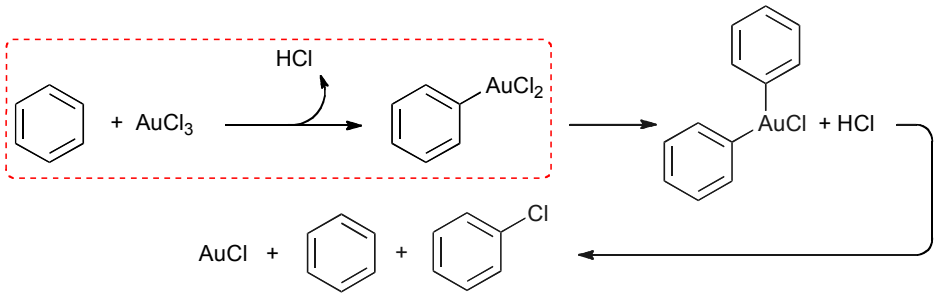

Scheme 2. $AuCl_3$–mediated auration of benzene.

Curiously, the potential of this novel reactivity mode of Au(III) for effecting further organic transformations was not explored until 70 years after Kharasch and Isbell's first report. These transformations have now become the subject of widespread scrutiny and the past few years have seen a number of methodologies which presumably exploit this C–H activation process. However, the fact that gold is also a potent π–acid has led to a degree of uncertainty surrounding the manner in which some of these transformations proceed. In some cases a Friedel–Crafts-type mechanism, not involving formation of a C–Au bond, is an equally plausible route to formation of the observed products and, in the absence of any evidence to support a C–H activation mechanism, such as isolated intermediates, it may be difficult to prove otherwise.

The first example of gold(III)–catalysed C_{sp2}–H functionalisation was reported by Hashmi *et al.*, in 2000.[9] The authors reported the transition metal–catalysed cycloisomerisation of terminal allenyl ketones to the corresponding furans. They observed subsequent polymerisation in the presence of a gold(III) catalyst, which was attributed to a Au(III) auration at the C–2 position of the furan. This process was then expanded to the $AuCl_3$–catalysed coupling of 2-methylfuran and methyl vinyl ketone[10] (Scheme 3). This coupling is proposed to proceed through arylgold(III) intermediate **I** (Scheme 4), formed by an electrophilic auration of 2–methylfuran, as observed in NMR spectroscopy studies. However, the authors do not exclude the possibility that gold acts as a Lewis acid in a Friedel–Crafts-type reaction (Scheme 4), considering that the reaction also proceeds under acidic conditions.

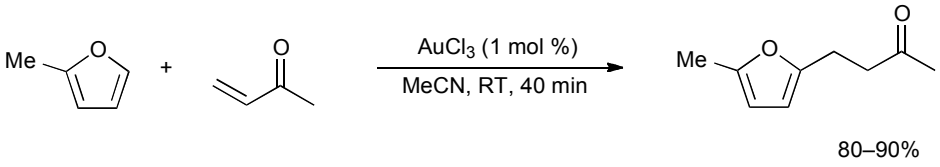

Scheme 3. $AuCl_3$ catalysed coupling of 2-methylfuran and methyl vinyl ketone.

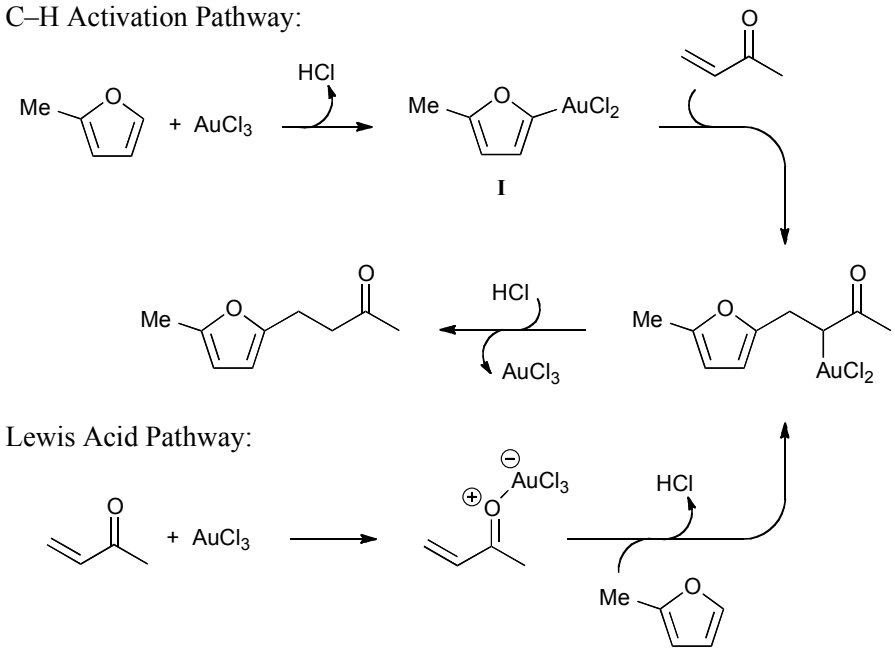

Scheme 4. Possible mechanistic pathways for gold(III)–catalysed C–C bond formation between 2-methylfuran and methyl vinyl ketone.

Urriolabeitia, Contel *et al.* have since investigated the design and synthesis of various iminophosphorane Au(III) complexes (Figure 1), as alternatives to the very hygroscopic and acidic $AuCl_3$ catalyst used in this reaction.[11,12] The authors have reported the successful addition of 2-methylfuran, and other electron–rich arenes, some of which were not suited to the acidic conditions of Hashmi's procedure, to methyl vinyl ketone. The products are generated in yields that match or surpass those previously reported, with these air– and moisture–stable organogold(III) catalysts.

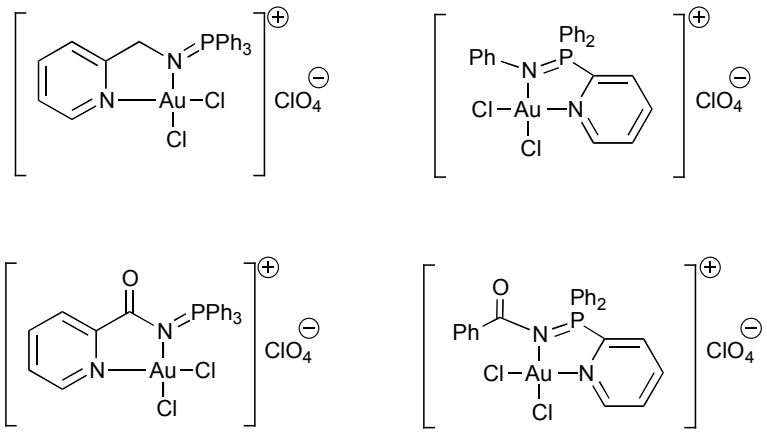

Figure 1. Au(III)-iminophosphorane complexes used for the addition of furans to methyl vinyl ketone.

Arcadi *et al.* developed a procedure for the addition of α,β–enones to indoles (Scheme 5).[13] It was proposed that the reaction proceeds *via* electrophilic C–H activation of the indole, at the C-3 position, to form an indolyl gold intermediate. Addition of this gold species to the α,β–enone generates a σ-alkyl gold complex, which undergoes a protodeauration step to liberate the addition product and release the catalyst. The proposed initial C–H activation step is supported by observation of the indolyl gold species, by mass spectrometry, in a solution containing the indole with a stoichiometric quantity of $NaAuCl_4{\cdot}2H_2O$.

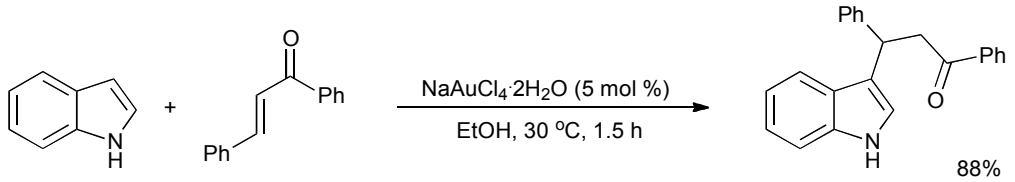

Scheme 5. Gold(III)–catalysed addition of indoles to α,β–enones.

This process was later extended to the alkylation of 7–azaindoles, again using α,β-enones in a Michael-type addition process.[14] However, possessing a much less activated C–3 position than indoles, these substrates required higher temperatures and longer reaction times.

Liu *et al.* reported the gold-mediated conjugate addition of α,β-enones to 4-hydroxycoumarins, with subsequent annulation furnishing the corresponding functionalised pyranocoumarins (scheme 6).[15] The $AuCl_3$ catalyst is proposed to act as a Lewis acid, activating the carbonyl of the enone towards 1,4-conjugate addition and then the resulting intermediate towards intramolecular annulation. The authors note that while alternative Lewis acids are also able to promote the tandem reaction, the $AuCl_3$ AgOTf pair display far superior reactivity and selectivity.

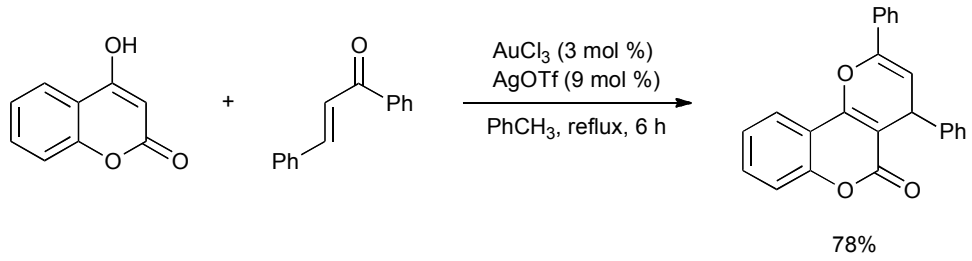

Scheme 6. Gold(III)–catalysed addition/ annulation of 4-hydroxycoumarins to α,β–enones.

Echavarren *et al.* reported the gold–catalysed annulation of 6–8 membered rings on indoles, *via* alkyne cyclisation (Scheme 7).[16] The selective formation of 7– or 8–membered ring compounds, from the same substrate, is achieved through regiochemical control exhibited by the oxidation state of the gold centre. Whereas Au(I) catalyst **1** promotes a 7-*exo*-dig process, use of $AuCl_3$ leads to 8–membered rings through an 8-*endo*-dig cyclisation. Furthermore, the authors observed an unexpected fragmentation of the 8–membered ring compounds, to produce C-2 allenylated indoles. Previous computational studies conducted by the authors indicate that the reaction may proceed through one of two energetically similar reaction pathways:[17] a Friedel–Crafts alkenylation or one involving a metal cyclopropyl carbene intermediate.

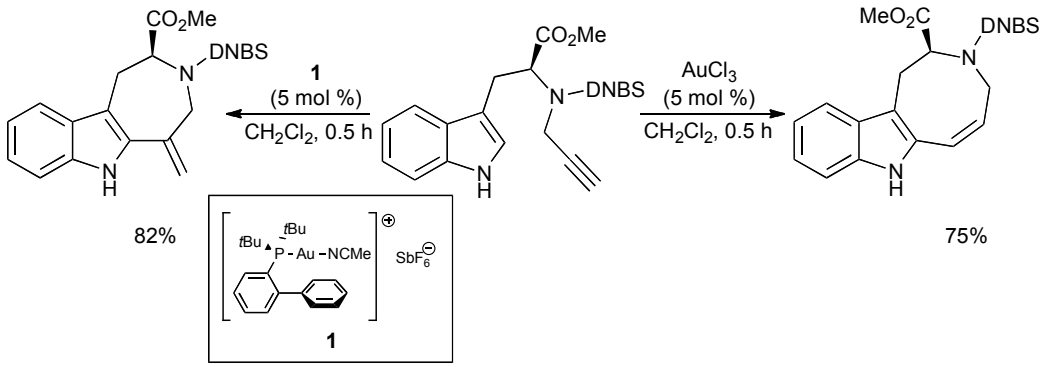

Scheme 7. Indole annulation showing the different reactivity observed for Au(I) and Au(III) catalysts.

The addition of arenes and indoles to electron–deficient alkyne substrates has also been reported (Schemes 8 and 9).[18] In this case, 5 mol % $AuCl_3$ affords only low product yields, but the addition of 15 mol % AgOTf as a co–catalyst delivers a highly reactive system, achieving good to excellent yields, under mild and solvent–free conditions. The authors note that mixing stoichiometric quantities of pentamethylbenzene and the Au(III) catalyst led to the disappearance of the aryl proton, as observed by ^{1}H NMR spectroscopy, which they attribute to a C–H activation reaction. Consequently, they propose that the hydroarylation proceeds *via* an arylgold(III) intermediate, formed in the first step of the reaction, and suggest that the silver salt may be required to generate a more electrophilic gold(III) species, *via* halide abstraction. However, they do not exclude the possibility that the gold(III) merely acts as a Lewis acid, activating the alkyne/alkene, as suggested by Reetz and Sommer for a similar process in which both Au(I) and Au(III) were found catalytically active for the hydroarylation of terminally substituted alkynes.[19] Interestingly, the authors observe that acetylenes lacking the conjugated carbonyl group undergo a Markovnikov type addition, with high (*Z*) selectivity (Scheme 8).

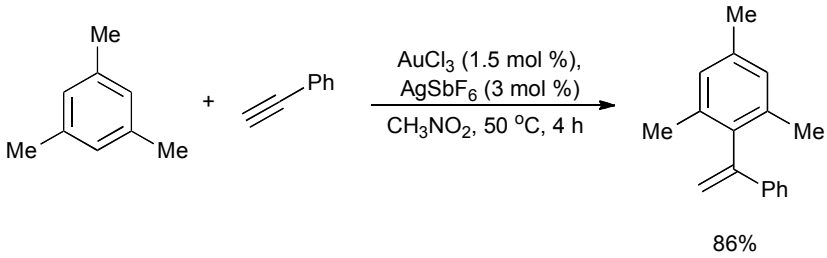

Scheme 8. $AuCl_3$/AgOTf catalysed coupling of pentamethylbenzene and ethyl propiolate. The reaction was also performed in solvent–free conditions to give the same yield in 1 hour.

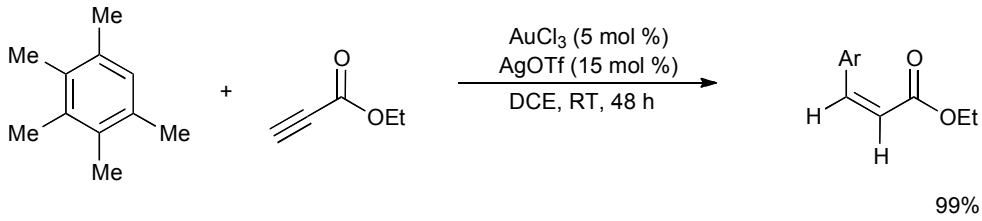

Scheme 9. $AuCl_3/AgSbF_6$ mediated hydroarylation of phenylacetylene.

The intermolecular hydroarylation of unactivated alkenes, with arenes and heteroarenes, was also reported (Scheme 10).[20] The $AuCl_3/AgSbF_6$ catalytic couple afforded products in good to excellent yields, with remarkable regioslectivity, under mild reaction conditions. The process was applicable to both aryl and aliphatic alkenes and did not appear particularly sensitive to steric hindrance, the hydroarylation of styrene with mesitylene proceeding to generate the corresponding product in 79% yield. The authors propose that the reaction proceeds through Au(III) coordination of the alkene, rather than direct auration of the arene, however they note that the latter pathway cannot be excluded.

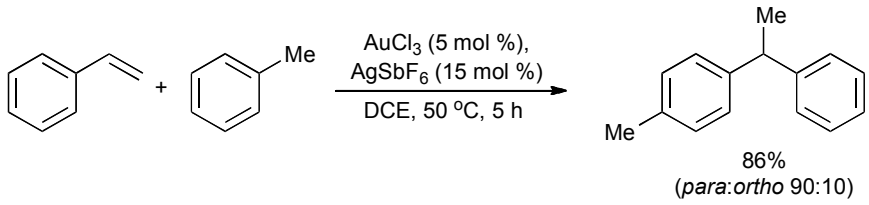

Scheme 10. Gold(III)–mediated hydroarylation of styrene with toluene.

He *et al.* also developed a novel route to 3-chromanols,[21] in a process proposed to exploit C–H activation in the intramolecular alkylation of arenes with epoxides (Scheme 11). This $AuCl_3$/AgOTf catalysed process gave good yields after only 4 hours at 50 ˚C with electron–rich arene substrates, however less electron–rich arenes required longer reaction times and higher temperatures. Notably, bromine substituents were well tolerated under the reaction conditions, leaving a useful handle for further transformations. Neither $AuCl_3$ nor AgOTf were able to effectively catalyse the reaction alone, with $AuCl_3$ giving a maximum of 20% product in the absence of silver. The proposed reaction mechanism proceeds through C–H activation of the arene, followed by addition to the tethered epoxide, although a second possible mechanism in which the gold catalyst acts purely as a Lewis acid to activate the epoxide is also mentioned. The authors note that the failure of other Lewis acidic catalysts, such as $BF_3{\cdot}Et_2O$, to successfully promote the reaction indicates that a Lewis acidic–mediated pathway is unlikely and points to one proceeding *via* C–H activation.

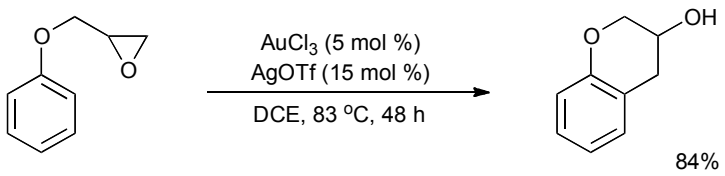

Scheme 11. $AuCl_3$/AgOTf catalysed synthesis of 3–chromanol.

This procedure later provided inspiration for Chen and Yang *et al.*, who applied the $AuCl_3$/AgOTf catalytic couple to the construction of catechin frameworks (Scheme 12).[22] Application of the gold(III)/silver couple to the aryl epoxide substrates resulted in only low yields of the desired product, however addition of thiourea ligand **2** led to greatly improved product formation. The authors attribute this influence to stabilization imparted by this bulky bidentate ligand to the Au(III) centre, noting that it offered superior performance compared to similar monodentate thioureas, phosphines and lutidine. As with He's procedure, a number of electron–withdrawing groups,

including halogens were well tolerated on the arene which is ultimately C–2 on the catechin product. However greater electron density was required on the arene which is presumed to undergo C–H activation.

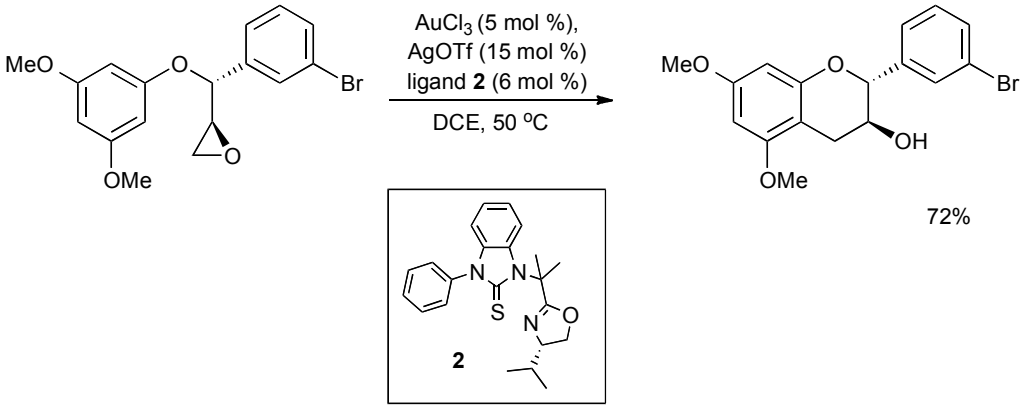

Scheme 12. Au(III)–mediated annulation of aryl epoxides to form catechin-based scaffold.

Pericàs *et al.* later developed a procedure for the cyclization of benzyl glycidyl ethers (Scheme 13), noting that the efficiency of the Lewis acidic catalysts $FeBr_3$ and $BF_3{\cdot}Et_2O$ appeared to be at odds with the findings of He *et al.*, in their cyclization of the structurally related aryl glycidyl ethers.[23] Accordingly, the authors performed a reinvestigation into this catalytic route to 3–chromanols. Their findings directly contradicted those of He *et al.*, observing that $FeBr_3$, $FeBr_3$/AgOTf and $BF_3{\cdot}Et_2O$ were able to promote the reaction, in fact generating higher yields under milder reaction conditions than $AuCl_3$/AgOTf. Thus, the authors conclude that the cyclization reactions of aryl and benzyl glycidyl ethers are clearly Lewis acid mediated processes and as such $AuCl_3$/AgOTf presents an unnecessarily expensive and less effective alternative to $FeBr_3$/ AgOTf.

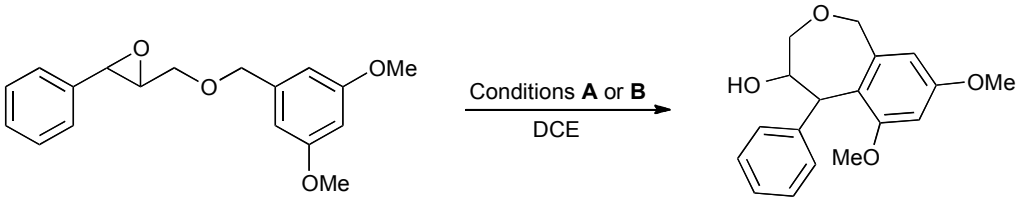

Scheme 13. Lewis acid–promoted cyclisation of benzyl glycidyl ethers. Conditons **A**: $FeBr_3$ (10 mol %), AgOTf (30 mol %), RT, 30 min (88%); Conditions **B**: $AuCl_3$ (2.5 mol %), AgOTf (7.5 mol %), 50 ^oC, 4 h (70%).

Wu *et al.* drew inspiration from He's work when developing their procedure for the ring–opening of aziridines (Scheme 14).[24] The authors reported that the $AuCl_3$/AgOTf catalytic couple outperformed other catalysts in the hydroarylation. Silver triflate was able to catalyse the reaction alone, albeit with a lower yield of 65%, as well as in the presence of other metal salts, such as $BiCl_3$, $YbCl_3$, $ZnCl_2$ and $BF_3 \cdot OEt$. These observations led the authors to consider that the silver cation may actually be the catalytic centre. However, given the superior performance of the gold/silver couple, they suggest that the silver may also act to generate a more electrophilic gold catalyst, as proposed by He *et al.*

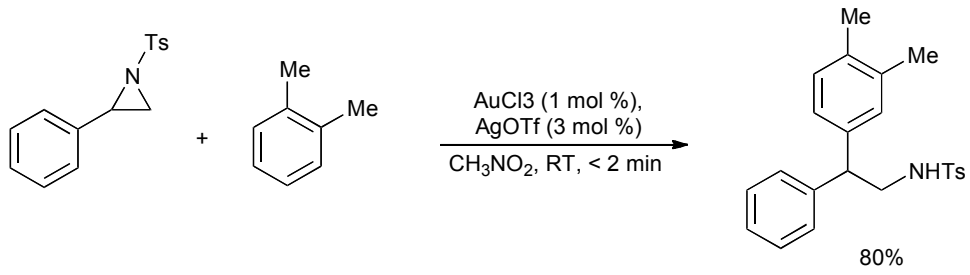

Scheme 14. $AuCl_3$/AgOTf catalysed ring opening of aziridines with electron–rich arenes.

Li and Skouta reported the gold(I) catalysed annulation of simple hydroxyaldehydes with alkynes to give products resembling the isoflavanone framework (Scheme 15).[25] This procedure does not entail C–H activation of

an arene, but the authors propose that the reaction proceeds *via* C_{sp2}–H activation of the aldehyde, through an oxidative addition step to generate an acyl gold(III) hydride **II** (Scheme 16). This gold(III) species then complexes with the phenylacetylene, in a hydrometalation step. Subsequent reductive elimination of **III** generates the new C–C bond and an α,β-unsaturated ketone **IV**, which then participates, with the hydroxy group, in a conjugate addition to give the new C–O bond and also regenerate the gold(I) catalyst. The authors base this proposal on their exclusion of alternative reaction pathways, such as initial reaction of the phenolic hydroxy group with the phenyl acetylene derivative or initial reaction of the terminal alkyne carbon with the aldehyde.

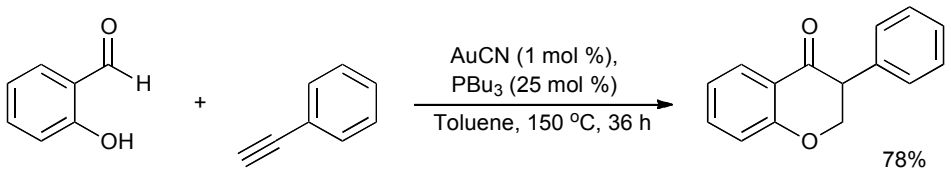

Scheme 15. Gold(I) catalysed annulation of salicylaldehyde with phenylacetylene.

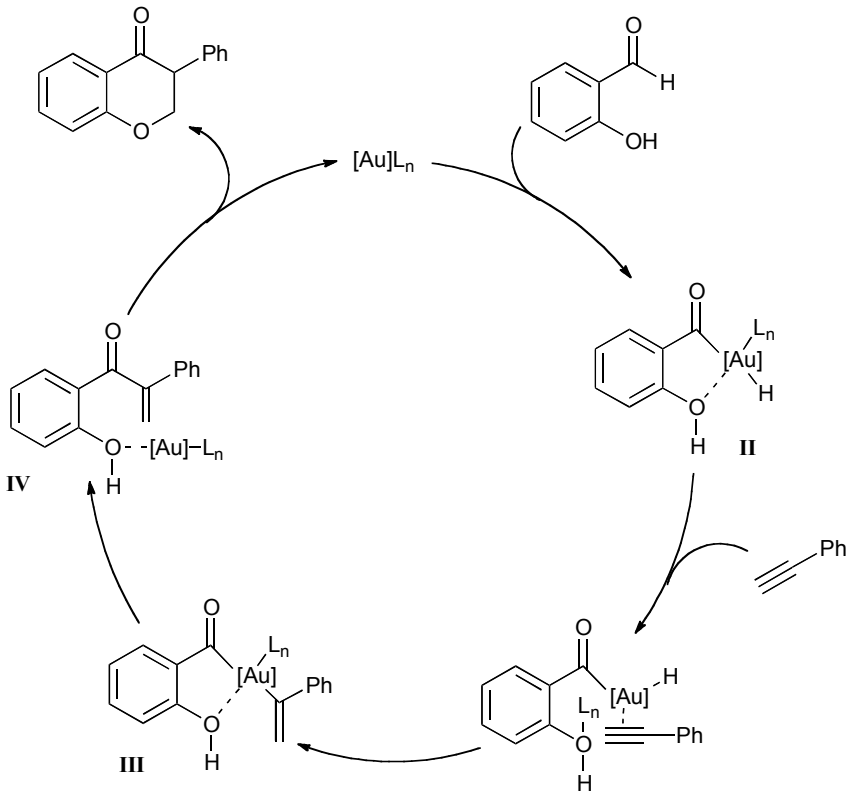

Scheme 16. Proposed reaction mechanism for salicylaldehyde cyclisation.

The direct functionalisation of arenes with primary alkyl triflates has also been reported.[26] In this reaction (Scheme 17), the authors note that there appear to be two competing reaction pathways: one leading to the desired linear product (**3**), which would proceed through an arylgold(III) intermediate; and another which follows a Friedel–Crafts-type pathway and leads to a branched product (**4**). The C–H auration pathway appears dominant for electron–rich arenes, whereas the Friedel–Crafts pathway takes over for the less electron–rich substrates, affording the branched product exclusively when using benzene. In support of the suggested mechanism, the authors show that stoichiometric dichlorophenylgold(III) reacts with n-butyl triflate to produce the linear product exclusively, albeit at a slow rate.

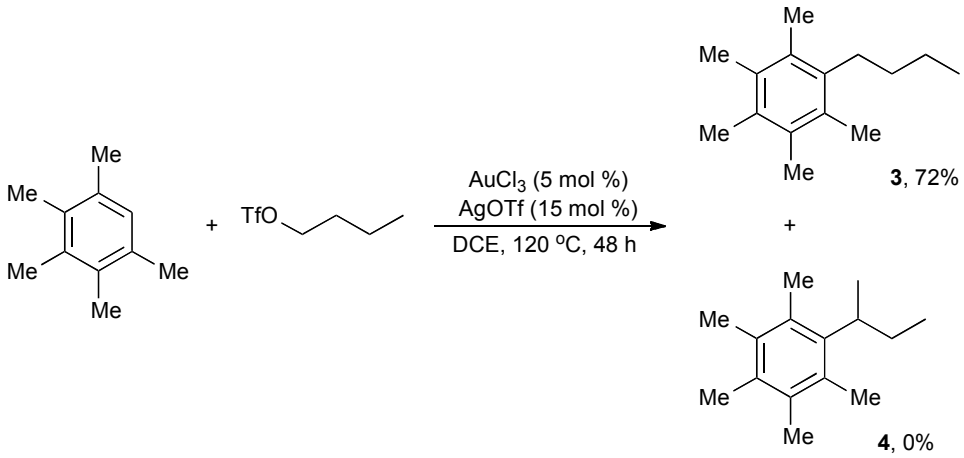

Scheme 17. $AuCl_3$/AgOTf catalysed coupling of pentamethylbenzene with pentyl trifluoromethanesulfonate.

The gold(III)–mediated addition of electron–rich arenes to imines, was reported by Li *et al.* (Scheme 18), generating the products in good yields.[27] $ZnCl_2$, $AlCl_3$ and $RuCl_3{\cdot}3H_2O$ catalysts were inactive, whereas the $AuCl_3$/AgOTf couple efficiently mediated the transformation, which the authors propose proceeds through a Friedel–Crafts type process.

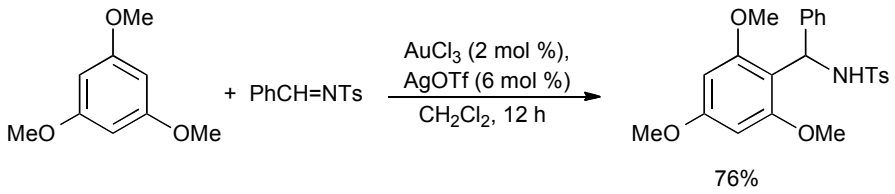

Scheme 18. Au(III)–catalysed addition of arenes to imines.

The benzylation of electron–rich arenes and heteroarenes with benzyl alcohols and carboxylates was achieved, in a gold(III)–mediated Friedel–Crafts-type process (Scheme 19), which generated products in good to excellent yields.[28] Although $AuCl_3$, $HAuBr_4$ and even PPh_3AuCl/AgOTf were able to promote the reaction, superior yields were obtained with $HAuCl_4$ for a number of arenes and heteroarenes under very mild reaction conditions. Good regioselectivities in favour of *para*-substitution are generally obtained with unsymmetrical arenes. Allylic alcohols can also be employed to achieve similar transformations.[29] Interestingly, when the benzyl acetates contain an α-stereocentre a high degree of stereoselectivity, favouring the *anti*–diastereomer, is observed. This was demonstrated by Bach *et al.* in their $AuCl_3$–mediated procedure, which generated the products in high yield under mild conditions (Scheme 20).[30]

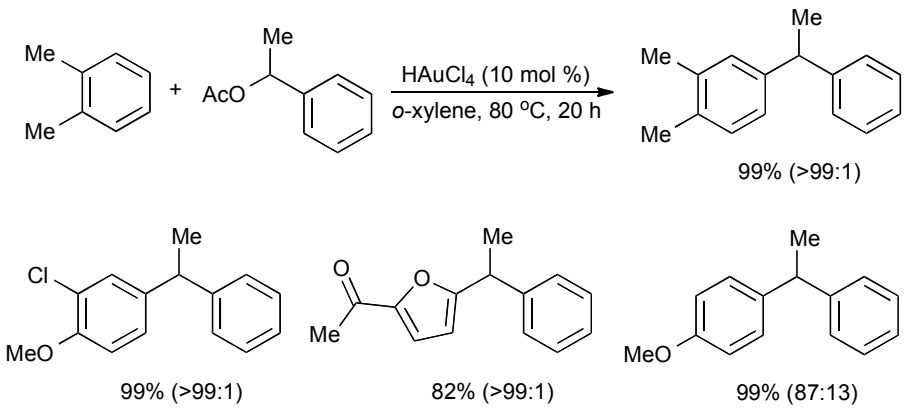

Scheme 19. Gold(III)–catalysed benzylation of *o*-xylene.

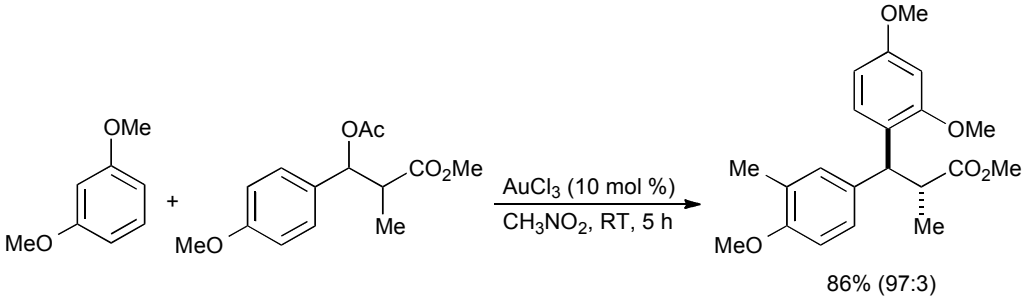

Scheme 20. Gold(III)–catalysed diastereoselective alkylation.

Li *et al.* employed Au(III) catalyst **5** (scheme 21) in the generation of allenes from propargylic alcohols and arenes *via* an S_N1-type process.[31] The authors propose gold(III) coordination to both the triple bond and hydroxy group of the alcohol, leading to generation of an ion pair intermediate. The steric bias of this intermediate then promotes nucleophilic attack at the C3 position, generating the desired allene products. Products resulting from nucleophilic attack at the propargylic position are also observed and thought to be a result of aryl coordination to the gold centre, this also allows the authors to rationalise their increased yield of this product with more coordinating nucleophiles, such as anisole.

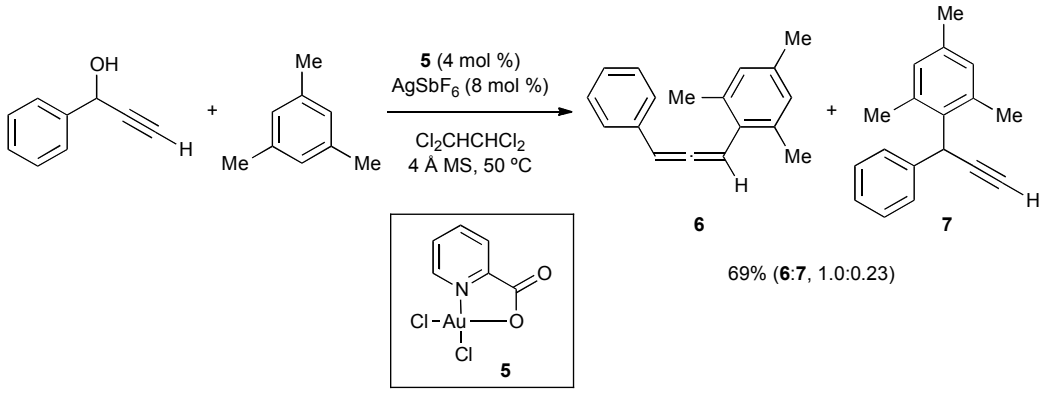

Scheme 21. Gold(III)–catalysed reaction of arenes with propargylic alcohols to generate allenes.

The synthetic utility of allenes was demonstrated by Liu *et al.* in their three-component tandem reaction between allene esters, Selectfluor and water to generate fluorinated indenes (scheme 22).[32] This gold-mediated process entails formation of C–C, C=O and C–F bonds in one synthetic step. The authors propose a Au(I)/Au(III) catalytic cycle (scheme 23) which entails activation of the allene by Au(I), nucleophilic addition of water and then oxidation of Au(I) by Selectfluor. The resulting Au(III) centre then performs a C_{sp2}–H activation, as supported by a primary kintetic isotope effect value of 2.3. Subsequent reductive elimination regenerates the Au(I) catalyst and leads to an intermediate, which the authors then propose undergoes a hydride-shift, oxidation and fluorination to furnish the final product.

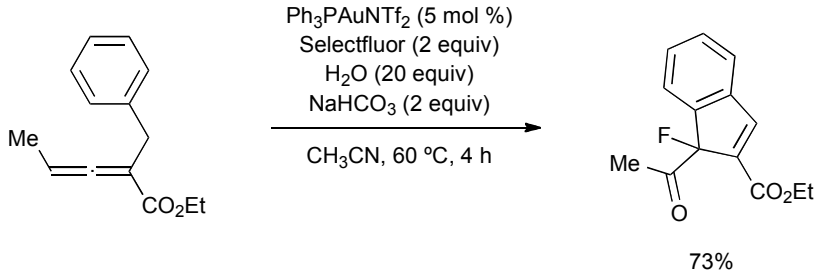

Scheme 22. Reaction of allene esters, Selectfluor and water to generate fluorinated indenes.

The construction of biaryls is also possible as demonstrated by Tse *et al.*, who employed Au(III) C–H activation in the development of a direct oxidative homocoupling procedure for electron–rich (hetero)arenes (Scheme 24).[33] This mild reaction, which may be performed under ambient conditions, tolerated a number of functional groups, notably including all of the halogens. The procedure is also applicable to neutral and electron–deficient arenes, although requiring higher temperatures and producing poorer yields. The authors note that although this reaction also proceeds in the presence of alternative Lewis acids, none of these catalysts display comparable reactivity to that of gold. Furthermore, they argue that the similar activity shown by the gold(I) catalysts $ClAuPPh_3$ and $(AcO)AuPPh_3$, to $HAuCl_4$, under the oxidative reaction conditions strongly supports a mechanism involving C–H activation.

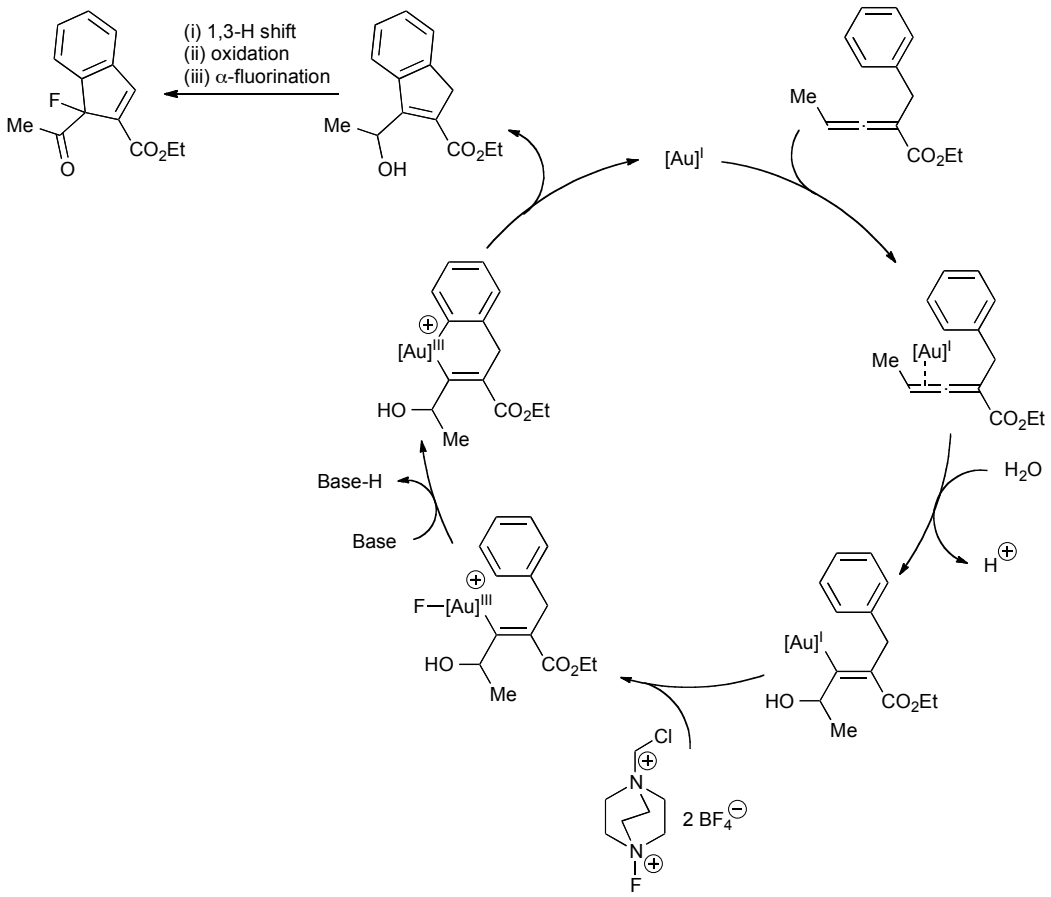

Scheme 23. Proposed Au(I)/Au(III) catalytic cycle. The authors performed an $O^{18}H_2$-labelling experiment, confirming the origin of the newly installed oxygen on the product.

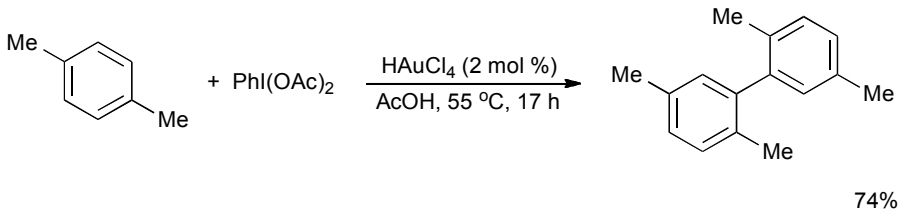

Scheme 24. $HAuCl_4$ catalysed homocoupling of *p*-xylene.

Fuchita *et al.*[34] used 2,6–lutidine as a ligand for Au(III), in a similar fashion to Liddle and Parkin,[3] allowing them to perform the C–H activation of a number of arenes and isolation of the resulting ligand–stabilised arylgold(III) compounds. Subsequent treatment of these organogold species with phenylacetylene, under very mild conditions, provided arylated alkynes in high yield (Scheme 25). This procedure benefits from mild reaction conditions and nearly quantitative C–C bond formation, following the lower yielding auration process step, however the necessary stoichiometic quantity of gold(III) is not ideal. Although the mechanism is not discussed, the alkynylation presumeably proceeds through an alkynyl arylgold(III) intermediate, which undergoes reductive elimination to generate the product and Au(I). Therefore in order to develop an overall catalytic process, the reoxidation of Au(I) to Au(III) is required.

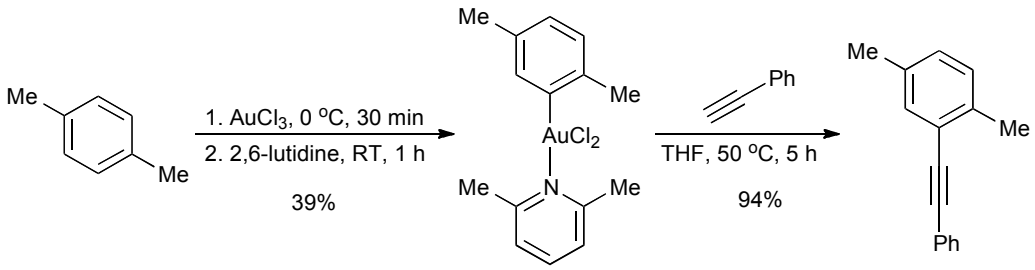

Scheme 25. C–H activation of *p*-xylene with $AuCl_3$, using 2,6–lutidine as a stabilising ligand, and subsequent functionalisation with phenylacetylene.

Several years later, Waser *et al.* reported the use of highly reactive and oxidising hypervalent iodine reagents in the the gold–catalysed direct akynylation of indoles and pyrroles (Scheme 26).[35] Their procedure provided easily deprotected silylacetylene products in good to excellent yields, achieving the same overall transformation as Fuchita *et al.* but with alkynyliodonium species, thus permitting the use of substoichiometric amounts of gold(I). The authors propose that this reaction may proceed *via* initial oxidation of the gold(I) chloride, by the alkynyliodonium species, to give a gold(III) acetylene complex. The gold(III) centre then performs C–H activation of the indole (or pyrrole), generating a organogold(III)

intermediate, which undergoes reductive elimination to give the alkynylated product and the regenerated gold(I) catalyst. However they do not exclude an alternative mechanism, involving gold–mediated addition of the indole to the alkyne, followed by β–elimination to give the product and release the gold catalyst. The reaction tolerates both electron–donating and electron–withdrawing groups on the indole, with the notable inclusion of bromine and iodine substituents. Alkynylation occurs preferentially at C-3 although in the case of substitution at this position, the C-2 product is accessed. Free pyrroles, not stable enough for Sonogashira cross–coupling, are compatible with this mild reaction to generate the C-2 alkynylated product preferentially. Waser *et al.* later extended this procedure to the alkynylation of thiophenes.[36]

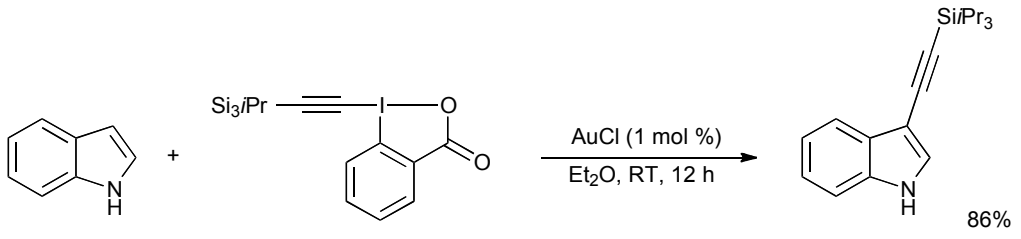

Scheme 26. Alkynylation of free indole catalysed by gold(I).

More recently, Nevado *et al.* took this concept further reporting the direct alkynylation of arenes starting from terminal alkynes.[37] Their gold–catalysed procedure employs a double C–H activation, achieving the ethynylation of electron–rich arenes with electron–poor alkynes, to provide synthetically challenging aryl propiolate products in good yields (Scheme 27). In seeking to elucidate the reaction mechanism, the authors conducted a series of NMR spectroscopy studies as well as kinetic isotope effect experiments, which indicated that neither the C_{sp} nor C_{sp2}–H bond breaking step is involved in the rate–limiting step. Based on their findings, the authors propose a reaction mechanism starting with C_{sp}–H activation, rather than C_{sp2}–H activation, to give a gold(I) acetylide, **V** (Scheme 28). This gold(I) intermediate is then oxidised, in the presence of $PhI(OAc)_2$, to generate gold(III) alkynyl complex **VI** which is then able to perform the C_{sp2}–H activation. Subsequent reductive

elimination provides the alkynylated product and regenerates the gold(I) catalyst.

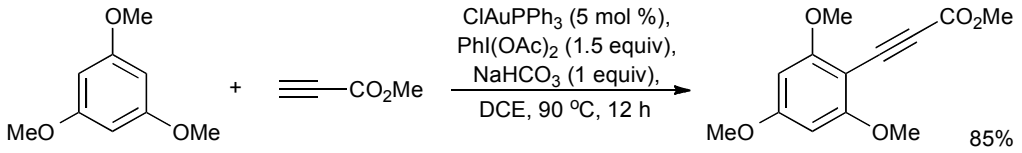

Scheme 27. Gold(I) catalysed ethynylation of 1,3,5-trimethoxybenzene.

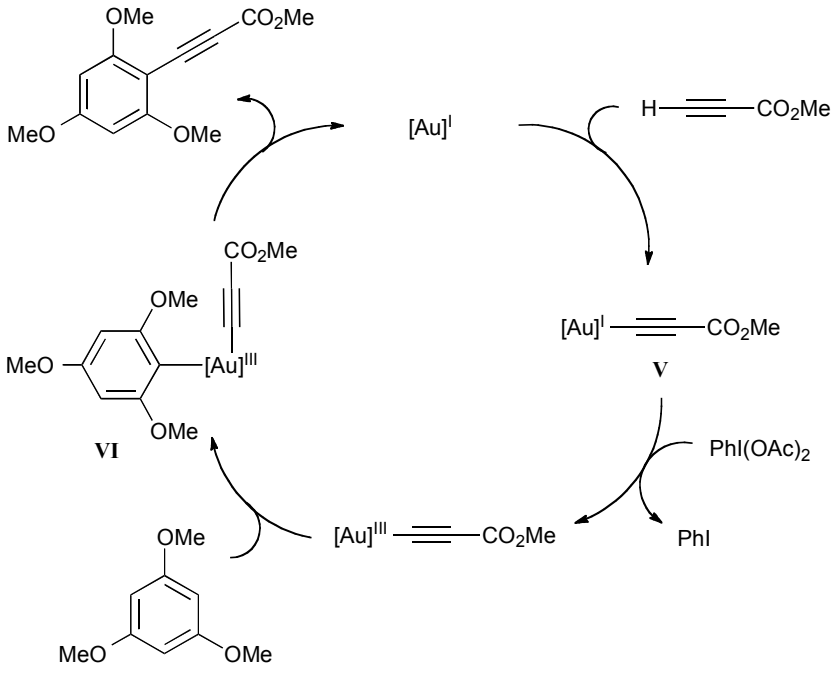

Scheme 28. Proposed mechanism for the gold(I) catalysed ethynylation of 1,3,5-trimethoxybenzene.

He *et al.* achieved nitrene insertion into aromatic C–H bonds in a Au(III) catalysed process for the formation of carbon–nitrogen bonds (Scheme 29).[38] Insertion of PhI=NNs (where Ns is *p*-nitrosulfonyl, which is easily deprotected from the product) into a number of arenes was achieved at room temperature in the presence of 2 mol % $AuCl_3$. The authors comment that this procedure was only applicable to benzene rings possessing three or more

substituents, which may be realated to the higher nucleophilicities of these substrates. The proposed mechanism proceeds through gold(III) arene **VII** (Scheme 30), formed *via* C–H activation, followed by activation of the nitrene by the Au(III) centre (**VIII)**, prompting an attack on the activated aryl carbon and consequent formation of the product as well as regeneration of the catalyst. The use of Lewis acidic metal ions and HCl in this system gave no product, lending strong support to the suggestion that the gold is performing C–H activation, rather than acting as a Lewis acid. Furthermore, the reaction of an arene with stoichiometric $AuCl_3$ quenched with D_2O resulted in aryl deuteration, indicating that direct metalation does occur in this process.

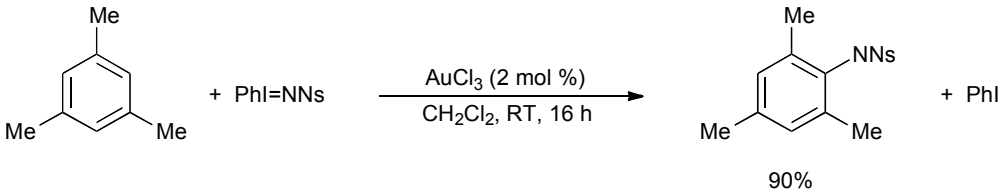

Scheme 29. $AuCl_3$ catalysed nitrene insertion. Ns = *p*-nitrosulfonyl.

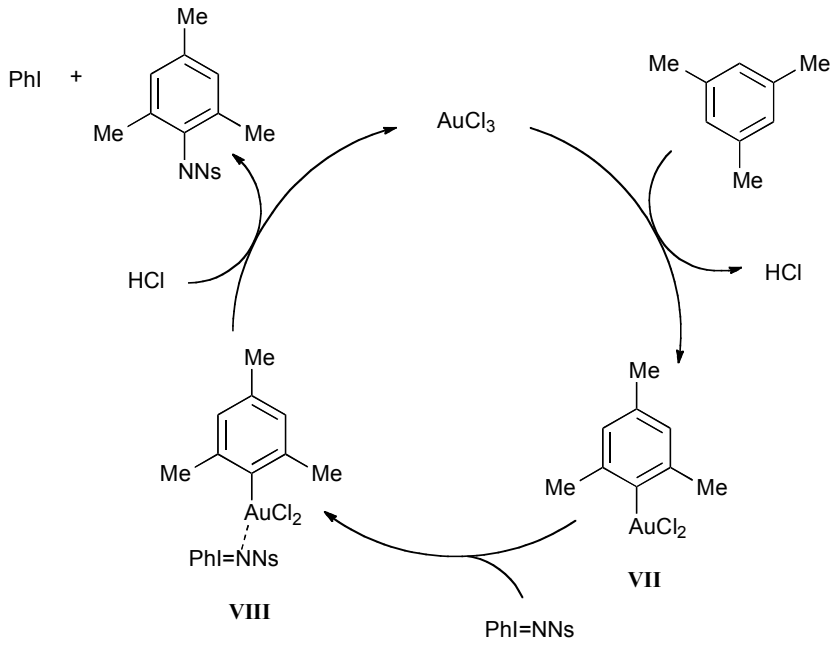

Scheme 30. Proposed reaction mechanism.

Wang *et al.* recently used gold(III) to catalyse the halogenation of a number of arenes (Scheme 31).[39] The authors describe the reaction as a dual activation process, involving activation of the *N*-halosuccinimide and also direct metalation of the arene, thereby utilizing both the Lewis acidity of gold as well as its ability to perform C–H activation. The use of other acids in this system, such as $FeCl_3$, $FeBr_3$, BF_3OEt_3 (commonly used to activate *N*-halosuccinimide), NH_4NO_3 and $ZrCl_4$, gave substantially lower yields. Furthermore, the use of $Pd(OAc)_2$, widely used to perform C–H activation, gave no product. The authors argue that these observations support their proposed dual activation reaction pathway. As observed with other Au(III) C–H activation procedures, electron–rich arenes generated high yields under mild conditions and with very low (0.01 mol %) catalytic loading. Whereas arenes bearing moderately electron–withdrawing groups required higher catalytic loading and longer reaction times and those with strongly electron–withdrawing groups were unreactive.

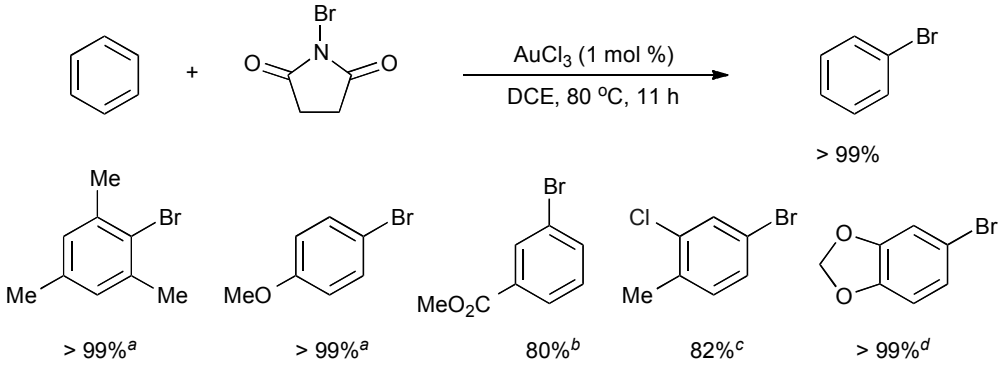

Scheme 31. $AuCl_3$ catalysed bromination of benzene. [a]0.01 mol % $AuCl_3$; [b]5 mol % $AuCl_3$; [c]60 °C; [d]0.5 mol % $AuCl_3$, RT.

The gold-mediated oxidative acetoxylation of hindered arenes was reported by Toullec, Michelet *et al.* (scheme 32).[40] The authors propose a mechanism in which the Au(I) centre is oxidised by the hypervalent iodine species, generating an $Au(III)(OAc)_2$ intermediate. Subsequent auration of the arene leads to liberation of an equivalent of acetic acid and formation of an arylgold(III) species, which then undergoes reductive elimination to furnish

the acetoxylated arene. However, for insufficiently hindered arenes, this arylgold(III) centre may go on to perform a second auration, leading to homocoupling of the arene.

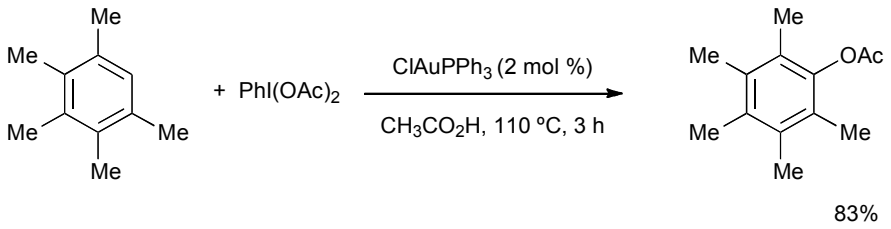

Scheme 32. Gold-mediated acetoxylation of hindered arenes.

The C–H activation, or direct metalation, of arenes by gold(III) is clearly a powerful process, providing a step and atom economical route to further functionalisation. The reactivity of gold, in this respect, is reflected in the high yields under mild reaction conditions. Intuitively, the selectivity of the strongly Lewis acidic gold(III) tends towards electron–rich arenes, with neutral and electron–poor substrates generally requiring more forcing conditions and generating poorer yields.

1.2.2 With Gold(I)

The functionalisation of an arene, following auration, is now an accepted route to diversification of the aryl nucleus, with the observation and isolation of aryl gold(III) reaction intermediates lending substantial support to such proposed mechanisms. However, the same has not been the case for Au(I), in fact, the C–H activation of an arene with Au(I) has only recently been demonstrated for the first time.[41]

This methodology, developed in our group, is the subject of chapter two and will be fully addressed therein. Almost simultaneously, Nolan *et al.* detailed the synthesis of an *N*-heterocyclic carbene-bound gold hydroxide and it's subsequent application to the C–H activation of electron-deficient arenes.[42] This gold(I) hydroxide and its synthetic applications[43] will be further discussed in chapter two.

In addition to these processes involving C–H activation, a number of methods for the gold(I)–mediated C–H functionalisation of arenes have been reported. All of these methods follow a common Friedel–Crafts step, in which the nucleophilic arene attacks an Au(I) stabilised carbocationic intermediate.

Genêt and Michelet *et al.* used $PPh_3AuCl/AgSbF_6$ to mediate the tandem Friedel–Crafts-type addition, of electron–rich (hetero)arenes to unactivated alkenes, following a carbocyclisation (Scheme 33).[44] The resulting cyclic functionalised carbo– or heterocycles were generated in good to excellent yields, under mild temperatures and short reaction times. The reaction is highly chemoselective, with arene addition to the alkyne not observed. A number of enynes and electron–rich (hetero)arenes were compatible with the system, including indole and bromine–substituted nucleophiles. The authors later developed an asymmetric version of this transformation, employing chiral bidentate phosphine ligands on the Au(I) centre to achieve good to excellent yields with up to 96% *ee*.[45]

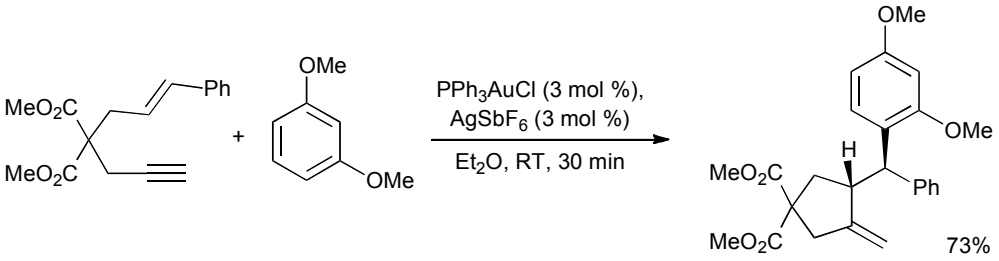

Scheme 33. Au(I)–catalysed tandem Friedel–Crafts-type addition/cyclisation.

Echavarren *et al.* reported the Au(I)–catalysed addition of electron–rich (hetero)arenes to 1,6-enynes (Scheme 34).[46] The reaction proceeds through a cyclopropyl metal carbene intermediate **IX**, which may react with the nucleophile at either the cyclopropane or the carbene, generating products **9** and **10**, respectively. Use of Au(I) catalyst **8** provided the best yields, under very mild conditions, for a number of electron–rich arenes and heteroarenes.

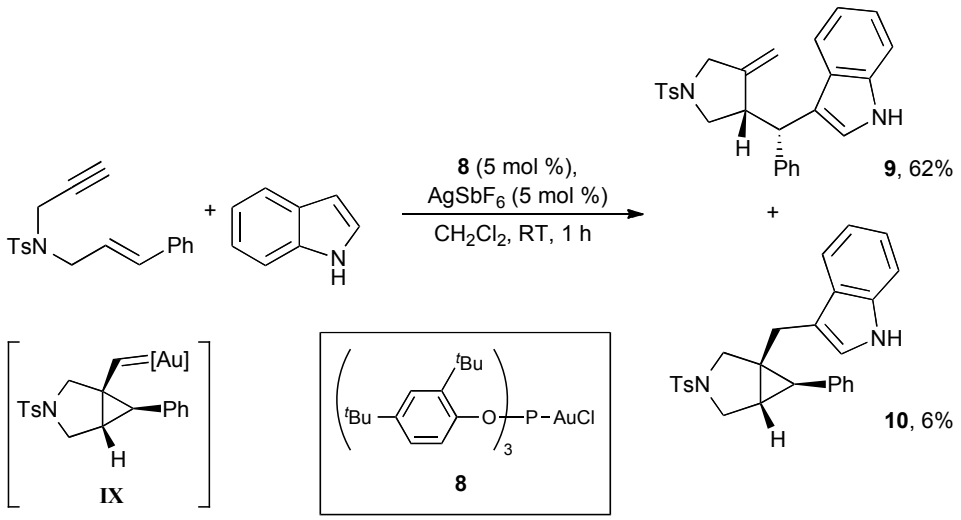

Scheme 34. Au(I)–catalysed arylation of 1,6-enynes.

Toste and Shapiro also utilised the reactivity of gold(I) carbenes in the rearrangement of alkynyl sulphoxides (Scheme 35).[47] Products are obtained in good to excellent yields under very mild reaction conditions. The authors propose that following a gold–mediated nucleophilic addition of the sulphoxide oxygen, to generate cyclised intermediate **X**, a subsequent sulphide release leads to intermediate **XI**. This gold(I) carbenoid then undergoes an intramolecular Friedel–Crafts alkylation, to provide the product and regenerated gold(I) catalyst.

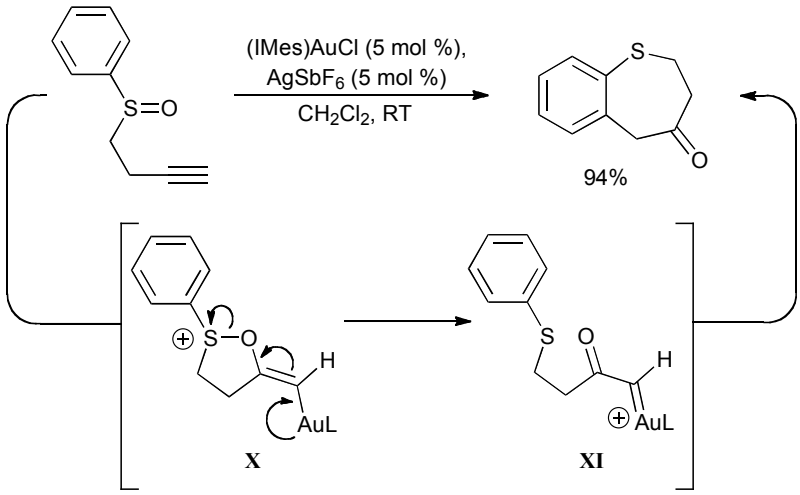

Scheme 35. Au(I)–catalysed rearrangement of alkynyl sulphoxides. IMes = bis(2,4,6-trimethylphenyl)imidazolin-2-ylidene.

Pale *et al.* employed the Lewis acidity of gold(I) in a Friedel–Crafts-type intramolecular reaction/ annulation of alkynylaziridines to generate spiro[isochroman-4,2'-pyrrolines] (Scheme 36).[48] The authors propose that the reaction proceeds *via* gold(I) coordination to both the alkyne and the nitrogen of the aziridine to form a transient allenyl intermediate, which was isolated in support of this pathway. This aminoallenylidene isochroman undergoes subsequent cyclisation, to give the corresponding spiro product.

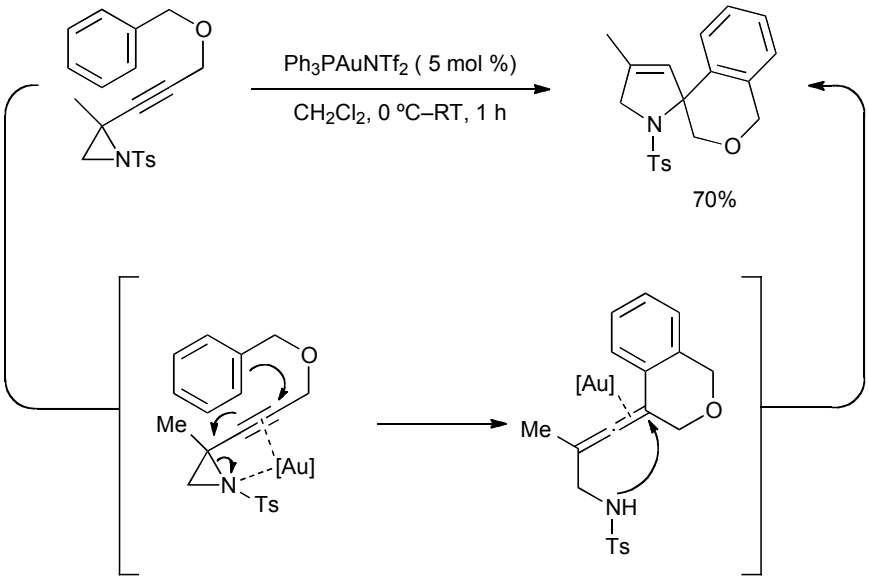

Scheme 36. Au(I)–catalysed allene formation/ annulation to form spiro derivative products.

The gold(I)-mediated formation of 3-acyloxindoles was reported by Zhang *et al.* (scheme 37).[49] The authors note that this oxidation/ cyclisation process generates products in good to excellent yields, the use of gold(I) catalysis meaning that synthetically useful handles, such as –Cl and –Br, remain intact. The absence of a primary kinetic isotope effect (k_H/k_D = 1.0) led the authors to propse that the C–H functionalisation proceeds *via* an electrophilic aromatic substitution step.

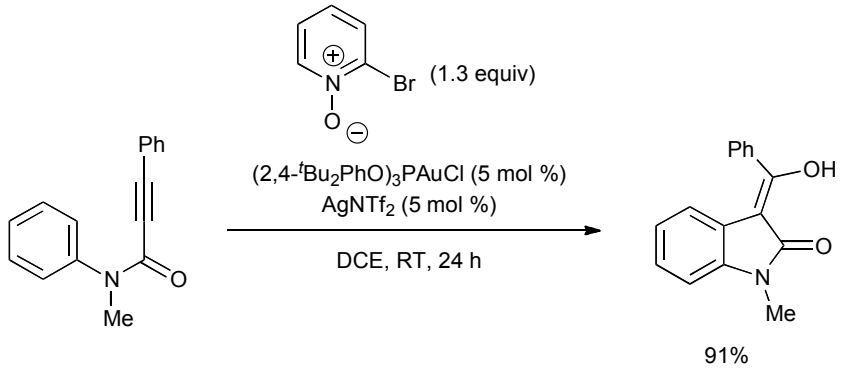

Scheme 37. Au(I)–catalysed formation of 3-acyloxindoles.

1.3 Alkyne C–H Functionalisation with Gold(I) and Gold(III)

The increased polarisation across a C_{sp}–H bond, compared to the aforementioned C_{sp2}–H bonds, translates to increased proton acidity and therefore facilitation of C–H activation processes. Consequently there are a large number of transformations which may proceed through C–H activation. However, the strong π-acidity of gold means that there is, again, an air of uncertainty surrounding mechanistic aspects of some of these processes. Being a soft Lewis acid, gold is attracted to areas of π electron density, and is used in such a capacity to effect a range of nucleophilic substitutions. In fact gold is often described as 'alkynophilic' owing to an apparent preference for alkynes over alkenes. Although, it is generally agreed that, this is more likely a preference of the incoming nucleophile for the lower lying alkyne LUMO than actual selectivity of gold, it does serve to highlight problems encountered in the elucidation of mechanistic pathways.

The Sonogashira cross–coupling reaction is a well–known and widely used route for the addition of an alkyne to an organic framework, proceeding through catalytic C–H activation of the alkyne. Typically the reaction employs palladium and copper catalysts, with copper responsible for alkyne activation and subsequent transmetalation to the organopalladium(II) intermediate, formed from oxidative addition of an organic halide to the Pd(0) catalyst. Reductive elimination releases the cross–coupled product and the regenerated Pd catalyst.[50]

Laguna *et al.* developed a Sonogashira cross–coupling reaction,[51] which uses gold(I) and gold(III) catalysts to perform the alkyne C–H activation and transmetalation to palladium, instead of copper(I) (Scheme 38). The gold–catalysed reactions were slightly slower than their copper–catalysed counterparts. However, the authors noted that generation of the alkyne homo-coupling product, a common problem in copper–catalysed systems, is completely avoided. Furthermore, this reaction offered greater operational simplicity, as pre-purification of reagents and exclusion of air were not required. The reaction was also performed with the water soluble

[PdCl(tppts)] and [AuCl(tppts)] (tppts = triphenylphosphine trisulfonate) in a biphasic CH_2Cl_2/H_2O solution, with good to excellent yields obtained for aryl iodides. The less reactive aryl bromides, which required heating in the previous system, did not generate useful quantities of product.

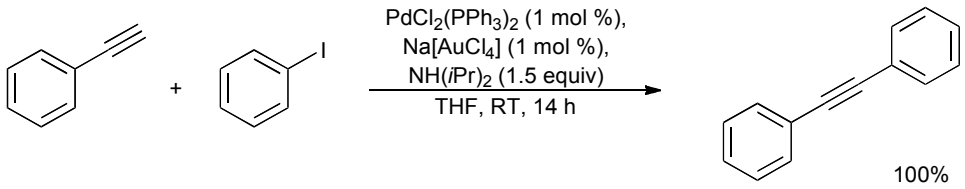

Scheme 38. Copper–free Sonogashira coupling reaction, with alkyne C–H activation with Au(III).

This copper–free Sonogashira cross–coupling provided a novel application of gold catalysis within an already very well established procedure. Furthermore, the coupling of gold and palladium cycles, in this manner, allows full exploitation of gold's ability to perform C–H activation while, through use of palladium, compensating for its reluctance to participate in the typical oxidative addition/reductive elimination catalytic pathway. While Au(I)–Au(III) redox chemistry is not completely inaccessible, examples are rare and generally require the presence of a strong oxidising agent, as such this catalyst pairing strategy is one that has since been adopted for other transformations.[52]

With this reactivity and limitations considered, the development of a Sonogashira cross–coupling, by Corma *et al.*, in which gold is able to replace both the copper and palladium catalysts[53] was an unanticipated extension to gold–catalysis. The authors rationalised that as gold had been shown to catalyse the Suzuki cross–coupling,[54] a role traditionally performed by palladium, and had also shown strong alkyne interactions, it should be able to perform the role of both metals in a copper– and palladium–free procedure. The use of 5 mol % Au/CeO_2, that is gold supported on a crystalline CeO_2 surface, in the cross–coupling of phenylactylene and iodobenzene provided the desired cross–coupling product in good yield, along with the alkyne

homocoupling product and a small amount of the iodobenzene homocoupling product. X–ray photoelectron spectroscopy showed the presence of Au(0), Au(I) and Au(III) in the gold supported catalyst and so effort was then directed towards uncovering which of these species was the active catalyst. The application of Au(I) and Au(III) complexes bearing Schiff base ligands (Figure 2) led the authors to conclude that, under the same conditions, the gold(III) complex predominantly led to formation of the alkyne homocoupling product in low yield whereas the gold(I) complex, bearing the same d^{10} configuration as palladium(0) and copper(I), gave the desired cross-coupling product (Scheme 39). Furthermore, they also note that the gold catalysts display similar activity to their palladium analogues and that colloidal gold(0) displays low reactivity towards either transformation.

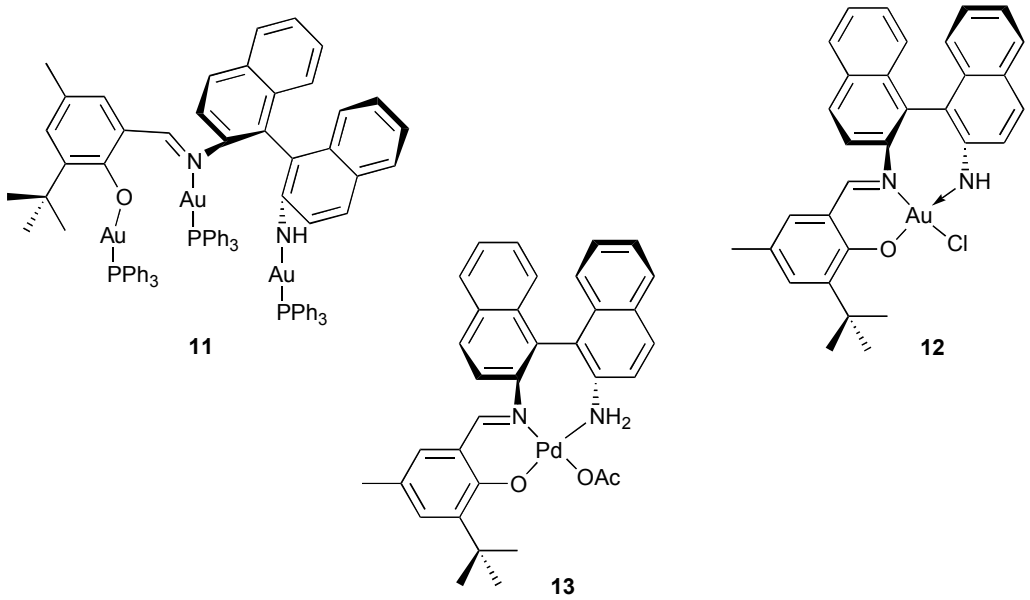

Figure 2. Au(I) and Au(III) complexes tested in the Cu– and Pd–free Sonogashira cross–coupling and the PdII) analogue also tested.

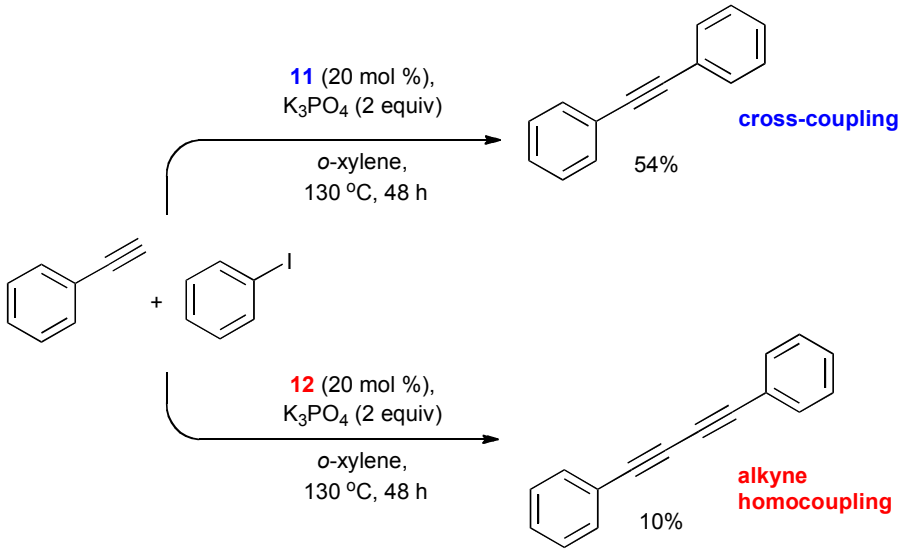

Scheme 39. Observed gold(I) and gold (III) reactivity in the copper–free Sonogashira coupling reaction.

Corma's proposal that gold(I) may be able to replace both the copper(I) and palladium(0) catalysts, in Sonogashira coupling procedures, offered an attractive alternative to the two–metal procedure and consequently attracted interest from a number of groups, aiming to improve upon the conditions and yields reported by Corma *et al.*

Antunes *et al.* used microwave irradiation, as an alternative to the high reaction temperatures, aiming to reduce the long reaction times and increase yields (Scheme 40).[55] After screening a number of gold–supported catalysts, Au/SiO_2 was selected as the most effective and used to catalyse the coupling of various aryl halides with phenyl acetylene. The authors note that although high yields were obtained when coupling electron–poor or neutral aryl iodides, the use of aryl bromides or iodides bearing electron–donating groups led to moderate product yields

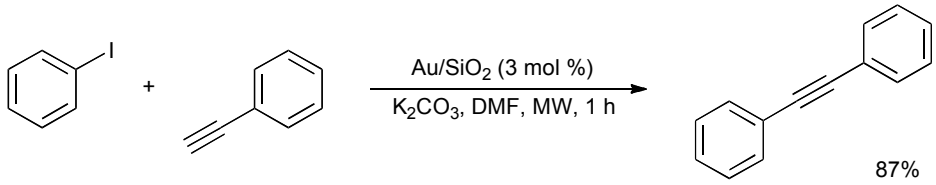

Scheme 40. Copper– and palladium–free Sonogashira coupling using an Au/SiO_2–supported catalyst and microwave irradiation.

Wang *et al.* also reported a copper– and palladium–free Sonogashira coupling of a number of terminal alkynes with aryl iodides and bromides (Scheme 41).[56] The cross–coupling products were obtained in good to excellent yields through use of a gold(I) iodide catalyst with the bidentate dppf ligand (dppf = 1,1'-bis(diphenylphosphino)ferrocene) in 1:1 molar ratio, the authors comment that any ratio of dppf to Au(I) less that 1:1 resulted in the reaction not going to completion.

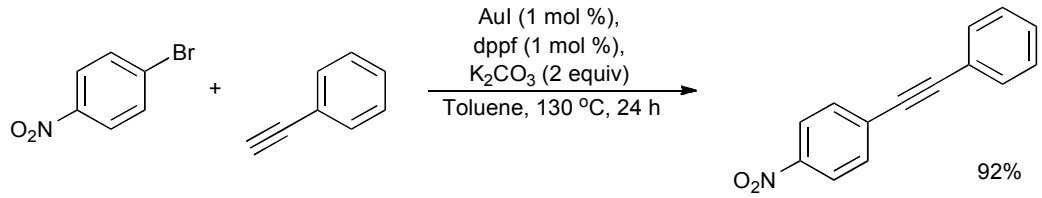

Scheme 41. Copper– and palladium–free Sonogashira coupling using a gold(I) iodide and dppf catalytic system. Dppf = 1,1'-bis(diphenylphosphino)ferrocene.

However, given the previously held conviction that gold was unable to participate in such redox chemistry, doubts remained over the validity of these reports and a recent publication by Echavarren *et al.*[57] calls into question the reactivity of these gold catalysts. The authors state that the description of gold(I) as being isoelectronic to Pd(0), accurate though it may be, does not indicate that the two metal centres will display the same reactivity. Aiming to learn more about this apparently contradictory reactivity of gold, a meticulous investigation into these copper– and palladium–free systems was conducted. Initially, the authors endeavoured to experimentally

substantiate any plausible mechanism through which this gold–catalysed coupling may proceed. One such pathway is the standard oxidative addition/transmetalation/ reductive elimination as typically observed for palladium, this pathway begins with oxidative addition of the aryl halide to gold(I) to give a gold(III) complex, a step deemed infeasible and therefore the pathway implausible. Another possible pathway begins with C–H activation of the alkyne, the viability of which is not contested, followed by oxidative addition of the aryl halide and reductive elimination of the product. Again, it is the oxidative addition step, to cationic alkynyl gold(I) complexes, which poses the problem and cannot be verified experimentally, suggesting that this pathway is also unlikely. This failure to determine a plausible mechanistic pathway for the reaction to follow, naturally, led the authors to examine the reproducibility of the reported Cu– and Pd–free coupling procedures. This too was unsuccessful and no cross–coupling products were obtained, using gold alone, however addition of small quantities of palladium (0.12 mol %) to these reactions promoted complete conversion to the product. Therefore, the authors conclude that any successful Au–catalysed and Pd–free Sonogashira couplings are a result of Pd contamination, rather than any comparative reactivity of these two d^{10} metal centres.

A subsequent rebuttal by Corma *et al.*[58] disputed these conclusions. Having performed kinetic and theoretical studies, the authors state that this reactivity is indeed possible in the absence of palladium impurities and is in fact a result of the formation and reactivity of gold nanoparticles. While their studies agree that a gold(I) centre would not be able to undergo oxidative addition in this reaction, a gold nanoparticle would. They therefore refute the claim that palladium impurities are a requirement for their reaction to proceed.

While Sonogashira cross–coupling reactions, in their palladium–, copper– and gold–catalysed forms, may well constitute the most versatile and widely employed method to achieve addition of an acetylenic group, these transformations are still limited by the requirement of a prefunctionalised aryl halide coupling partner. Moreover, the generality of the procedure is limited, electron–rich arenes and/or electron–poor alkynes being more challenging

substrates. Alkynes have also been used as nucleophiles in a number of Au–mediated couplings.

Li and Yao developed a gold(I) promoted procedure for the alkynylation/cyclization of acetylenic aldehydes with terminal alkynes,[59] to give 1-alkynyl-1*H*-isochromene products (Scheme 42). The use of alternative electron–donating phosphine ligands in the procedure gave none of the desired product, with only a small amount generated when there was no phosphine used at all. The absence of water also prevented product formation, indicating that it plays a key role in the reaction. The reaction appears to require the presence of an *o*-alkynyl group on the aldehyde-bearing substrate, with benzaldehydes giving no product when applied to the reaction conditions. The authors rationalise that the *o*-alkynyl acts as a chelating–activating group. The proposed mechanism proceeds *via* initial C–H activation of the alkyne, in the presence of mild base, to generate a gold acetylide. This then chelates to the alkynyl benzaldehyde, through the alkynyl and carbonyl groups, activating the carbonyl for reaction with the acetylide and subsequent attack of the triple bond gives a vinylgold intermediate, which undergoes protonolysis to give the product and regenerated catalyst.

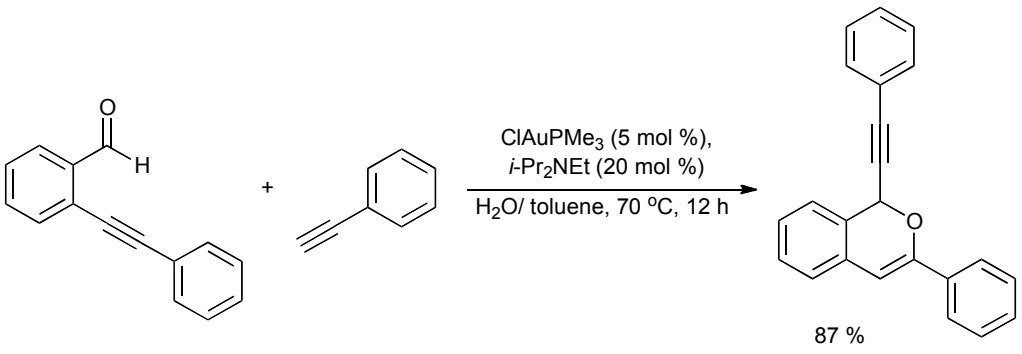

Scheme 42. Gold(I) catalysed alkynylation/cyclization of 2-(phenylethynyl) benzaldehyde with phenylacetylene.

Wang *et al.* performed the gold(I)–catalysed arylmethylation of terminal alkynes,[60] in a procedure which demonstrates the potential for exploitation of the Au–C bond as a nucleophile in substitution reactions (Scheme 43). The

electrophilic reaction partner, of the terminal alkyne, contains a trichloroacetimidoxyl leaving group, which performs two important roles. The reaction proceeds through initial C–H activation of the terminal alkyne to provide the Au–C bond, as verified by an H/D exchange study. In this auration step, the basic nitrogen of the trichloroacetimidoxyl group removes the acidic terminal proton of the alkyne, thus generating the gold acetylide. The resulting protonated trichloroacetimidoxyl group is now a much better leaving group and consequently more susceptible to attack of the gold acetylide, allowing formation of the benzylacetylene derivative products in good yield and the neutral trichloroacetamide leaving group, which does not interfere with the reaction or activity of the gold catalyst.

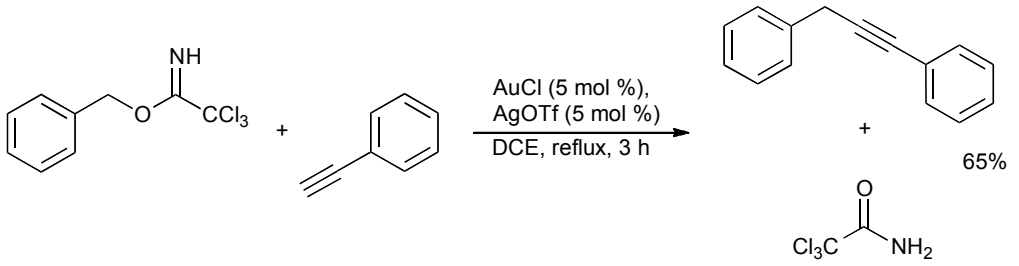

Scheme 43. Gold(I) catalysed coupling of benzylic trichloroacetimidate with phenylacetylene.

Multicomponent approaches to the one–step construction of complex molecular frameworks offer obvious benefits, in terms of step and atom economy. Along with increased operational simplicity, facilitation of product isolation and catalyst recovery, this approach allows for a much more financially and environmentally favourable synthetic strategy. The application of gold catalysis to this field has amplified the environmental advantages, allowing for the development of milder methodologies, benefiting from the high reactivity of gold towards π-electron density and also, generally more so in the case of gold(III), solubility in water meaning that it may be used in place of other, more harmful, organic solvents.

Li and Wei employed gold(I) and gold(III) catalysts in their three–component coupling of aldehydes, alkynes and amines (Scheme 44).[61] They found that Au(III) salts outperformed Au(I) and $AuBr_3$ was selected as the best catalyst, being the cheapest as well as most reactive of the gold salts. The authors propose a mechanism proceeding *via* C–H activation of the alkyne by Au(I), which in the case of $AuBr_3$ catalysed reactions, may be generated *in situ* by reduction of Au(III) by the alkyne. The resulting gold acetylide intermediate reacts with the imminium ion, generated from the aldehyde and secondary amine, to give the product and free the Au(I) catalyst for further reaction. Interestingly, the reaction required the complete exclusion of air and also did not proceed cleanly in organic solvents, where low yields and increased generation of by-products were observed.

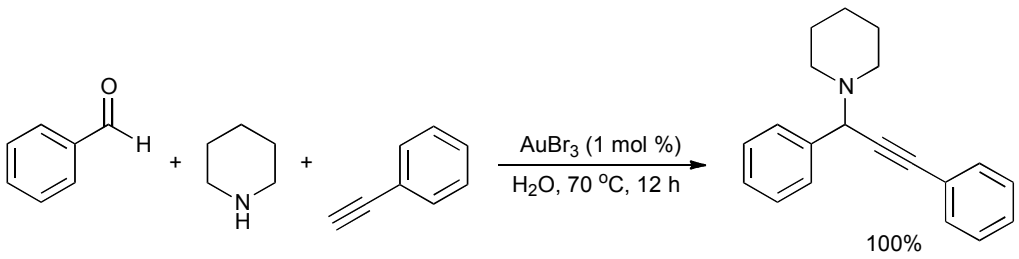

Scheme 44. Gold(III) catalysed three–component coupling of benzaldehyde, piperidine and phenylacetylene.

Wang *et al.* later extended this transformation to a Au(III)–catalysed cyclisation of the 3-component coupling products, generating quinoline derivatives in high yields under very mild conditions.[62]

The gold(III) catalysed A^3 coupling of aldehydes, alkynes and amines was also performed by Wong and Che *et al.*, using gold(III) salen complexes (Scheme 45).[63] The reactions were very mild, proceeding in water at 40 °C to give excellent yields, in the presence of 1 mol % of the gold(III) catalyst. Furthermore, the use of chiral prolinol derivatives as the amine component in this system, allowed the formation of the corresponding propargylamine products in good yields, with excellent diastereoselectivities observed (84:16–99:1 over 5 examples).

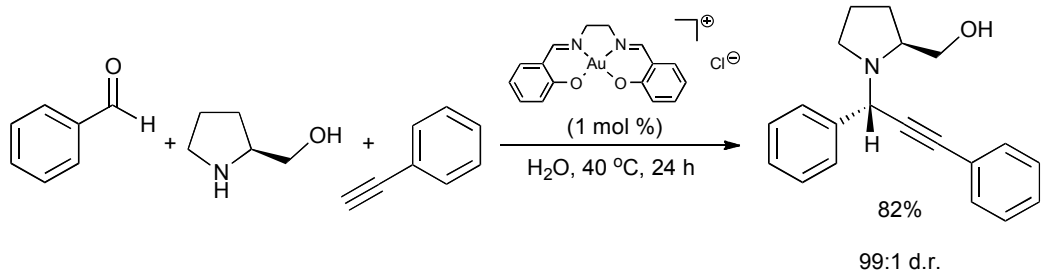

Scheme 45. Three–component coupling catalysed by a gold(III) salen complex.

Li *et al.* later reported the A^3 coupling of α-oxyaldehydes, alkynes and amines to give the corresponding α-oxyamines (Scheme 46) in good yields and with moderate diastereoselectivity.[64] Again, this procedure could be promoted by both gold(I) and gold(III) salts, with gold(I) catalyst showing superior reactivity and AuI selected as the catalyst of choice. The AuI catalysed reaction could also be performed at 0 °C, although generating a lower yield of 58% product. Use of organic solvents, in place of water, was not beneficial and resulted in decreased yields. Silver and copper catalysts were also tested but were not active in this system.

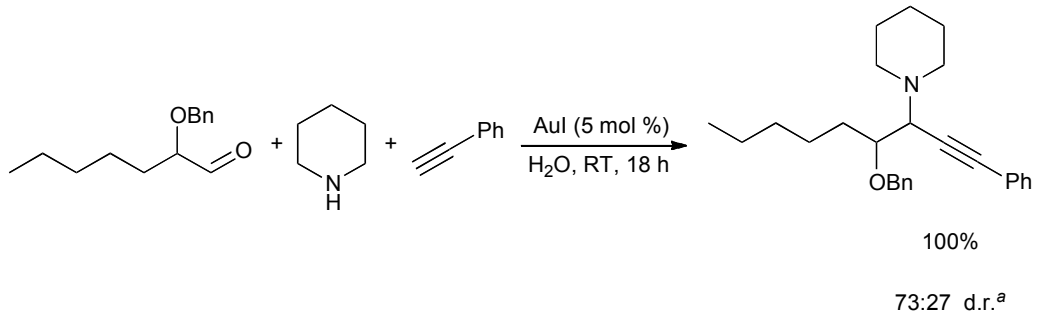

Scheme 46. Gold(I) catalysed three–component coupling of α-benzoxyaldehyde, piperidine and phenylacetylene. [a]^{1}H NMR analysis of crude reaction mixtures provided *dr* values but absolute configuration was not determined.

The 3-component coupling of an aldehyde, terminal alkyne and triethyl orthoformate was reported by Wang *et al.* (Scheme 47).[65] The authors propose that the reaction proceeds *via* gold(I) C–H activation of the alkyne. However, they note that the ability of AgOTf to promote the reaction alone, albeit in lower yield, indicates that another pathway, in which the gold(I) acts as a Lewis acid in a Prins-type reaction may also be considered.

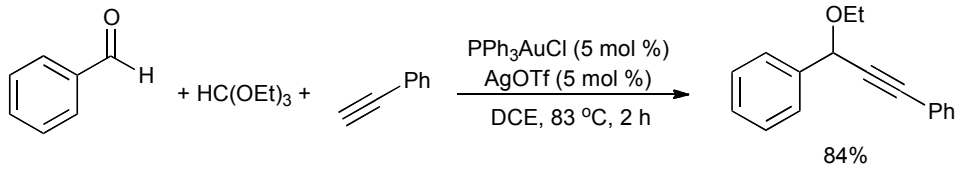

Scheme 47. Gold(I)–mediated three-component coupling of benzaldehyde, triethyl orthoformate and phenylacetylene.

Lui and Yan extended these gold–catalysed multicomponent couplings to the formation of new carbon–nitrogen bonds (Scheme 48).[66] Their procedure employed Au(III) catalysts, the best being $NaAuCl_4 \cdot 2H_2O$, having observed much poorer yields with Au(I). They also tested the activity of copper catalysts, finding them unable to generate good yields in this system. The reaction proceeded either using water as the solvent or under solvent-free conditions, both of which are an advantage from an environmental standpoint, as is the low reaction temperature. The authors extended this procedure to the coupling of optically pure amino acid derivatives with alkynes and aldehydes, observing preservation of enantiomeric purity in the products.

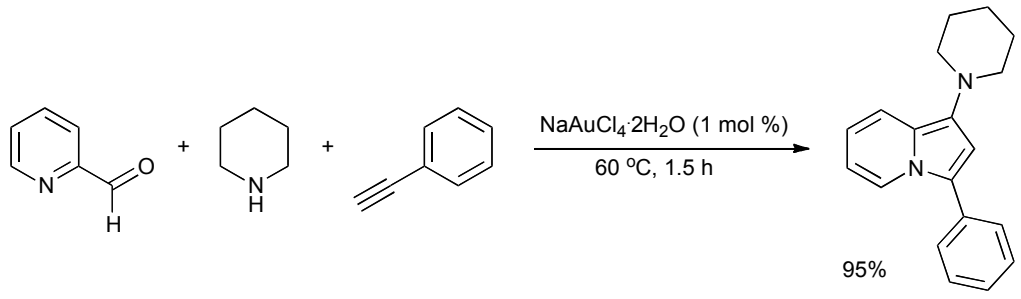

Scheme 48. Gold(III) catalysed three–component coupling of pyridine-2-carboxaldehyde, piperidine and phenylacetylene

1.4 Alkane C–H Functionalisation with Gold(I) and Gold(III)

With the smallest s-orbital contribution, C_{sp3}–H bonds are the least acidic and therefore offer the greatest challenge for performing C–H activation. Consequently there are far fewer examples of this class of activation with gold, compared to the C_{sp2}–H and C_{sp}–H activation.

Periana *et al.* developed the first reaction of this class in 2004.[67] Cationic gold was able to activate an unactivated methane C_{sp3}–H bond, in the oxidation of methane to methanol (Scheme 49). The procedure employed metallic gold, in the presence of concentrated sulphuric acid and a selenic acid oxidising agent, at 180 ^{o}C to produce methanol in high yield, with turnover numbers of up to 30 observed. The production of low levels of CH_3D, when the reaction is carried out in D_2O, supports the formation of an Au–CH_3 intermediate. DFT calculations indicate that both Au(I) and Au(III) species are *via*ble catalysts for this reaction, which proceeds through electrophilic auration and subsequent oxidative functionalisation.

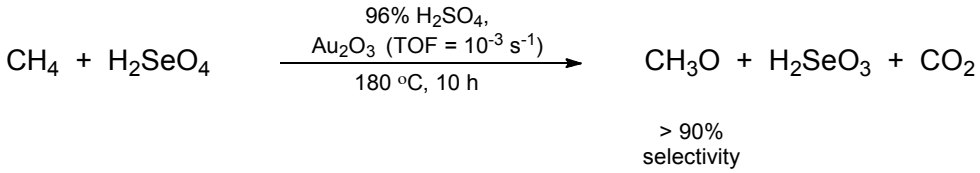

Scheme 49. Gold–catalysed oxidation of methane to methanol.

Hashmi, Laguna *et al.* reported a gold–catalysed benzylic C–H activation, under ambient conditions.[68] During a study into the gold–mediated cyclization of alkynyl benzylic alcohols, an unexpected dimerisation, resulting in the formation of eight new bonds, was observed in the presence of additional nucleophilic substituents, like the ester groups as shown in Scheme 50. From this scheme it is clear that, following gold–coordination to the alkyne, there are two groups poised for nucleophilic attack: the hydroxyl group, which leads to the expected cyclization product (**15**), or the ester carbonyl, leading to dimerisation (**14**). From here, the reaction pathway (Scheme 51) is

proposed to proceed through intramolecular addition of the hydroxyl to give an activated tricyclic form of the benzyl alcohol (**XIII**), which reacts with a second molecule of the starting material to generate the dibenzyl ether (**XIV**). At this point a proposed C–H activation occurs at the benzylic position, to generate a gold–carbon bond, which may receive additional stabilisation from coordination of the adjacent carbonyl group (**XV**). Insertion of the alkyne, into the Au–C bond (**XVI**) followed by protodemetalation (**XVII**) and migration of the double bond leads to the dimerisation product (**14**). The authors present the direct auration of acetone, verified with X–ray crystallographic analysis, as support for the proposed benzylic C–H activation. This, along with the exclusion of an alternative radical reaction pathway, leads the authors to conclude that experimental evidence strongly supports a reaction mechanism including benzylic C–H activation.

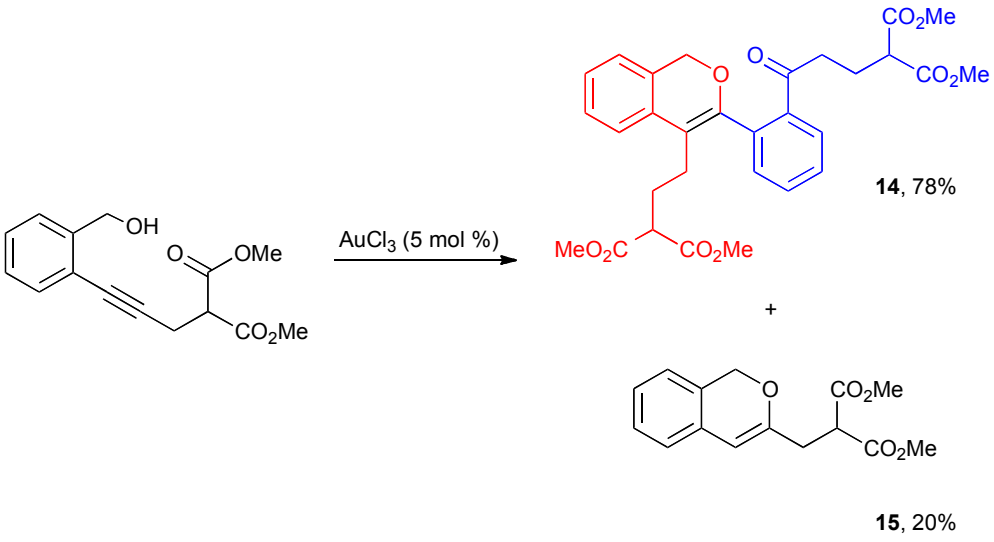

Scheme 50. Gold(III)–catalysed dimerisation *via* C–H activation at a benzylic postion.

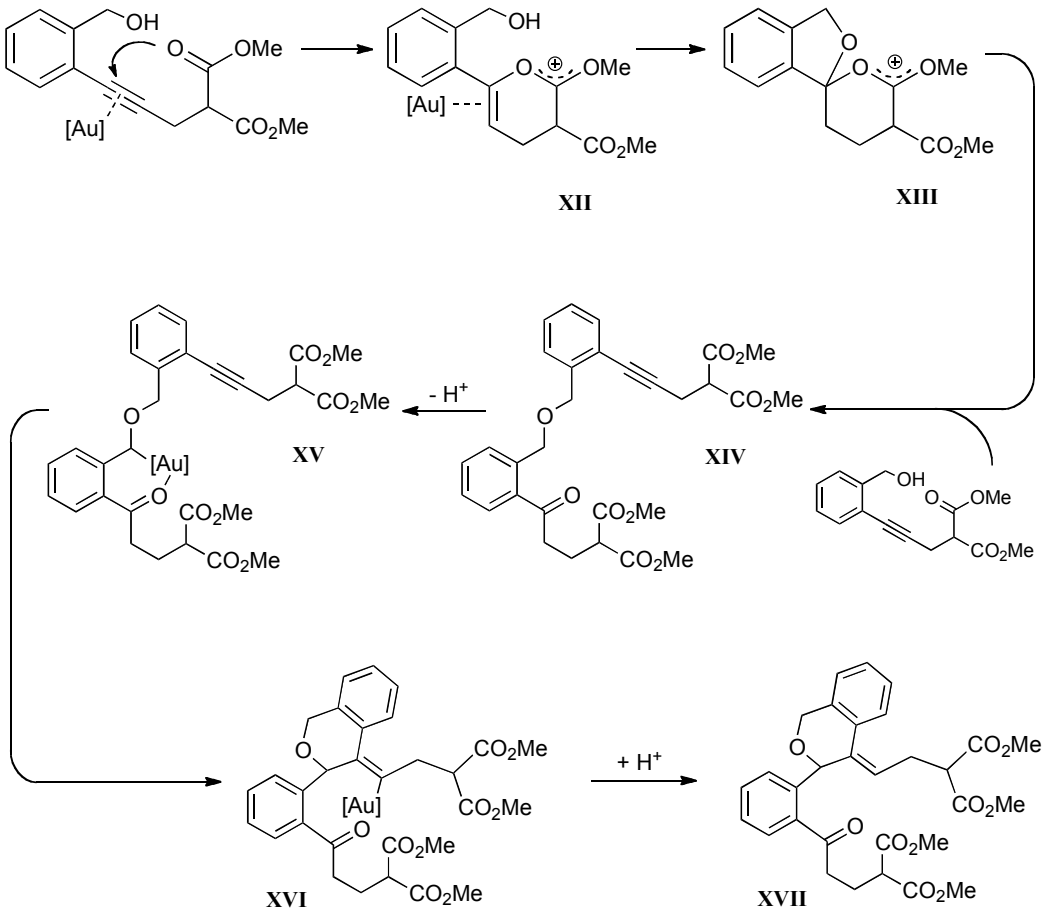

Scheme 51. Proposed mechanism for the formation of dimerisation product **15**, proceeding through C–H activation at the benzylic position of intermediate **XIV**.

The Au(I)–mediated insertion of a carbene into a C_{sp3}–H bond was demonstrated by Nolan *et al.*, who performed transfer of the carbene unit from ethyl diazoacetate to primary and tertiary C–H bonds of alkanes (Scheme 52).[69] The authors favoured the use of (IPr)AuCl as the Au(I) source, with halide abstractor $NaBAr_4$ employed to generate the active catalyst. Using 2,3-dimethylbutane as the substrate, in which both primary and tertiary C–H bonds are available, the authors observed high selectivity towards the primary functionalised product **16**. Interestingly, this regioselectivity is completely reversed with use of the copper(I) catalyst (IPr)CuCl, which preferentially formed tertiary functionalised product **17**, under the same conditions; the authors attribute this to electronic effects. There is no reaction in the absence

of halide scavenger $NaBAr_4$, in keeping with the authors proposal that the active catalyst is a cationic gold species, which mediates carbene transfer from the azide and C_{sp3}–H bond insertion, as previously proposed for a similar procedure.[70]

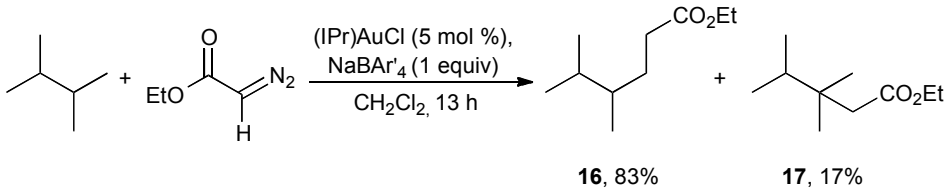

Scheme 52. Au(I)–mediated reaction of 2,3-dimethylbutane with ethyl diazoacetate. IPr = 1,3-bis(diisopropylphenyl)imidazol-2-ylidene; $NaBAr_4$ = sodium tetrakis(3,5-bis(trifluoromethyl)phenyl)borate.

The Au(I)–catalysed cycloisomerisation of 1,5–enynes terminated by C_{sp3}–H bond insertion was reported by Toste *et al.*, who generated the corresponding cyclised products in high yields under mild reaction conditions (Scheme 53).[71] The authors propose that the transformation proceeds *via* an initial Au(I) complexation of the alkyne, inducing intramolecular addition of the alkene and thus generating intermediate **XVIII**. This Au(I) carbenoid then invokes an intramolecular C_{sp3}–H bond insertion to generate the tetracyclic product. This mechanism is supported by a deuteration study, consistent with the *intramolecular* interaction of the C_{sp3}–H bond with the Au(I) carbenoid. Subsequent DFT calculations performed by Zhang *et al.*, verify this mechanistic pathway and highlight the importance of the cycloalkyl substituent ring size: for smaller rings (less than 7-membered) intermediate **XVIII** follows a ring expansion pathway, generating a tricyclic product. On the other hand, for larger rings the C–H insertion pathway is favoured. The authors note that this observation is a result of kinetic, rather than thermodynamic, control.[72]

Insertion of cationic gold carbene intermediates into C_{sp3}–H bonds was also observed by Echavarren *et al.*, generating complex by-products in their gold(I)–catalysed addition of carbonyl compounds to 1,*n*-enynes (where *n* = 5 or 6).[73]

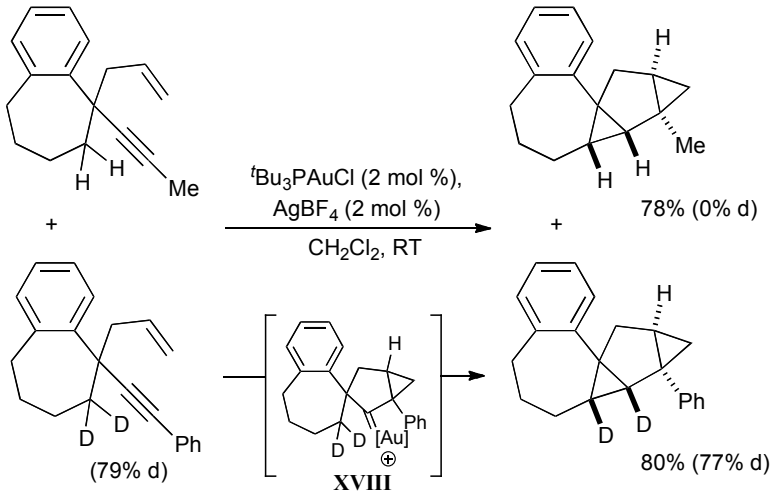

Scheme 53. Au(I)–catalysed cycloisomerisation. (d = deuteration)

Formation of a gold(I) carbene was also proposed by Liu and Bhunia, in their procedure for the 1,3-addition of a C_{sp3}–H bond to this alkenylcarbenoid intermediate (Scheme 54).[74] Bicyclo[3.2.1]oct-6-en-2-one products were generated in high yield, in this gold(I)–catalysed procedure, which is proposed to proceed *via* gold carbenoid **XIX** (Scheme 55). Based on deuterium labelling studies, the authors suggest that the sp^3 hybridised H–$C(OMe)_2$ bond is cleaved by an intramolecular hydride transfer, induced by the gold carbene carbon, to generate Au(I) allyl intermediate **XX**. The authors note that this process constitutes the first 1,3-addition of a C_{sp3}–H bond to a metal carbenoid, C_{sp3}–H insertion being more typically observed.

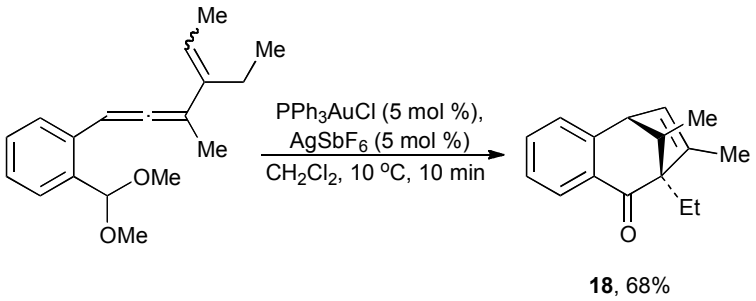

Scheme 54. 1,3-addition of a C_{sp3}–H bond to a Au(I) carbenoid.

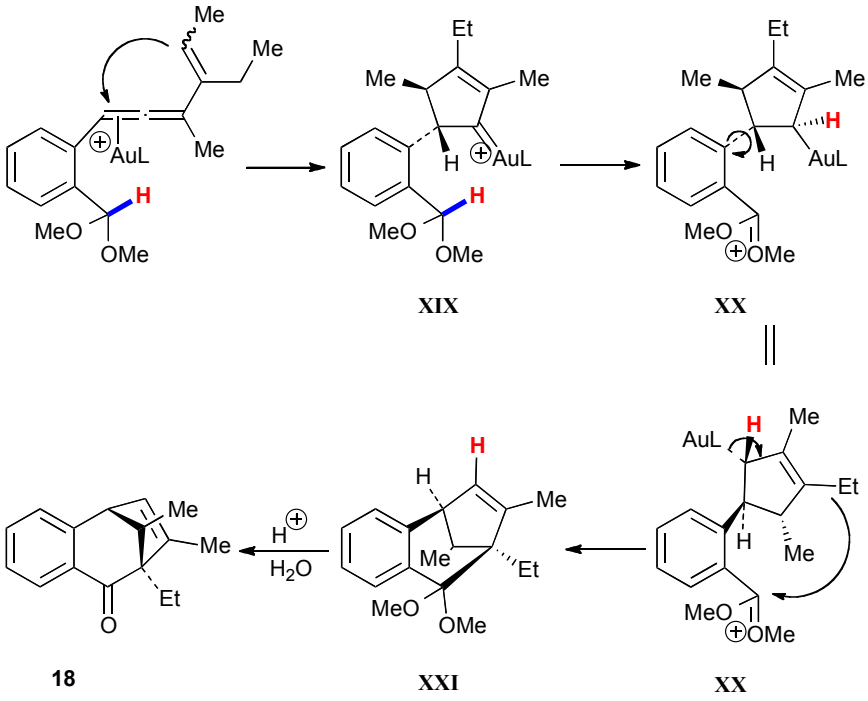

Scheme 55. Proposed mechanism of 1,3-addition to Au(I) carbenoid intermediate **XIX**.

Gagosz *et al.* reported the Au(I)–catalysed hydroalkylation of a range of alkynyl ethers, proceeding through a 1,5-hydride shift/cyclisation sequence (Scheme 56).[75] The authors propose that 6-*exo* activation of alkynyl ethers, by gold(I) catalyst **19**, promotes a 1,5-hydride shift, from the C_{sp3}–H α to the oxygen to the alkyne. Subsequent cyclisation of the resulting vinylgold species generates the products in high yields, for a number of alkynyl ether

substrates. Thus, through activation of a terminal alkyne, with electrophilic gold(I), a C_{sp3}–H bond is replaced with a new C–C bond.

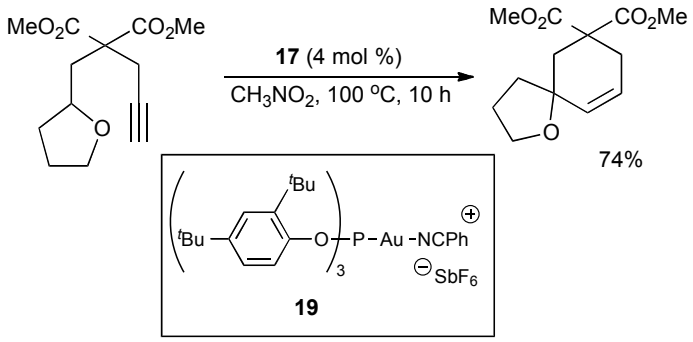

Scheme 56. Au(I)–mediated 1,5-hydride shift/cyclisation.

A remarkable gold-catalysed oxidative C_{sp3}– C_{sp3} coupling, employing air as the oxidant, was reported by Zhu *et al.* (scheme 57).[76] The reaction proceeds under mild conditions to perform the coupling of tertiary amines with nitroalkanes or ketones, generating the α-C–H functionalised amine products in excellent yields. Mass spectrometry identified a cationic iminium species as the key intermediate, leading the authors to propose a pathway in which an iminium gold(I) hydride complex is formed (scheme 58). In the presence of air, this iminium species is then trapped by the nitroalkane to generate the product and liberate a gold(III) species. This species is then able to interact with another amine to generate an iminium ion, once again leading to product formation and this time liberation of the gold(I) catalyst.

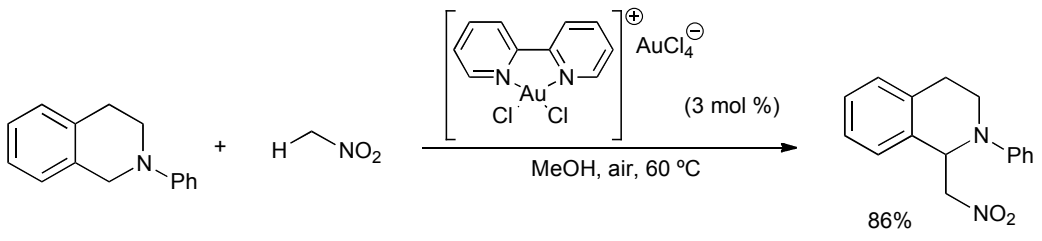

Scheme 57. Gold-catalysed oxidative C–C coupling using air as the oxidant.

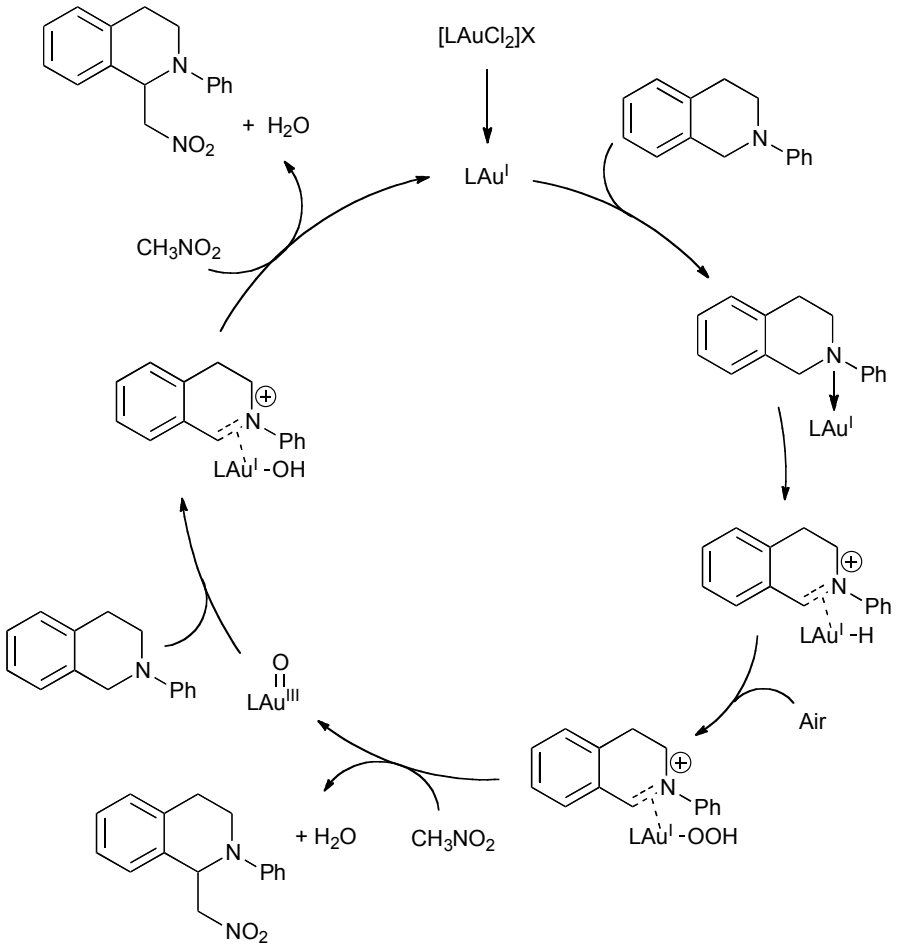

Scheme 58. Gold-catalysed oxidative C–C coupling using air as the oxidant.

The authors later applied this system to the phosphination of C_{sp3}–H bonds, using similar amine starting materials, this procedure generated α-amino phosphonic products.[77]

A procedure for the gold-catalysed amidation of benzylic C–H bonds was developed by Feng *et al.* (scheme 59).[78] A gold(III) catalyst/ *N*-bromosuccinimide (NBS) system was used to perform the functionalisation of the C_{sp3}–H bonds, generating the corresponding amines in good to excellent yields. The authors propose that the reaction begins with reaction of the sulfonylamide and NBS to form an *N*-bromosulfonylamide, which then interacts with the reduced Au(I) catalyst to form a gold nitrene complex. This complex

then combines with the benzylic C–H bond, *via* a 3-membered transition state, to generate the product and liberate the Au(I) catalyst.

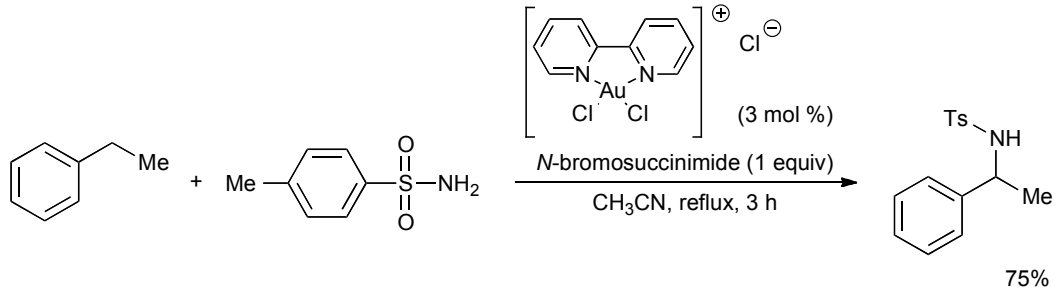

Scheme 59. Gold-catalysed amidation of benzylic C–H bonds.

1.5 Conclusions

C–H functionalisation is clearly a powerful synthetic tool, providing a highly economic means to increase the complexity of unactivated frameworks. This review has outlined the advances in the area involving the functionalisation of arenes, alkynes and alkanes using gold(I) and gold(III) catalysts. Some transformations covered in this review can be performed with other transition metals and even strong acids. In these cases, it is important to achieve low loadings of the gold catalyst in order to be competitive with the cheaper alternatives. In other examples though, the transformations are unique to gold, opening new avenues of reactivity. The potential of gold–catalysis in this field is only just beginning to be realised and will undoubtedly continue to gain momentum over the coming years. With increased exploitation of both gold(I) and gold(III) catalysts, in this area, will come a greater understanding of the reactivity modes of the metal centres and aptitude for catalyst design and application.

Chapter Two: Gold(I) C–H Activation of Arenes[i]

2.1 Introduction

Recent years have seen gold catalysis take great strides in the area of C–H functionalisation, as summarised in the previous chapter. Embarking on this project, we sought to develop a novel procedure for aryl C–H functionalisation, specifically aiming to construct biaryl species, in-keeping with previous work in the group (scheme 60).[79]

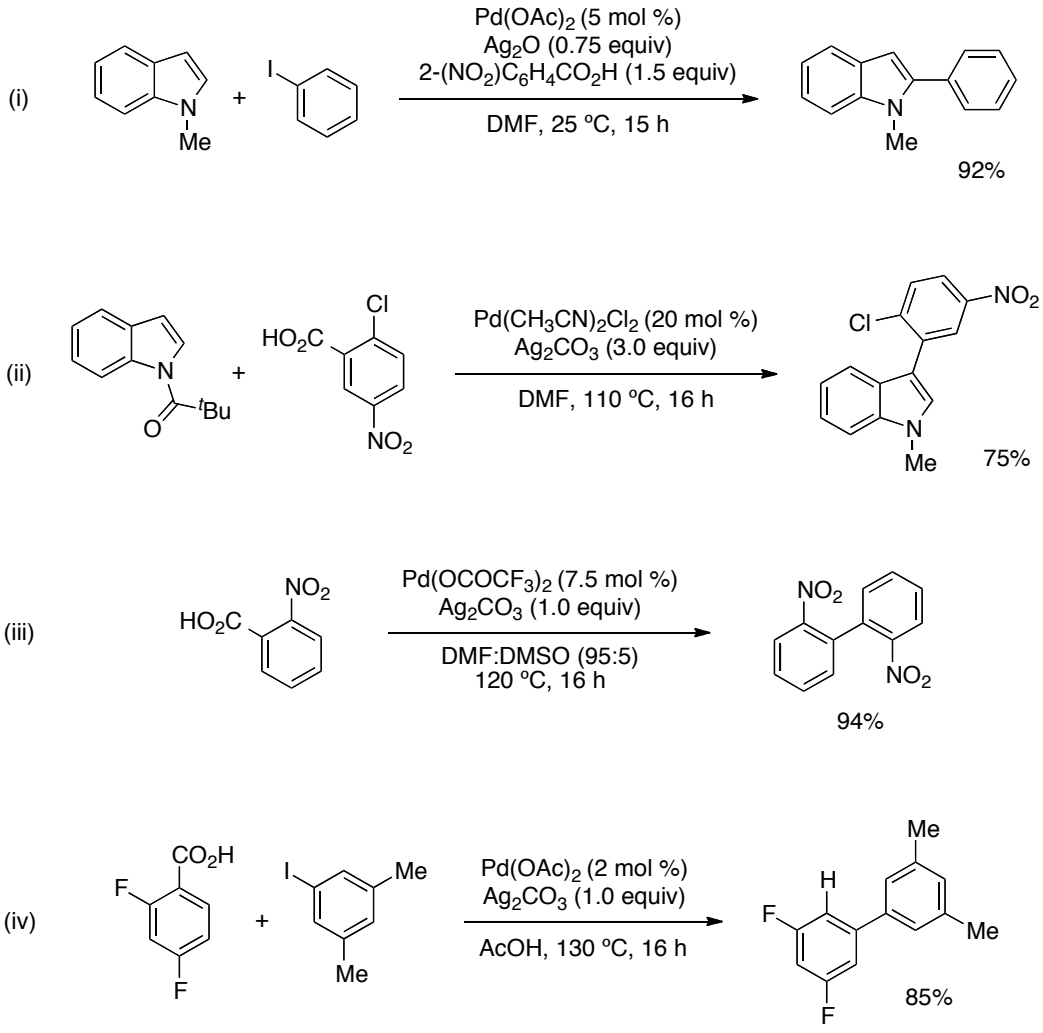

Scheme 60. Examples of protocols developed in the group for the formation of biaryl species.

[i] This project was conducted in collaboration with Dr Pengfei Lu, although his contributions will not be discussed. See reference 41 for complete details of the project.

With the exception of the highly nucleophilic indole, these processes all require harsh conditions, demanding the use of high temperatures and long reaction times. We aimed to develop milder C–H arylation methodologies and in order to achieve this we sought to employ the potent reactivity of gold salts. As discussed in chapter one, the ability of gold(III) to perform aromatic C–H activation, under remarkably mild reaction conditions, was well established. On the other hand, the same process for gold(I) salts was not known.[80] We decided to investigate this potential new mode of reactivity for gold(I), hoping to harness it in a mild C–H arylation process. As gold-mediated aryl C–H activation was fast becoming a cornerstone of many transformations, it was invariably achieved with gold(III) salts. Although the use of gold(I) was also known for the functionalisation of arenes, any intermediate aryl gold(I) species were not the result of a C–H activation step (scheme 61). Instead they were constructed via transmetallation from the corresponding lithium, magnesium or boronic acid species.[81, 52(a), 82] So despite the great stability and synthetic utility of these aryl gold(I) species, the poor step and atom economy associated with their construction meant that they were rarely employed.

Gold(III) aryl C–H activation is generally believed to proceed via electrophilic aromatic substitution, a process seemingly precluded for the lower oxidation state gold(I). We therefore decided to investigate the potential of gold(I) salts towards the C–H activation of arenes as the first stage of the overall project.

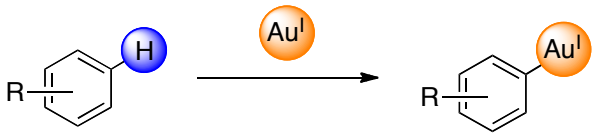

Scheme 61. General scheme for the desired aryl C–H activation with gold(I).

The aim of this investigation was to devise and optimise a gold(I) C_{sp2}–H activation procedure, specifically aimed at aryl C–H activation. Successful development of such a process would provide a novel route to the construction of aryl gold(I) species, with greater step and atom economy than those previously

reported. It would also, whether successful or not, allow us an insight to the viability of a gold(I) mediated aryl C–H functionalisation process.

2.2 Optimisation of the reaction conditions

Our initial efforts were focused towards screening a range of arenes against C–H activation with gold(I) salts. The general experiment design took literature procedures, as discussed in chapter one, into account. With this in mind, the use of silver salts was deemed necessary for halide abstraction and consequent generation of a more active cationic gold(I) species. As the aim of the reaction is to achieve a C–H bond cleavage, with concurrent C–Au bond formation, the inclusion of a base was also deemed necessary. A number of arenes were screened against variations on these conditions, with the use of $AgSbF_6$ and DBU leading to our first success. We were delighted to observe that when the electron-deficient 1,3,5-trifluorobenzene was submitted to C–H activation with $ClAuP^tBu_3$ the corresponding aryl gold(I) species was generated in 60% yield (entry 1, table 1). We then took this substrate forward to the optimisation of our reaction conditions, as outlined in table 1.

Taking these initially successful reaction conditions forward, we established that no product was generated in the absence of a silver source (entry 2), presumably a consequence of the lack of a halide abstracting species. The use of caesium pivalate as the base led to an increase in yield to 64% (entry 3). We were disappointed to note that the use of Na_2CO_3 and pivalic acid led to a substantially lower yield of 15% (entry 4), however K_2CO_3 and pivalic acid were a far more successful combination and generated the product in 89% yield (entry 5). Substituting $AgSbF_6$ for the basic Ag_2O, in the presence of pivalic acid but absence of an additional base, led to a decrease in yield (entry 6). Finally, the use of Ag_2O along with the combination of K_2CO_3 and pivalic acid, led to 100% product formation.

A survey of solvents revealed that the apolar DCE led to a poor yield of 5% (entry 7). Although the use of other polar solvents, such as DMA and THF, did lead to generation of the desired product in good yields (entries 9 and 10) none were a match for the 100% yield obtained in DMF.

Table 1. Optimisation of the gold(I) C–H activation of 1,3,5-trifluorobenzene.

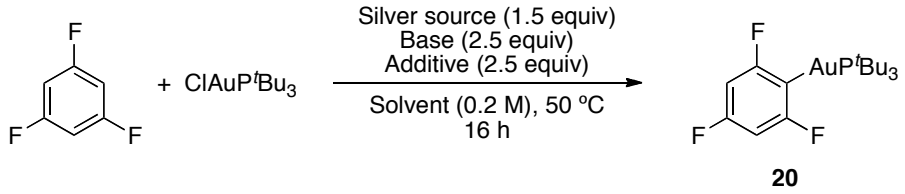

20

Entry	Silver source	Base	Additive	Solvent	Yield (%)[a]
1	$AgSbF_6$	DBU	-	DMF	60
2	-	DBU	-	DMF	0
3	$AgSbF_6$	CsOPiv	-	DMF	64
4	$AgSbF_6$	Na_2CO_3	PivOH	DMF	15
5	$AgSbF_6$	K_2CO_3	PivOH	DMF	89
6[b]	Ag_2O	-	PivOH	DMF	37
7[c]	Ag_2O	K_2CO_3	PivOH	DMF	100
8	Ag_2O	K_2CO_3	PivOH	DCE	5
9	Ag_2O	K_2CO_3	PivOH	DMA	78
10	Ag_2O	K_2CO_3	PivOH	THF	58

All reactions used 4.5 equivalents of 1,3,5-trifluorobenzene and 1.0 equivalent of ClAuP^{t}Bu$_3$. [a] Yields were determined by ^{1}H NMR spectroscopy, using an internal standard. [b] 1.25 equivalents of Ag_2O. [c] 0.75 equivalents Ag_2O and 1.75 equivalents of K_2CO_3.

Throughout the screening and optimisation processes, all of the reactions had been stirred at 50 ºC for 16 hours. An investigation into the reaction time revealed that the C–H activation of this substrate reached completion after only 2 hours (entry 2, table 2). Further decreasing the reaction time, to 1 hour, led to a decreased although still excellent yield of 92% (entry 3). The 82% product yield after 30 minutes (entry 4) demonstrates how fast this reaction is. This is further highlighted by the 5 minute reaction (entry 5), which shows that the product is generated in 10% yield even after this very short time. A 5 minute reaction was also conducted with a pre-mixing of all other reagents, in order to allow formation of any active gold species, prior to addition of the 1,3,5-

trifluorobenzene. In this case the product yield was slightly increased to 16% (entry 6), suggesting that there may be a small induction period in the reaction. This would account for the reactions of the silver salt, base and pivalic acid with the gold(I) species.

Table 2. Optimisation of the gold(I) C–H activation of 1,3,5-trifluorobenzene.

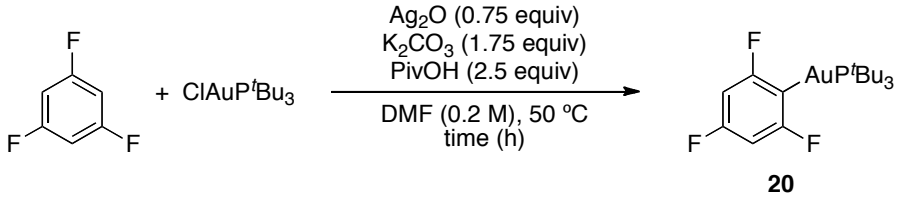

20

Entry	Reaction Time	Yield (%)[a]
1	16 hour	100
2	2 hour	100
3	1 hour	92
4	30 mins	82
5	5 mins	10
6[b]	5 mins	16

All reactions used 4.5 equivalents of 1,3,5-trifluorobenzene and 1.0 equivalent of ClAuP^{t}Bu$_3$. [a] Yields were determined by ^{1}H NMR spectroscopy, using an internal standard. [b] 1,3,5-trifluorobenzene was added after stirring all other reagents for 10 minutes.

Although we were delighted with the mild reaction temperature of 50 ºC, we also performed this C–H activation reaction at room temperature (scheme 62). The reaction time for this reduced temperature was 16 hours, as we anticipated that the reaction would likely be slower.

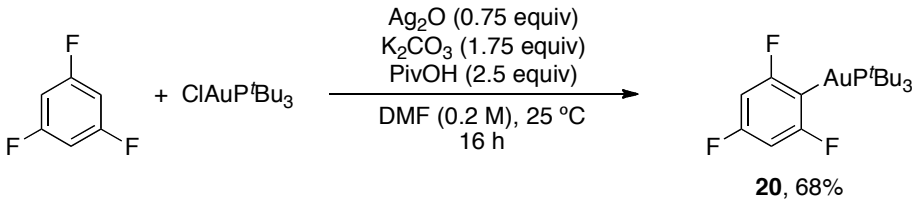

Scheme 62. General scheme for the desired aryl C–H activation with gold(I).

After these 16 hours, the desired product was generated in 68% yield. Although we were very happy to note that this reaction does work at room temperature, it was also apparent that the reaction was considerably slower under these conditions. We therefore decided to continue operating at the original temperature of 50 ºC.

We were, of course, conscious that developing a gold(I) C–H activation procedure employing an excess of silver would inevitably prompt questions about the role that this silver is playing. Our initial use of this second coinage metal was with the intention that it would act as a halide abstractor, removing a chloride from the gold(I) salt, to generate an active, cationic gold(I) species. Whilst our strategy did indeed allow us to access the desired aryl gold(I) product, in order to confirm that this auration is achieved *via* gold(I) C–H activation, we must also assess the possibility that the excess silver may be responsible for the C–H activation with subsequent transmetallation leading to our product. We therefore conducted a number of reactions with a reduced quantity of silver (table 3). Working on the assumption that one equivalent of the silver, in our standard reaction mixture, is very quickly consumed in the abstraction of a chloride anion from the gold salt, we selected to use 0.9 equivalents of silver. Under these conditions all of the silver would be consumed in halide abstraction and leave no surplus to perform a C–H activation.

Table 3. Optimisation of the gold(I) C–H activation of 1,3,5-trifluorobenzene.

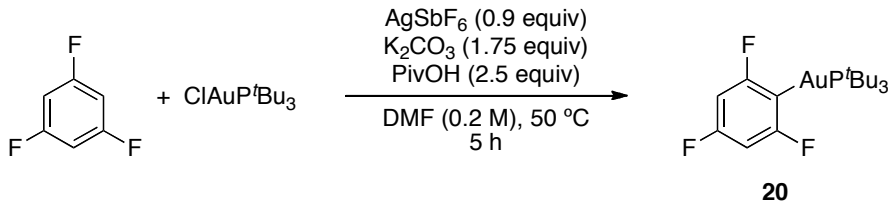

20

Entry	$AgSbF_6$	K_2CO_3	PivOH	Yield (%)[a]
1 [b]	0.9 equiv	1.75 equiv	2.5 equiv	20
2	0.9 equiv	1.75 equiv	2.5 equiv	50
3	0.9 equiv	2.5 equiv	2.5 equiv	98

All reactions used 4.5 equivalents of 1,3,5-trifluorobenzene and 1.0 equivalent of ClAuP^{t}Bu$_3$. [a] Yields were determined by ^{1}H NMR spectroscopy, using an internal standard. [b] The ClAuP^{t}Bu$_3$ and $AgSbF_6$ were mixed in DMF at 50 ºC for 30 minutes, before filtration into a solution of the remaining reagents.

Our first approach was to perform a reaction in which the gold salt and silver were mixed for 30 minutes, in order to generate the desired active cationic gold species, before being filtered into a solution of the remaining reagents (entry 1, table 3). Although this reaction led to a yield of only 20%, the fact that any product was formed at all was still encouraging. It is likely that some of the gold(I) species was lost in filtration, contributing to the decreased yield. The filtration process also resulted in greater dilution of the reaction, which would undoubtedly lead to a slower reaction and less overall product formation. Mixing all reagents, with the reduced quantity of silver under otherwise standard reaction conditions, led to 50% product formation (entry 2). Again, formation of the desired product is encouraging although it is still somewhat lower than we would have hoped. As the optimised reaction conditions employ silver in the form of silver(I) oxide, a base, this decreased yield may be due to a reduction in the basic species present in the reaction mixture. In the next reaction, the absence of basic silver oxide was compensated by an increase in the amount of potassium carbonate (entry 3). In this case the product was observed in 98% yield. The results of these reactions, even those leading to lower product yield, appear to

suggest that it is indeed gold(I), not silver(I), that is responsible for the C–H activation.

Also noteworthy, is that during optimisation all reactions were conducted under an atmosphere of nitrogen. Subsequent investigation revealed that this was not necessary and that conducting the reactions under air has absolutely no detrimental effect on product formation. This consideration adds to operational simplicity of the procedure, which along with the mild reaction conditions and excellent product yield, make this an attractive method for the generation of an aryl gold(I) species.

2.3 Scope of the reaction

Using our optimised reaction conditions, we set out to explore the scope of this C–H activation procedure with $ClAuP^tBu_3$. The results are shown below in scheme 63.

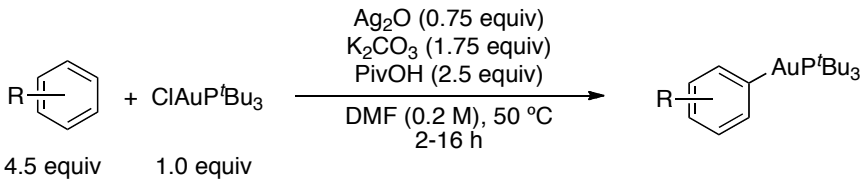

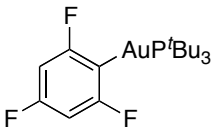

20, 100%[a]

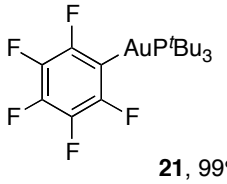

21, 99%[a]

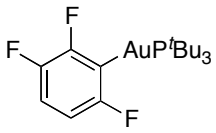

22, 99%[a]

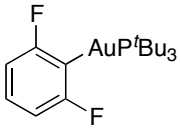

23, 83%[b]

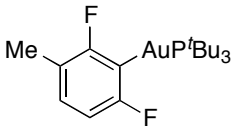

24, 63%[b]

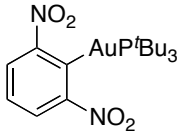

25, 83%[b]

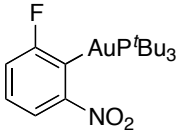

26, 99%[b]

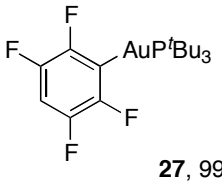

27, 99%[b]

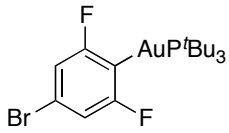

28, 83%[b]

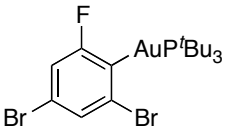

29, 99%[b]

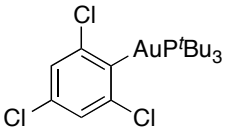

30, 63%[b]

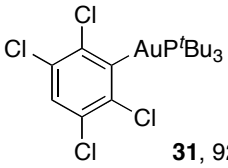

31, 92%[b]

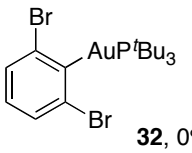

32, 0%[b]

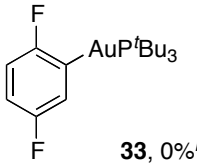

33, 0%[b]

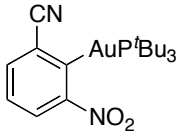

34, 0%[b]

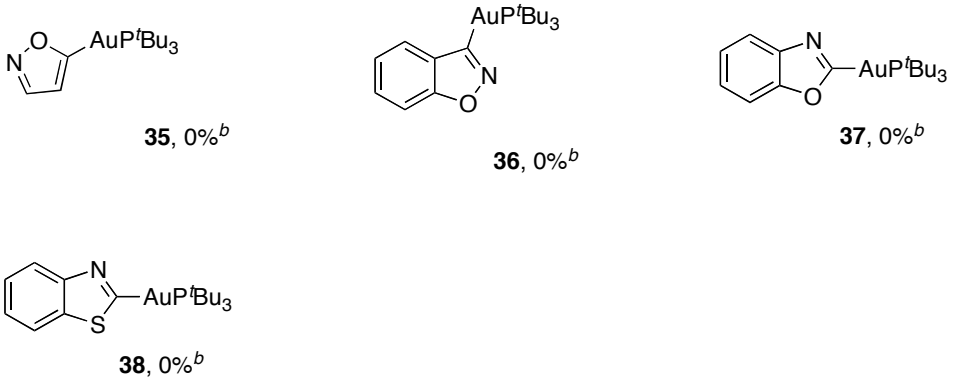

Scheme 63. Scope of the C–H activation with ClAuP^{t}Bu$_3$. All yields are of isolated pure material. ^{a} 2 hour reaction time. ^{b} 16 hour reaction time.

A number of electron-deficient arenes underwent successful C–H activation, generating the corresponding aryl gold(I) products **21-31** in good to excellent yields. Having optimised the reaction conditions with 1,3,5-trifluorobenzene, it became apparent that perfluorinated arenes are highly amenable to this auration, generating products **20**, **21**, **22**, **23** and **27** in excellent yields. The C–H activation is less successful with slightly more electron-rich arenes, as demonstrated by the lower yield of product **24**. This unambiguous preference of gold(I) for the activation of electron-deficient arenes is in complete contrast to that of gold(III) for electron-rich arenes.

The successful application of 1,3-dinitrobenzene, 1,3,5-trichlorobenzene and 1,2,4,5-tetrachlorobenzene, to our reaction conditions, led to the generation of aryl gold(I) products **25**, **30** and **31** and demonstrated that this auration is not limited to fluorinated arenes.

Also noteworthy, is the formation of products **28** and **29** containing an untouched bromine substituent. This would not be possible in the presence of metals, such as palladium or copper, which are prone to oxidative addition. The maintenance of such a reactive handle offers the prospect of further transformations.

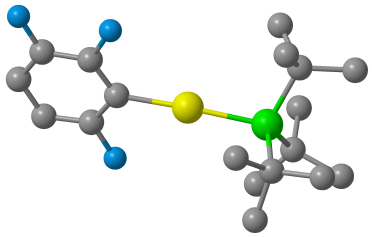

Figure 3. Structure of **22** as determined by X-ray crystallography. This structure highlights the requirement of two electron-withdrawing substituents *ortho*- to the site of activation.

These aurations exhibit extremely high regioselectivity, with the gold(I) salt invariably activating the most electron-deficient C–H bond. With the structure of a number of these aryl gold(I) products confirmed by X-ray crystallography, it is also apparent that the site of activation must possess two *ortho*- electron-withdrawing groups (figure 3). This is further exemplified by the lack of product **33**, which does not offer such a position and product **32**, in which the position between the two bromine substituents is inaccessible due to sterics. Formation of product **34** is also not possible, under these conditions, possibly as a result of slightly increased pK_a at the position between the two electron-withdrawing substituents. The lack of products **35-38** highlights a further limitation of this procedure, with the corresponding heteroarenes apparently unable to undergo auration under these reaction conditions. It is also possible that the lack of *ortho*-substituents, in products **35-38**, results in a C–Au(I) bond which is unstable in the reaction medium.

The C–H activation is also compatible with a number of ligands on the gold(I) salt (scheme 64). For the phosphine ligands, it is evident that higher product yields are obtained when more strongly σ-donating species are appended to the gold(I) centre. A corresponding drop in yields is observed with stronger π-acceptors, with triphenylphosphite gold(I) chloride leading to only 37% yield of the corresponding aryl gold(I) product **42**. The cone angle of the phosphine ligands does not appear to have any impact on the success of the auration reaction. This is very well exemplified by the comparable yields of products **20**

and **39**, incorporating tri-*tert*-butylphosphine (cone angle 182º) and triethylphosphine (cone angle 132º), respectively.[83] The electron-donating N-heterocyclic carbene IPr was also employed as a ligand for gold(I), generating product **40** in excellent yield.

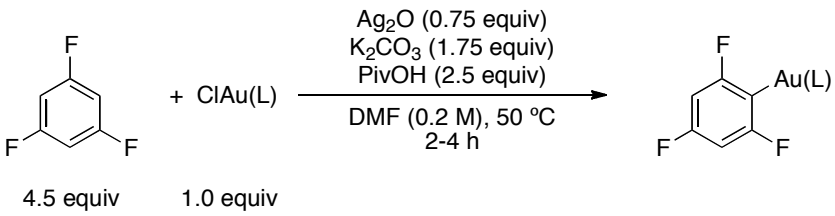

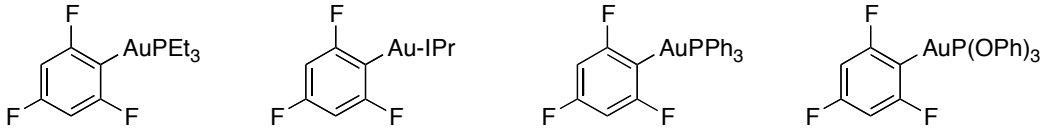

Scheme 64. Scope of the C–H activation with different ligands on the gold(I) salt. Yields are of isolated pure material. The yield of **42** was determined by ^{1}H NMR analysis with the use of an internal standard. [a] 2 hour reaction time. [b] 4 hour reaction time.

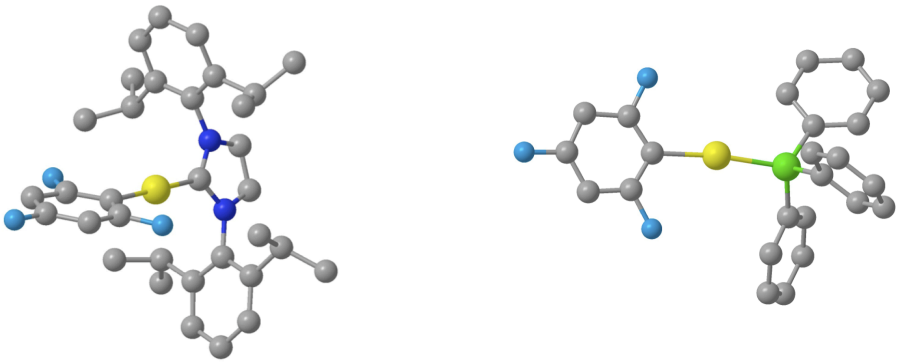

Figure 4. Structures of **40** (left) and **41** (right) as determined by X-ray crystallography.

With the exception of triphenylphosphitegold(I) chloride, all of these gold(I) salts lead to high yields of their corresponding aryl gold(I) products. The lowest yielding of these salts is triphenylphosphinegold(I) chloride, which still led to the formation of product **41** in 88% yield. This salt may be applied to the C–H activation of a number of arenes, as shown is scheme 65, generating aryl gold(I) products **43**-**47** in excellent yields.

Although slightly lower than their tri-*tert*-butylphosphine counterparts, products **43**-**47** were all generated and isolated in excellent yields. This, along with the great operational simplicity and step economy of the process, highlights the advantages of using this C–H activation procedure for the generation of aryl gold(I) species.

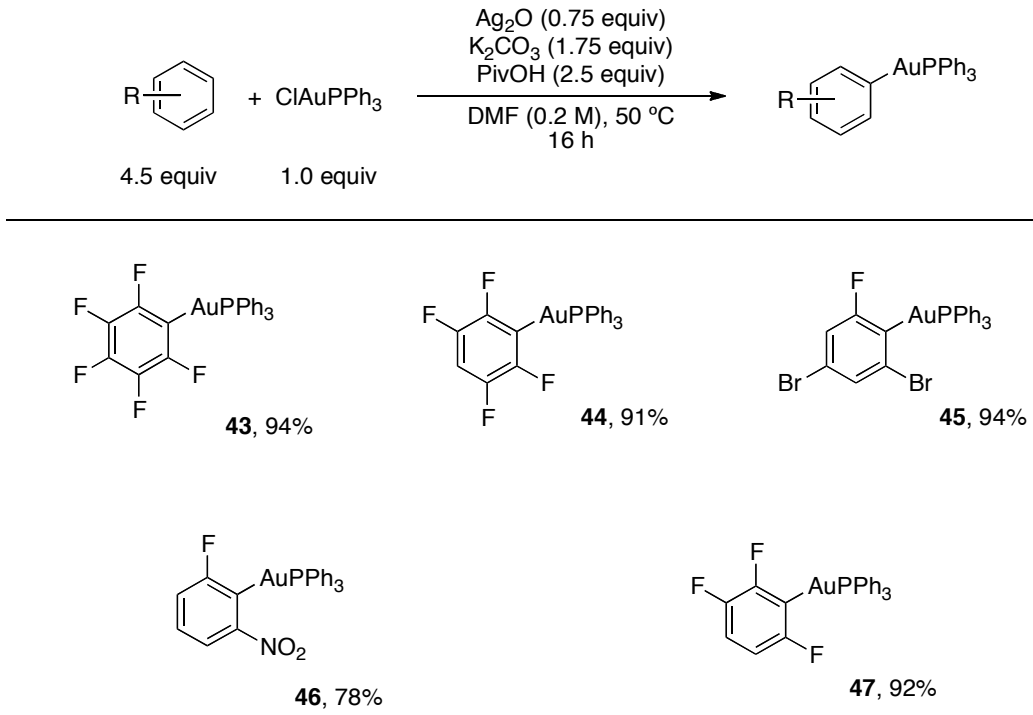

Scheme 65. Scope of the C–H activation with $ClAuPPh_3$. Yields are of isolated pure material.

2.4 Mechanistic proposal

We next set out to explore the mechanism of this procedure. Having conducted the optimisation and explored the scope of the auration, we were delighted to have gained a new route to access a number of aryl gold(I) species. However, our initial ambition was to investigate the potential of this C–H activation in order to employ it in a procedure to achieve the overall C–H functionalisation of our starting arene. With this in mind, gaining greater insight into how this auration takes place would offer a distinct advantage in the design of any such procedure.

The required use of silver in our procedure prompted us to investigate the potential that it may be the silver(I), and not the gold(I), species that is responsible for the C–H activation. After the use of substoichiometric quantities of silver (see optimisation), it was determined that it was indeed the gold(I) species undertaking the C–H activation.

Our next step was to determine a kinetic isotope effect of this C–H activation process. We conducted this experiment with 1,3-dinitrobenzene and 1,3-dinitrobenzene-d_4 (scheme 66). The ratio of products **25**:**25-d$_3$** was determined, by mass spectrometric analysis, to be 100:20. Giving a high primary kinetic isotope effect of 5.0 (k_H/k_D = 100/20 = 5.0), indicating that the C–H bond breaking is involved in the rate-determining step of the auration reaction.

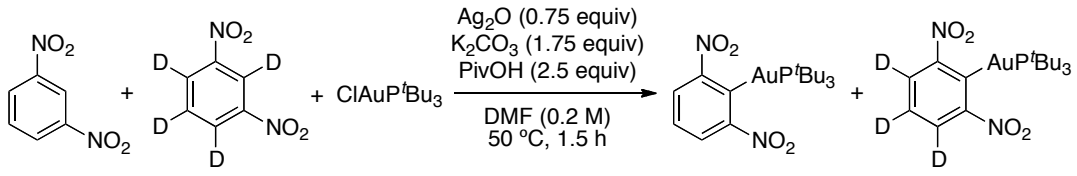

Scheme 66. Kinetic isotope effect experiment using 1,3-dinitrobenzene and it's deuterated counterpart. The ratio of products **25**:**25-d$_3$** was 100:20, as determined by mass spectrometry.

A more detailed investigation into the reagents employed under the optimised reaction conditions (table 4) was conducted. The aim was to determine which

reagents were most crucial to the performance of the reaction and thereby gain a greater understanding of the role that each species plays in the auration.

Table 4. Standard conditions for the gold(I) C–H activation of 1,3,5-trifluorobenzene and variations.

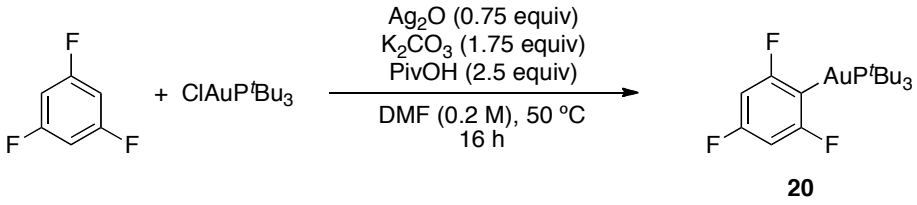

20

Entry	Ag_2O	K_2CO_3	PivOH	Yield (%)[a]
1	0.75 equiv	1.75 equiv	2.5 equiv	100
2	2.0 equiv	-	2.5 equiv	62
3	-	1.75 equiv	-	0
4	0.75 equiv	-	-	73

All reactions used 4.5 equivalents of 1,3,5-trifluorobenzene and 1.0 equivalent of ClAuP^{t}Bu$_3$. [a] Yields were determined by ^{1}H NMR spectroscopy, using an internal standard.

Our standard reaction conditions lead to the generation of the desired product **20** in 100% yield (entry 1, table 4). The exclusion of potassium carbonate (with increase in the amount of silver oxide to compensate for the increased acidity of the reaction mixture) had a detrimental effect on the reaction, with a drop in yield to 62% (entry 2). On the other hand, the use of potassium carbonate alone was not able to facilitate the reaction, no product was generated in the absence of silver oxide and pivalic acid (entry 3). This result was entirely expected, as in the absence of a silver species there would be no halide abstractor to generate the active gold(I) species. The reaction with only silver oxide led to formation of the product in 73% (entry 4), demonstrating that this basic silver species is able to promote this auration in the absence of potassium carbonate and pivalic acid, albeit with a lower yield.

This brief investigation appears to demonstrate that each of these reagents is necessary and important to the overall success of the reaction. Clearly each reagent plays a pertinent role in this reaction, although the more specific details are yet to be elucidated. That the desired product is formed, to some extent, in the absence of one or more of these species may be a result of a differing route being taken in these cases rather than their lack of value.

A potential drawback of using the gold(I) chloride salt, as the starting source of gold, is that halide abstraction (or the lack thereof) may interfere with determining how necessary each reagent is to the success of the C–H activation. Based on the reagents in our reaction mixture, we hypothesised that our active gold(I) species may likely be a gold(I) pivalate. ^{31}P NMR analysis of the reaction mixture, in the absence of an arene, showed that a species with a shift of 85 ppm was generated. NMR analysis of gold(I) pivalate showed the same signal to be present, appearing to confirm that this is the gold(I) species generated after halide abstraction. Whether this is the species that is then responsible for the C–H activation, either alone or in the presence of other reagents, was the aim of our next investigation (table 5).

The *in situ* formation of a gold(I) pivalate species suggests that a concerted metalation deprotonation (CMD) pathway, as previously proposed for palladium(II)-mediated processes, may be in place.[84] Such a pathway would proceed through a six-membered transition state, in which the coordinated pivalate ligand acting as a base, to abstract the aryl proton, with concurrent formation of the carbon–gold(I) bond (scheme 67). This mechanism would also be consistent with the observed high primary kinetic isotope effect.

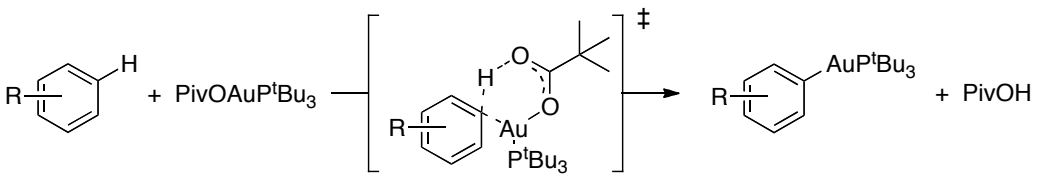

Scheme 67. Concerted metalation deprotonation pathway proceeding via a six-membered transition state to generate an aryl gold(I) product.

With the aim of verifying whether our auration is indeed proceeding through a CMD mechanism, we submitted tri-*tert*-butylphosphinegold(I) pivalate to the C–H activation of 1,3,5-trifluorobenzene in DMF at 50 ºC for 16 hours. Disappointingly, the desired product **20** was not observed under these conditions (entry 1, table 5). This clearly indicates that the reaction mechanism is more complex than the interaction between the gold(I) pivalate and arene alone.

The addition of 1.75 equivalents of potassium carbonate led to the formation of the desired product in a very low yield of 7% (entry 2). Considering that this addition of a base led to promotion of the reaction, it is perhaps not surprising that no product is observed in the presence of both potassium carbonate and pivalic acid (entry 3). Also unsurprisingly, addition of all reagents required under the optimised conditions led to 100% yield of product **20** (entry 4). Our use of gold(I) pivalate, rather than gold(I) chloride, was intended to negate the use of a silver source and so the use of silver oxide should no longer be essential to reaction success. A substantial decrease in the amount of silver oxide resulted in a relatively minor drop in product yield to 76% (entry 5). This appears to confirm that, although the inclusion of silver oxide is undeniably leading to increased product yield, it is no longer crucial as a source of silver. It is perhaps the basicity of this silver species, which is having a beneficial effect on product formation.

With this in mind, we next assessed the effect of basic sources of silver on the progress of the reaction. The addition of silver pivalate alone was enough to facilitate the formation of product **20** in 34% yield (entry 6). Silver oxide was also able to promote the C–H activation alone, with 0.75 equivalents leading to 30% yield (entry 7) and 2.0 equivalents giving 64% of product **20** (entry 8). In comparison, use of the non-basic silver hexafluoroantimonate was not able to promote the auration to any significant degree, with 1.0 equivalent leading to only 4% product (entry 9) and 0.25 equivalents not leading to the generation of any product at all (entry 10). These results confirm that it is indeed the basicity of these silver species that is crucial to their successful mediation of the C–H activation.

Table 5. Standard conditions for the gold(I) C–H activation of 1,3,5-trifluorobenzene and variations.

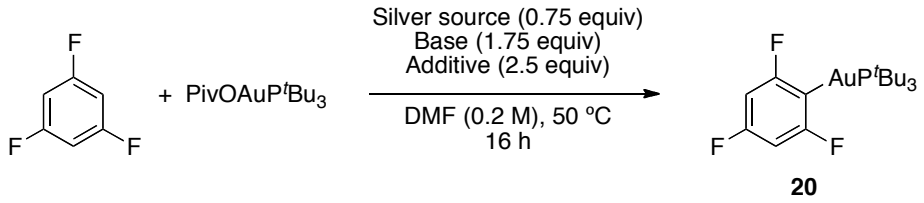

20

Entry	Silver source	Base	Additive	Yield (%)[a]
1	-	-	-	0
2	-	K_2CO_3	-	7
3	-	K_2CO_3	PivOH	0
4	Ag_2O	K_2CO_3	PivOH	100
5[b]	Ag_2O	K_2CO_3	PivOH	76
6[c]	AgOPiv	-	-	34
7	Ag_2O	-	-	30
8[d]	Ag_2O	-	-	64
9[e]	$AgSbF_6$	-	-	4
10[f]	$AgSbF_6$	-	-	0
11	Ag_2O	-	PivOH	64
12	Ag_2O	K_2CO_3	-	98
13[g]	Ag_2CO_3	-	-	100
14[h]	Ag_2CO_3	-	-	100
15[i]	Ag_2CO_3	-	-	100
16[j]	Ag_2CO_3	K_2CO_3	-	100
17[k]	-	Cs_2CO_3	-	80

All reactions used 4.5 equivalents of 1,3,5-trifluorobenzene and 1.0 equivalent of ClAuP^{t}Bu$_3$. Unless otherwise stated, reactions used 0.75 equivalents silver source, 1.75 equivalents base and 2.5 equivalents acid. [a] Yields were determined by ^{1}H NMR spectroscopy, using an internal standard. [b] 0.1 equivalents silver oxide. [c] 1.0 equivalents AgOPiv. [d] 2.0 equivalents of Ag_2O. [e] 1.0 equivalent $AgSbF_6$. [f] 0.25 equivalents $AgSbF_6$. [g] 2.0 equivalents of Ag_2CO_3. [h] 1.0 equivalent of Ag_2CO_3. [i] 0.5 equivalents of Ag_2CO_3. [j] 0.25 equivalents of Ag_2CO_3 and 1.0 equivalent K_2CO_3. [k] 1.0 equivalent of Cs_2CO_3.

The use of silver oxide with pivalic acid, presumably leading to the *in situ* formation of silver pivalate, was able to promote the reaction and led to 64% product yield (entry 11). However, it would seem apparent that the role of pivalic acid in this auration lies in the generation of the gold(I) pivalate species. Indeed, in the absence of pivalic acid the desired product **20** is observed in an excellent yield of 98% (entry 12). Given that neither the silver oxide or potassium carbonate are able to mediate the reaction this successfully individually, it seemed possible that the *in situ* formation of silver carbonate was taking place and that it was this species responsible. Indeed, to our delight, the use of silver carbonate led to the quantitative product yields that we were generating under our standard conditions (entries 13, 14 and 15).

Bearing in mind that under our standard reaction conditions we assume that one whole equivalent of silver (out of the 1.5 available) is used to abstract the chloride from the initial gold(I) species, it seemed logical that the reaction should also work with lower equivalents of silver, perhaps in conjunction with potassium carbonate. We were pleased to observe that this was the case, with 0.25 equivalents of silver carbonate and 1.0 equivalent of potassium carbonate leading to 100% product yield (entry 16). Aiming to determine whether alternative carbonates were also able to facilitate the auration, we also tested the use of caesium carbonate, which led to 80% of the desired product (entry 17). Indicating that alternative carbonates are able to mediate the reaction, although with less success than silver carbonate.

Having established that our C–H activation conditions lead to the *in situ* formation of gold(I) pivalate. That this gold pivalate is not capable of performing the auration of 1,3,5-trifluorobenzene independently but that the addition of silver carbonate (another species likely formed *in situ*) is sufficient to promote the reaction to 100% product formation. We considered the possibility that the reaction is an equilibrium (scheme 68).

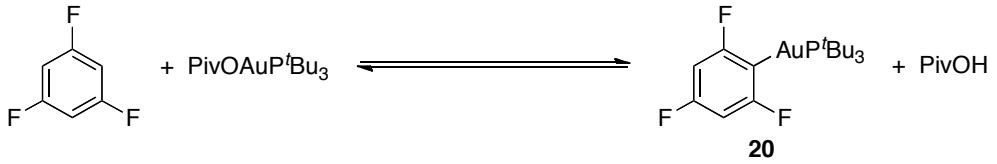

Scheme 68. Potential equilibrium of our C–H activation reaction.

In such a case, the additional basic species would be necessary for consumption of the pivalic acid, thus driving the reaction towards formation of the desired product. However, we would expect that combination of the gold(I) pivalate and arene would lead to some formation of the desired product, even in the absence of an additional base. Aiming to investigate the reverse reaction, we combined aryl gold(I) product **20** and pivalic acid in DMF (table 6).

Table 6. Standard conditions for the gold(I) C–H activation of 1,3,5-trifluorobenzene and variations.

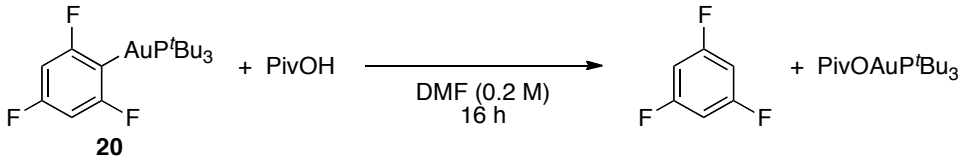

Entry	Temperature (ºC)	Result[a]
1	50	95% aryl gold(I) **20** and 5% gold(I) pivalate
2	70	83% aryl gold(I) **20** and 17% gold(I) pivalate

All reactions used 1.0 equivalent of aryl gold(I) species **20** and 2.0 equivalents of pivalic acid. [a] Results determined by ^{31}P NMR analysis.

After 16 hours at 50 ºC the major species in solution was still the aryl gold(I) species **20**, with only 5% generation of gold(I) pivalate (entry 1, table 6). Increasing the temperature to 70 ºC led to an increase in the formation of gold(I)

pivalate to 17%, however the major species in solution is still the aryl gold(I) compound **20**. These results, along with previous observations, appear to discount the proposal that the C–H activation is an equilibrium.

These results do not support our initial proposal of a concerted metalation deprotonation pathway, which proceeds with the intramolecular assistance of a coordinated pivalate ligand, through a six-membered transition state (scheme 69). We also do not appear to be able to rationalise the requirement for additional base being the result of an equilibrium. We must therefore deduce that the proton abstraction is the result of intermolecular carbonate assistance (scheme 69). Aryl deprotonation, by silver carbonate, occurs with concurrent formation of the gold(I)–carbon bond to generate the aryl gold(I) product, silver bicarbonate and silver pivalate. Of course, there are a number of basic species present in our reaction mixture, which have also shown their capability for facilitating this auration (table 5). It is therefore only logical to expect that this intermolecular proton abstraction may be performed by multiple species, rather than by silver carbonate exclusively.

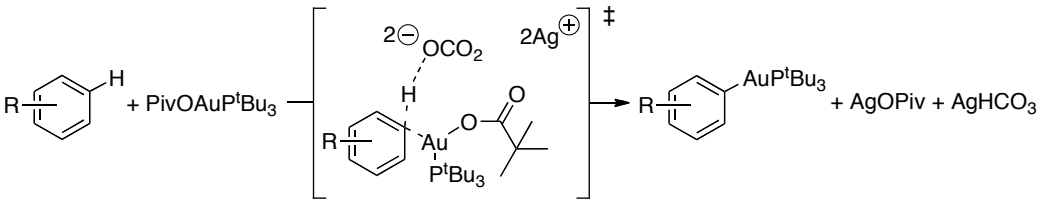

Scheme 69. Concerted metalation deprotonation pathway with silver carbonate performing the intermolecular proton abstraction.

This pathway would justify the required presence of an additional base and also account for the high primary kinetic isotope effect. However, we cannot exclude the potential that the deprotonation is facilitated by π-coordination of the gold(I) species (scheme 70).

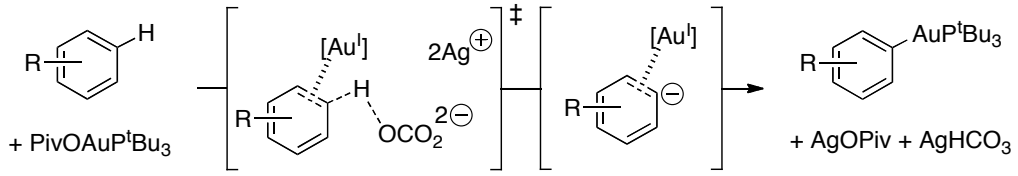

Scheme 70. Deprotonation aided by π-coordination of gold(I).

Our efforts to elucidate the mechanism of this C–H activation necessitated that we also consider alternatives to the CMD pathway. Given that at least two species are responsible for the deprotonation and auration of the starting arene (one being the gold(I) pivalate and the other most likely silver carbonate, likely in conjunction with additional basic species) an alternative mechanism could be envisaged (scheme 71). This route would entail initial deprotonation of the arene, by one of the basic species, to generate an anion. Subsequent interaction with the cationic gold(I), formed via halide abstraction by silver, would then lead to generation of the aryl gold(I) product.

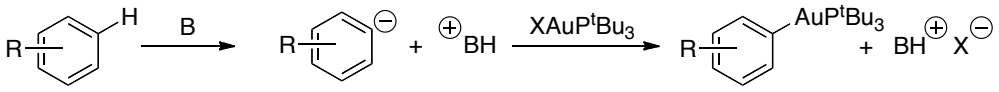

Scheme 71. Alternative reaction mechanism for the auration, based on deprotonation and subsequent interaction with gold(I).

An experiment in the absence of a gold(I) salt, but in the presence of D_2O, was conducted with 1,3-dinitrobenzene (scheme 72). After 16 hours, under otherwise standard C–H activation conditions, 30% of the deuterated arene was observed by ^{1}H NMR spectroscopy. This 30% compares to the 83% yield of aryl gold(I) product **25**. This reaction demonstrates that the species employed under our optimised reaction conditions, along with those generated *in situ*, are unable to deprotonate the starting arene to any significant degree. Certainly not to the extent that auration takes place in the presence of a gold(I) species.

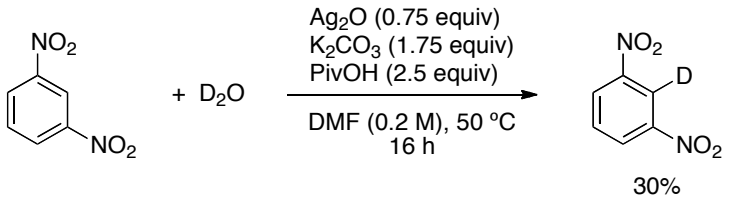

Scheme 72. Deuteration of 1,3-dinitrobenzene under our standard C–H activation conditions, in the absence of gold(I). This deuteration compares to 83% of product **25**. The reaction employed 100 equivalents of D_2O.

Taking these results into consideration, it seems implausible that our gold(I) C–H activation is proceeding through a pathway involving deprotonation before interaction with the gold(I) (scheme 71). In addition, our observation of such a high primary kinetic isotope effect is not in-keeping with such a mechanism.

Concurrent work by Nolan *et al.* led to the development of an alternative route to the construction of aryl gold(I) products. The authors detailed the synthesis of an *N*-heterocyclic carbene-bound gold(I) hydroxide from the corresponding gold(I) chloride (scheme 73).[42] The described procedure for the generation of gold(I) hydroxide **48** is operationally simple, with the authors noting that it may be performed under air using technical grade solvents. The use of inexpensive sodium or potassium hydroxides led to excellent yields of **48**, the structure of which was unequivocally confirmed by x-ray crystallography.

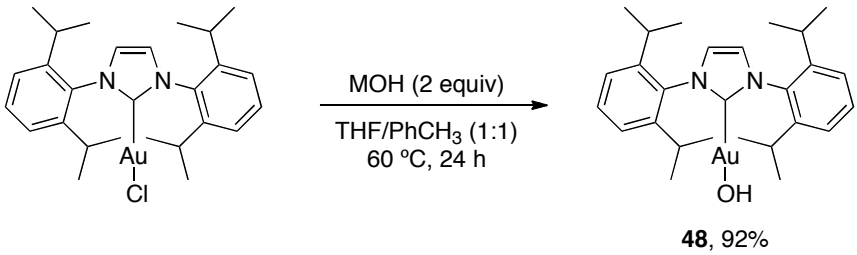

Scheme 73. Reaction of gold(I) chloride with metal hydroxide to generate gold(I) hydroxide **48**, where M = Na or K (both giving 92% yield of **48**).

Further investigation, by Nolan and Boogaerts, into the reactivity of this gold(I) hydroxide (**48**) led to the development of a procedure for the carboxylation of a number of electron-deficient (hetero)arenes.[43] The process employs gold(I) catalyst **48**, under very mild reaction conditions, to generate excellent yields of the arenes, carboxylated at the most acidic position.

A subsequent report from the Nolan group demonstrated the versatility of this gold(I) hydroxide, with its application to the decarboxylation of a number of aromatic carboxylic acids.[85] Under comparatively high reaction temperatures, hydroxide **48** promotes liberation of carbon dioxide with simultaneous formation of the corresponding aryl gold(I) species. The products are obtained in excellent yields, with auration invariably occurring at the site of decarboxylation.

However, it was the initial report into the formation gold hydroxide (**48**) that detailed its application to the C–H activation of tetra- and penta-fluorobenzene (scheme 74). The corresponding aryl gold(I) products are formed in excellent yields after 24 hours at 80 ºC. The obvious similarities between this system and our own prompted us to question whether our auration may also proceed via initial *in situ* formation of a gold(I) hydroxide. However, Nolan *et al.* comment that the C–H activation of 1,3,5-trifluorobenzene, under these conditions, was unsuccessful (scheme 75) and led only to isolation of unreacted gold(I) hydroxide.

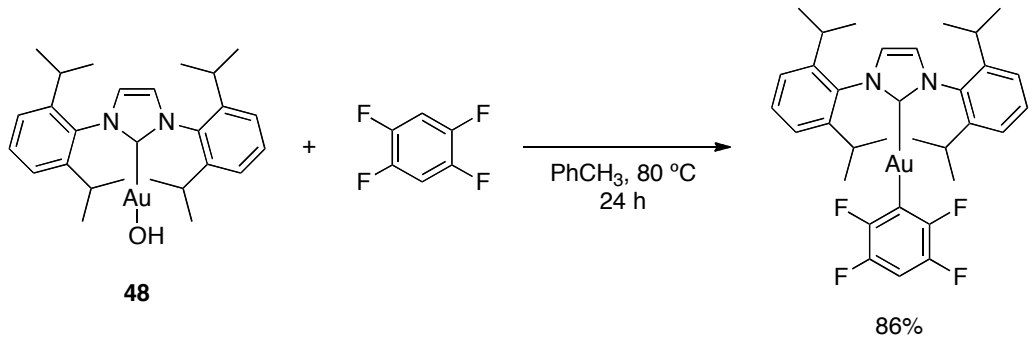

Scheme 74. Reaction of gold(I) hydroxide **48** with 1,2,4,5-tetrafluorobenzene to generate an aryl gold(I) product.

Nolan *et al.* note that this a consequence of the pK_a values involved, with gold(I) hydroxide **48** able to perform the auration of (hetero)arenes possessing a pK_a value lower than its own (p$K_{a\ DMSO}$ = 30.4). The auration of 1,3,5-trifluorobenzene, with a p$K_{a\ DMSO}$ of 31.5, is therefore not possible with this system.

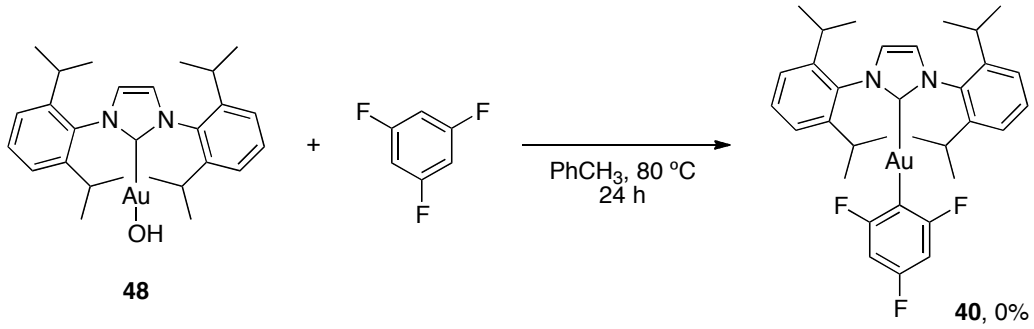

48 **40**, 0%

Scheme 75. Unsuccessful combination of gold(I) hydroxide **48** with 1,3,5-trifluorobenzene.

Under our conditions, the same *N*-heterocyclic carbene-bound gold(I) chloride may be submitted to the C–H activation of 1,3,5-trifluorobenzene and generate the corresponding product **40** in excellent yield. This observation led us to doubt that our C–H activation proceeds through a mechanism that involves the formation of a gold(I) hydroxide intermediate.

In summary, experimental observations suggest that out gold(I) C–H activation is proceeding via a concerted metalation deprotonation pathway, with intermolecular assistance from carbonate and pivalate bases in solution. This proposal is in-keeping with the high primary kinetic isotope effect of 5.0 and also the requirement for additional basic species, when gold(I) pivalate is pre-formed. However, we cannot preclude a pathway involving proton abstraction facilitated by π-coordination of gold(I).

2.5 Development of a silver-free C–H activation protocol

Our gold(I) C–H activation procedure allows us to access a number of aryl gold(I) species in excellent yield, with significantly increased step economy over previous methods for their construction. The great operational simplicity and mild reaction conditions make this an attractive route to these compounds, which may then be applied to further transformations. The reagents necessary to facilitate this auration are each inexpensive and readily available, with their roles explored as part of our mechanistic investigation.

However, the evident affinity of gold(I) for electron-deficient arenes offered the prospect to further simplify this procedure. As demonstrated by Nolan *et al.*, application of a strong base to these arenes will result in loss of the most acidic proton. In the presence of cationic gold(I), a species isolobal with a proton, this will allow auration to occur in this position (scheme 76). We therefore conducted a brief investigation into the potential use of such comparably forcing conditions with $ClAuP^tBu_3$.

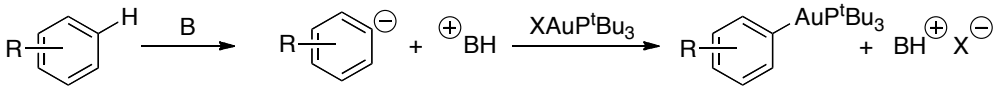

Scheme 76. Our envisaged application of a strong base to the deprotonation and subsequent auration of electron-poor arenes.

Part of our investigation into the mechanism of the gold(I) C–H activation procedure entailed conducting deuteration studies, in the absence of a source of gold. While those pertinent to the mechanistic discussion were mentioned in the previous section (scheme 74), a number of additional deuteration experiments were performed. Over the course of these reactions, it became apparent that high levels of deuteration could be achieved in the absence of silver (table 7). As expected, strong bases were sufficient to achieve loss of the most acidic proton.

Table 7. Deuteration studies with 1,3-dinitrobenzene.

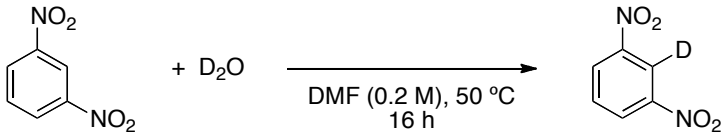

Entry	Ag_2O	MOH	K_2CO_3	PivOH	Yield (%)[a]
1	0.75 equiv	-	1.75 equiv	2.5 equiv	30
2	-	-	1.75 equiv	2.5 equiv	4
3	-	NaOH (2.0 equiv)	1.75 equiv	2.5 equiv	34
4	-	KOH (2.0 equiv)	1.75 equiv	2.5 equiv	40
5	-	NaOH (1.0 equiv)	1.75 equiv	-	92
6	-	NaOH (2.0 equiv)	1.75 equiv	-	94
7	-	NaOH (2.0 equiv)	-	-	96
8	-	KOH (2.0 equiv)	-	-	96

All reactions used 1.0 equivalent of 1,3-dinitrobenzene and 100 equivalents of D_2O. [a] Yields of deuterated products determined by ^1H NMR analysis, using an internal standard.

As mentioned previously, our standard C–H activation conditions, in the absence of gold(I), lead to 30% deuteration of 1,3-dinitrobenzene (entry 1, table 7). The exclusion of silver oxide leads to a decrease in deuteration, to 4% (entry 2), and substitution of either sodium or potassium hydroxide in its place raises deuteration to comparable levels (entries 3 and 4). In the absence of pivalic acid, we observe a substantial rise in deuteration (entries 5 and 6). The presence of 2.0 equivalents of either sodium or potassium hydroxide leads to 96% deuteration (entries 7 and 8). This near quantitative deuteration is compared to the 83% yield of aryl gold(I) product **25**, achieved under our C–H activation conditions. Our next step was to see whether these conditions for deuteration could be applied to an auration procedure (table 8).

Table 8. Silver-free auration of 1,3,5-trifluorobenzene.

20

Entry	Base	Yield (%)[a]
1	NaOH (4.0 equiv)	94
2	KOH (4.0 equiv)	92
3	KO^{t}Bu$_3$ (4.0 equiv)	100

All reactions used 1.0 equivalent of ClAuP^{t}Bu$_3$ and 4.5 equivalents of 1,3,5-trifluorobenzene. [a] Results determined by ^{1}H NMR analysis, using an internal standard.

Our initial concern was that halide abstraction would be less efficient in the absence of silver, with a detrimental impact on the auration reaction. However, the use of 4.0 equivalents of either sodium or potassium hydroxide led to excellent yields of the corresponding aryl gold(I) product (entries 1 and 2, table 8). The use of potassium *tert*-butoxide led to quantitative formation of the desired product (entry 3), now offering the same yield as our standard C–H activation procedure.

Having previously explored the scope of our C–H activation reaction, we did not conduct a similar exploration with this procedure. The similarity with the system developed by Nolan *et al.* made this largely redundant. We did however note that a few of the species that were either unsuccessful or low yielding under the previous system, generated higher yields of their corresponding aryl gold(I) products under these more forcing reaction conditions (scheme 77).

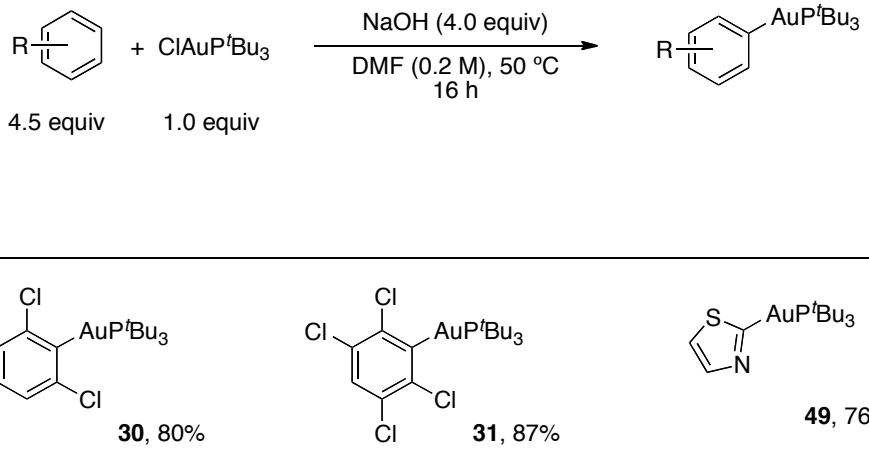

Scheme 77. Silver-free auration of electron-deficient arenes. All yields are of isolated pure material.

Under our standard C–H activation conditions, submission of 1,3,5-trichlorobenzene had led to 63% of the aryl gold(I) product **30**, whereas submission of the same arene to these more basic conditions led to 80% of product **30**. An even greater rise was observed for thiazole, which led to only 26% product under the previous conditions, but gave 76% of product **49** in the presence of sodium hydroxide.

Having believed that such alternative conditions were available, we were pleased to note that these basic species could indeed be employed to achieve the auration of electron-deficient arenes. The successful implementation of these conditions provides a more atom economical route to a number of aryl gold(I) species. The requirement of only NaOH, in place of Ag_2O, K_2CO_3 and PivOH, greatly reduces the cost of the auration reactions and also enhances their operational simplicity. Work is continuing in the group to determine the scope of arenes that are compatible with these basic conditions.

2.6 Conclusions

At the outset of this project, our aim was to establish the viability of an aryl C–H activation procedure with gold(I). The corresponding gold(III) process was developed over 80 years ago and has since found itself a foundation of a number of transformations, which cleverly exploit formation of the carbon–gold(III) bond to achieve further functionalisation. The remarkable reactivity of gold(I) and gold(III) towards C–H functionalisation has been demonstrated in a number of processes, we envisaged harnessing this reactivity to develop a mild gold(I) C–H activation procedure.

Our desire to achieve this transformation was fuelled not only by a desire to expand upon the known reactivity of gold(I) salts, but also to provide a novel route to the generation of aryl gold(I) species. Our preliminary investigations allowed us a glimpse of the potential reactivity of aryl gold(I) compounds, towards cross-coupling, in the presence of a palladium species (scheme C1). This experiment was only conducted on an NMR scale but highlighted the feasibility of transmetalation from gold(I) to palladium(II). An almost simultaneous report, by Hashmi *et al.*, had taken this preliminary study to its logical conclusion, demonstrating the successful application of aryl gold(I) species to a palladium-mediated cross-coupling, with aryl halides[52(a)].

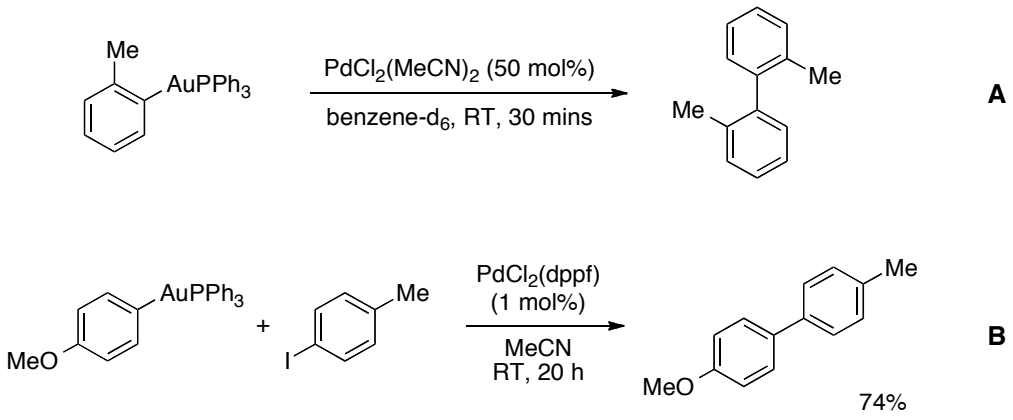

Scheme C1. Aryl gold(I) species employed with sources of palladium(II) to achieve biaryl formation. **A**: Our preliminary study, performed in an NMR tube. Complete conversion was achieved, as confirmed by GC-MS analysis. **B**: Cross-coupling reported by Hashmi *et al.*.

Our initial experimental design anticipated that a silver source and a base would be required for abstraction of a halide and proton, respectively. With this very basic experimental design, we set out to determine the finer details by screening a number of potential candidates for each role against an array of arenes. We were delighted to observe the successful formation of an aryl gold(I) complex, with the application of $ClAuP^tBu_3$ to the electron-deficient 1,3,5-trifluorobenzene, in the presence of DBU and $AgSbF_6$. Further optimisation of the reaction conditions led us to realise that the use of Ag_2O, K_2CO_3 and pivalic acid would allow us to generate the same aryl gold(I) product (**20**) in 100% yield.

With these optimised conditions in hand, we set out to explore the scope of this auration. A number of electron-deficient arenes were submitted to these conditions and the corresponding aryl gold(I) species were generated in excellent yields. This reaction is highly regioselective, with auration invariably occuring at a position between two electron-withdrawing groups. The procedure benefits from great operational simplicity and remarkably mild reaction conditions. Our observation of a high primary kinetic isotope effect (of 5.0) and the *in situ* formation of a gold(I) pivalate led us to conclude that the C–H activation proceeds via a concerted metalation deprotonation pathway, with intermolecular assistance from an additional basic species.

We also determined that the auration of electron-deficient arenes could also be achieved in the presence of an excess of strong base. Under these conditions we believe that the reaction proceeds via a more straightforward acid-base reaction. This silver-free procedure has since been developed and expanded upon, to include a greater range of (hetero)arenes.[86]

The evident affinity of gold(I) for electron-deficient arenes is in contrast to that of gold(III) for electron-rich arenes. Although both gold(I) and gold(III) C–H activation procedures operate, with great success, under very mild reaction conditions.

2.7 Experimental

2.7.1 General Information

All reactions were carried out in disposable vials using reagents obtained from commercial sources and used without further purification. Column chromatography was carried out on silica gel, particle size 40–63 μm, using flash techniques. Analytical thin layer chromatography was performed on pre-coated silica gel F_{254} plates with visualisation under UV light. Melting points were obtained using a Gallenkamp hot stage apparatus and are uncorrected. IR spectra were recorded using a Bruker Tensor 37 FTIR machine and are quoted in cm^{-1}. ^{1}H NMR spectra, recorded at 400 MHz, are referenced to the residual solvent peak at 7.26 ppm ($CHCl_3$) and quoted in ppm to 2 decimal places with coupling constants (*J*) to the nearest 0.1 Hz. ^{13}C NMR spectra, recorded at 101 MHz, are referenced to the solvent peak at 77.0 ppm ($CDCl_3$) and quoted in ppm to 1 decimal place with coupling constants (*J*) to the nearest 0.1 Hz. ^{31}P NMR spectra were recorded at 162 MHz, in $CDCl_3$ and quoted in ppm to 2 decimal places and with coupling constants (*J*) to the nearest 0.1 Hz.

2.7.2 Experimental Procedures

General procedure for the optimisation of the gold(I) C–H activation

A mixture of $ClAuP^tBu_3$[87] (8.8 mg, 0.02 mmol), 1,3,5-trifluorobenzene (9 μL, 0.09 mmol) and the desired additives were stirred at 25-50 ºC in the solvent (0.10 mL, 0.20 M). After the selected reaction time, the resulting mixture was filtered through a plug of cotton wool, washing with CH_2Cl_2. The filtrate was concentrated under reduced pressure and ^{1}H NMR analysis, using *p*-xylene as an internal standard, allowed detection and quantification of product **20**.

General procedure A: Synthesis of aryl gold(I) compounds via C–H activation

A mixture of the desired gold(I) chloride[86] (0.06 mmol), Ag_2O (10.5 mg, 0.045 mmol), K_2CO_3 (14.7 mg, 0.105 mmol), pivalic acid (15.3 mg, 0.15 mmol) and the arene (0.27 mmol) in DMF (0.3 mL, 0.20 M) was stirred at 50 ˚C. After 16 hours, the resulting mixture was filtered through a plug of cotton wool, which was washed with CH_2Cl_2 and the filtrate concentrated under reduced pressure.

The crude product was purified by column chromatography to afford products **20**-**47**.

General procedure B: Synthesis of aryl gold(I) compounds via silver-free C–H activation

A mixture of the desired gold(I) chloride (0.06 mmol), NaOH (9.6 mg, 0.24 mmol) and the arene (0.27 mmol) in DMF (0.3 mL, 0.20 M) was stirred at 50 ˚C. After 16 hours, the resulting mixture was filtered through a plug of cotton wool, which was washed with CH_2Cl_2 and the filtrate concentrated under reduced pressure. The crude product was purified by column chromatography to afford products **30**, **31** and **49**.

2.7.3 Characterisation Data

2,4,6-Trifluorophenyl(tri-*tert*-butylphosphine)gold(I) **20**

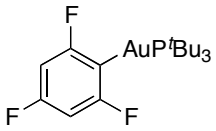

General procedure A was applied with ClAuP^{t}Bu$_3$ (26.4 mg, 0.06 mmol) and 1,3,5-trifluorobenzene (27 μL, 0.27 mmol) for 2 h. Column chromatography (*n*-hexanes:CH_2Cl_2 90:10) afforded product **20** as a white solid (31.5 mg, 100%); m.p. 132–134 ℃; R_f 0.40 (*n*-hexanes:CH_2Cl_2 70:30); IR: 1618, 1588, 1400, 1100, 992; ^{1}H NMR (400 MHz) δ 6.57 (ddd, 2H, *J* = 9.4, 4.7, 1.6 Hz), 1.56 (d, 27H, *J* = 13.1 Hz); ^{13}C NMR (100 MHz) δ 168.3 (dddd, *J* = 43.2, 29.0, 15.0, 3.5 Hz), 161.6 (dt, *J* = 242.1, 14.1 Hz), 98.5 (dddd, *J* = 36.2, 24.0, 4.7, 3.0 Hz), 39.2 (d, *J* = 16.3 Hz), 32.4 (d, *J* = 4.6 Hz); ^{19}F NMR (367 MHz,) δ –87.25 (apparent t, 2F, *J* = 6.6 Hz), –116.09 (t, 1F, *J* = 6.9 Hz); ^{31}P NMR (162 MHz) δ 92.25 (t, *J* = 6.0 Hz); MS (EI) *m/z* 530 (M+, 100); HRMS (EI) calcd. $C_{18}H_{29}AuF_3P$: (M+) 530.1621; found: (M+) 530.1621.

Pentafluorophenyl(tri-*tert*-butylphosphine)gold(I) **21**

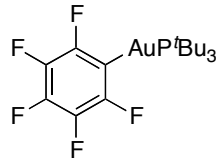

General procedure A was applied with ClAuP^{t}Bu$_3$ (26.4 mg, 0.06 mmol) and pentafluorobenzene (30 μL, 0.27 mmol) for 2 h. Column chromatography (*n*-hexanes:CH_2Cl_2 90:10) afforded product **21** as a white solid (33.8 mg, 99%); m.p. 114– 116 ℃; R_f 0.52 (*n*-hexanes: CH_2Cl_2 70:30); IR: 1501, 1452, 1435, 950; ^{1}H NMR (400 MHz) δ 1.56 (d, 27H, *J* = 13.3 Hz); ^{13}C NMR (100 MHz) δ 39.4 (d, *J* = 16.9 Hz), 32.4 (d, *J* = 4.5 Hz); ^{19}F NMR (367 MHz) δ –117.77—118.09 (m, 2F), –160.57 (t, 1F, *J* = 20.0 Hz), –163.50—164.05 (m, 2F); ^{31}P NMR (162 MHz) δ 92.24 (quint., *J* = 7.0 Hz); MS (EI) *m/z* 566 (M+, 100); HRMS (EI) calcd. $C_{18}H_{27}AuF_5P$: (M+) 566.1427; found: (M+), 566.1427.

2,3,6-Trifluorophenyl(tri-t*ert*-butylphosphine)gold(I) **22**

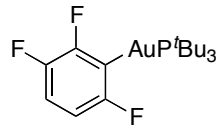

General procedure A was applied with ClAuP^{t}Bu$_3$ (26.4 mg, 0.06 mmol) and 1,2,4-trifluorobenzene (28 μL 0.27 mmol) for 2 h. Column chromatography (*n*-hexanes:CH_2Cl_2 90:10) afforded product **22** as a white solid (31.4 mg, 99%); m.p. 108–110 ℃; R_f 0.42 (*n*-hexanes: CH_2Cl_2 70:30); IR: 1482, 974, 843, 798; ^{1}H NMR (400 MHz) δ 6.84–6.69 (m, 2H), 1.56 (d, 27H, *J* = 13.1 Hz); ^{13}C NMR (100 MHz) δ 113.9 (dd, *J* = 20.5, 9.4 Hz), 109.4 (ddt, *J* = 34.6, 5.1, 3.6 Hz), 39.2 (d, *J* = 16.4 Hz), 32.4 (d, *J* = 4.5 Hz); ^{19}F NMR (565 MHz) δ –94.80 (dd, 1F, *J* = 18.6, 5.5 Hz), –112.72—112.93 (m, 1F), –145.09—145.24 (m, 1F); ^{31}P NMR (162 MHz) δ 92.02 (dd, *J* = 12.6, 6.1 Hz); MS (ESI) *m/z* 553 ([M+Na]+, 100); HRMS (ESI) calcd. $C_{18}H_{29}AuF_3NaP$: ([M+Na]+), 553.1511; found: ([M+Na]+) 553.1511.

2,6-Difluorophenyl(tri-*tert*-butylphosphine)gold(I) **23**

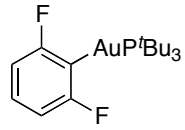

General procedure A was applied with ClAuP^{t}Bu$_3$ (26.4 mg, 0.06 mmol) and 1,3-difluorobenzene (26 μL, 0.27 mmol) for 16 h. Column chromatography (*n*-hexanes:CH_2Cl_2 90:10) afforded product **23** as a white solid (25.6 mg, 83%); m.p. 126–128 ℃; R_f 0.33 (*n*-hexanes: CH_2Cl_2 70:30); IR: 1433, 1200, 1172, 950, 778; ^{1}H NMR (400 MHz) δ 7.09–6.95 (m, 1H), 6.88–6.78 (m, 2H), 1.56 (d, 27H, *J* = 13.1 Hz); ^{13}C NMR (100 MHz) δ 170.2–169.3 (m), 127.3 (t, *J* = 8.4 Hz), 109.7 (dt, *J* = 30.8, 2.9 Hz), 39.2 (d, *J* = 16.1 Hz), 32.4 (d, *J* = 4.6 Hz); ^{19}F NMR (565 MHz) δ –88.31 (d, 2F, *J* = 6.5 Hz); ^{31}P NMR (162 MHz) δ 92.22 (t, *J* = 6.3 Hz); MS (EI) *m/z* 512 (M+, 100); HRMS (EI) calcd. $C_{18}H_{30}AuF_2P$: (M+), 512.1214; found: (M+), 512.1214.

2,6-Difluoro-5-methylphenyl(tri-*tert*-butylphosphine)gold(I) **24**

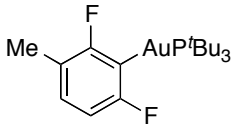

General procedure A was applied with ClAuP^{t}Bu$_3$ (26.4 mg, 0.06 mmol) and 2,4-difluorotoluene (31 μL, 0.27 mmol) for 16 h. Column chromatography (*n*-hexanes:CH_2Cl_2 90:10) afforded product **24** as a white solid (20.0 mg, 63%); m.p. 96–98 ℃ ; R_f 0.40 (*n*-hexanes: CH_2Cl_2 70:30); IR: 1449, 955, 795; ^{1}H NMR (400 MHz) δ 6.84 (apparent q, 1H, *J* = 7.9 Hz), 6.77–6.72 (m, 1H), 2.19 (s, 3H), 1.56 (d, 27H, *J* = 13.0 Hz); ^{13}C NMR (100 MHz) δ 128.7 (dd, *J* = 8.1, 5.2 Hz), 119.1–118.3 (m), 109.3 (dt, *J* = 30.9, 3.2 Hz), 39.2 (d, *J* = 15.9 Hz), 32.4 (d, *J* = 4.6 Hz), 15.0 (s); ^{19}F NMR (565 MHz) δ – 91.19 (d, 1F, *J* = 6.0 Hz), –92.95 (d, 1F, *J* = 6.2 Hz); ^{31}P NMR (162 MHz) δ 92.30 (t, *J* = 6.3 Hz); MS (EI) *m/z* 526 (M+, 100); HRMS (EI) calcd. $C_{19}H_{32}AuF_2P$: (M+), 526.1870; found: (M+), 526.1870.

2,6-Dinitrophenyl(tri-*tert*-butylphosphine)gold(I) **25**

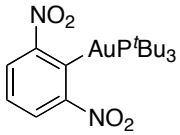

General procedure A was applied with ClAuP^{t}Bu$_3$ (26.4 mg, 0.06 mmol) and 1,3-dinitrobenzene (45.4 mg, 0.27 mmol) for 16 h. Column chromatography (*n*-hexanes:EtOAc 95:5) afforded product **25** as a white solid (28.3 mg, 83%); m.p. 231–233 ℃; R_f 0.15 (*n*-hexanes: EtOAc 95:5); IR: 1515, 1334, 1172, 808; ^{1}H NMR (400 MHz) δ 8.19 (dd, 2H, *J* = 8.0, 1.3 Hz), 7.33 (t, 1H, *J* = 8.0 Hz), 1.55 (d, 27H, *J* = 13.3 Hz); ^{13}C NMR (100 MHz) δ 162.7 (d, *J* = 93.6 Hz), 158.8 (d, *J* = 2.0 Hz), 127.5 (d, *J* = 2.9 Hz), 126.1 (s), 38.9 (d, *J* = 17.2 Hz), 32.3 (d, *J* = 4.5 Hz); ^{31}P NMR (162 MHz) δ 91.28 (s); MS (EI) *m/z* 566 (M+, 100); HRMS (EI) calcd. $C_{18}H_{30}AuN_2O_4P$: (M+), 566.1604; found: (M+), 566.1604.

2-Fluoro-6-nitrophenyl(tri-*tert*-butylphosphine)gold(I) **26**

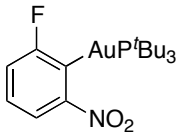

General procedure A was applied with ClAuP^{t}Bu$_3$ (26.4 mg, 0.06 mmol) and 1-fluoro-3-nitrobenzene (29 μL, 0.27 mmol) for 16 h. Column chromatography (*n*-hexanes:EtOAc 95:5) afforded product **26** as a pale yellow solid (31.9 mg, 99%); m.p. 160–162 ℃; IR: 2954, 1510, 1338, 1213, 798; ^{1}H NMR (400 MHz) δ 7.94 (d, 1H, *J* = 7.9 Hz), 7.25-7.22 (m, 1H), 7.16 (td, 1H, *J* = 7.9, 6.2 Hz), 1.57 (d, 27H, *J* = 13.2 Hz); ^{13}C NMR (100 MHz) δ 168.0 (dd, *J* = 230.3, 2.3 Hz), 158.1 (d, *J* = 19.8 Hz), 153.7 (dd, *J* = 93.9, 69.0 Hz), 126.7 (d, *J* = 7.3 Hz), 119.6 (t, *J* = 2.9 Hz), 118.6 (dd, *J* = 32.3, 2.2 Hz), 39.1 (d, *J* = 16.9 Hz), 32.4 (d, *J* = 4.4 Hz); ^{31}P NMR (162 MHz) δ 91.86 (d, *J* = 3.9 Hz); MS (EI) *m/z* 539 (M+, 100); HRMS (EI) calcd. $C_{18}H_{30}AuFNO_2P$: (M^+), 539.1656; found: (M^+), 539.1645.

2,3,5,6-Tetrafluorophenyl(tri-*tert*-butylphosphine)gold(I) **27**

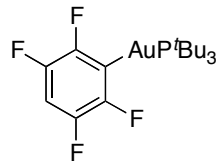

General procedure A was applied with ClAuP^{t}Bu$_3$ (26.4 mg, 0.06 mmol) and 1,2,4,5-tetrafluorobenzene (30 μL, 0.27 mmol) for 16 h. Column chromatography (*n*-hexanes:EtOAc 95:5) afforded product **27** as a white solid (32.5 mg, 99%); m.p. 120–122 ℃; IR: 2953, 1452, 1189, 1173, 888, 705; ^{1}H NMR (400 MHz) δ 6.68 (tt, 1H, *J* = 9.9, 9.6 Hz), 1.57 (d, 27H, *J* = 13.2 Hz); ^{13}C NMR (100 MHz) δ 149.9-148.2 (m), 147.1-145.2 (m), 102.8 (t, *J* = 23.4 Hz), 39.4 (d, *J* = 16.1 Hz), 32.4 (d, *J* = 4.4 Hz); ^{31}P NMR (162 MHz) δ 92.10 (apparent p, *J* = 6.8 Hz); MS (EI) *m/z* 548 (M+, 100); HRMS (EI) calcd. $C_{18}H_{28}AuF_4P$: (M^+), 548.1525; found: (M^+), 548.1515.

2,6-Difluoro-4-bromophenyl(tri-*tert*-butylphosphine)gold(I) **28**

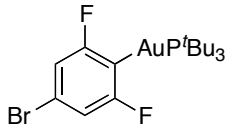

General procedure A was applied with ClAuP^{t}Bu$_3$ (26.4 mg, 0.06 mmol) and 1-bromo-3,5-difluorobenzene (31 μL, 0.27 mmol) for 16 h. Column chromatography (*n*-hexanes:EtOAc 95:5) afforded product **28** as a white solid (28.3 mg, 83%); m.p. 120–122 ℃; IR: 2997, 1579, 1392, 1171, 983, 834; ^{1}H NMR (400 MHz) δ 6.99 (dd, 2H, *J* = 4.1, 1.5 Hz), 1.56 (d, 27H, *J* = 13.1 Hz); ^{13}C NMR (100 MHz) δ 168.5 (ddd, *J* = 234.0, 26.4, 3.7 Hz), 142.0 (dt, *J* = 124.0, 62.4 Hz), 118.2 (t, *J* = 11.0 Hz), 113.5 (apparent dt, *J* = 35.2, 3.3 Hz), 39.2 (d, *J* = 16.2 Hz), 32.4 (d, *J* = 4.4 Hz); ^{31}P NMR (162 MHz) δ 92.35 (t, *J* = 6.1 Hz); MS (EI) *m/z* 590 (M+, 100); HRMS (EI) calcd. $C_{18}H_{29}AuBrF_2P$: (M^+), 590.0817; found: (M^+), 590.0808.

2,4-Dibromo-6-flourophenyl(tri-*tert*-butylphosphine)gold(I) **29**

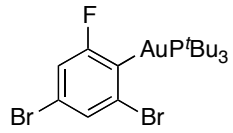

General procedure A was applied with ClAuP^{t}Bu$_3$ (26.4 mg, 0.06 mmol) and 1,3-dibromo-5-fluorobenzene (34 μL, 0.27 mmol) for 16 h. Column chromatography (*n*-hexanes:EtOAc 95:5) afforded product **29** as a white solid (38.7 mg, 83%); m.p. 168–170 ℃; IR: 2997, 1579, 1392, 1171, 983; ^{1}H NMR (400 MHz) δ 7.45 (s, 1H), 7.12 (d, 1H, *J* = 4.8 Hz), 1.56 (d, 27H, *J* = 13.1 Hz);^{13}C NMR (100 MHz) δ 166.3 (dd, *J* = 235.2, 3.6 Hz), 161.1 (dd, *J* = 97.0, 64.3 Hz), 134.4 (dd, *J* = 25.2, 4.2 Hz), 129.5 (t, *J* = 3.7 Hz), 118.6 (d, *J* = 9.6 Hz), 116.1 (dd, *J* = 35.3, 3.0 Hz) 39.4 (d, *J* = 16.2 Hz), 32.6 (d, *J* = 4.5 Hz); ^{31}P NMR (162 MHz) δ 91.19 (d, *J* = 5.5 Hz); MS (EI) *m/z* 566 (M+, 100); HRMS (EI) calcd. $C_{18}H_{29}AuBr_2FP$: (M+H), 652.0096; found: (M+), 651.0098.

2,4,6-Trichlorophenyl(tri-*tert*-butylphosphine)gold(I) **30**

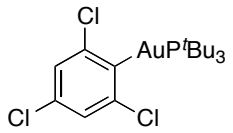

General procedure A was applied with ClAuP^{t}Bu$_3$ (26.4 mg, 0.06 mmol) and 1,3,5-trichlorobenzene (49.0 mg, 0.27 mmol) for 16 h. Column chromatography (*n*-hexanes:EtOAc 95:5) afforded product **30** as a white solid (21.8 mg, 63%); m.p. 206–208 ℃; IR: 2955, 1334, 1172, 1055, 808; ^{1}H NMR (400 MHz) δ 7.25 (s, 2H), 1.56 (d, 27H, *J* = 13.1 Hz); ^{13}C NMR (100 MHz) δ 172.0 (d, *J* = 99.5 Hz), 143.7 (d, *J* = 3.6 Hz), 131.4 (s), 125.9 (d, *J* = 3.9 Hz), 39.4 (d, *J* = 16.0 Hz), 32.6 (d, *J* = 4.5 Hz); ^{31}P NMR (162 MHz) δ 90.88 (s); MS (EI) *m/z* 566 (M+, 100); HRMS (EI) calcd. $C_{18}H_{29}AuCl_3P$: (M+), 578.0738; found: (M+), 578.0734.

2,3,5,6-Tetrachlorophenyl(tri-*tert*-butylphosphine)gold(I) **31**

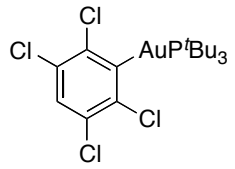

General procedure A was applied with ClAuP^{t}Bu$_3$ (26.4 mg, 0.06 mmol) and 1,2,4,5-tetrachlorobenzene (58.3 mg, 0.27 mmol) for 16 h. Column chromatography (*n*-hexanes:EtOAc 95:5) afforded product **31** as a white solid (33.8 mg, 92%); m.p. 202–204 ℃; IR: 2955, 1355, 1149, 1055, 854; ^{1}H NMR (400 MHz) δ 7.23 (s, 1H), 1.58 (d, 27H, *J* = 13.1 Hz); ^{13}C NMR (100 MHz) δ 177.8 (d, *J* = 97.6 Hz), 138.3 (d, *J* = 4.4 Hz), 130.8 (d, *J* = 7.3 Hz), 128.2 (s), 39.4 (d, *J* = 16.1 Hz), 32.4 (d, *J* = 4.4 Hz); ^{31}P NMR (162 MHz) δ 90.40 (s); MS (EI) *m/z* 614 (M+, 100); HRMS (EI) calcd. $C_{18}H_{28}AuCl_4P$: (M^+), 614.0315; found: (M^+), 614.0296.

2,4,6-Trifluorophenyl(triethylphosphine)gold(I) **39**

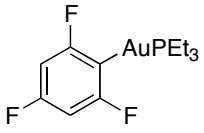

General procedure A was applied with ClAuPEt$_3$ (21.0 mg, 0.06 mmol) and 1,3,5-trifluorobenzene (27 μL, 0.27 mmol) for 2 h. Column chromatography (*n*-hexanes:CH_2Cl_2 90:10) afforded product **39** as a brown oil (26.2 mg, 98%); R_f 0.37 (*n*-hexanes: CH_2Cl_2 70:30); IR: 1618, 1587, 1402, 1103, 991; 1H NMR (400 MHz) δ 6.57 (ddd, 2H, *J* = 9.4, 5.0, 1.7 Hz), 1.87 (dq, 6H, *J* = 9.3, 7.7 Hz), 1.26 (dt, 3H, *J* = 17.9, 7.7 Hz); 13C NMR (100 MHz) δ 168.3 (dddd, *J* = 232.1, 28.6, 14.7, 4.0 Hz), 163.9–158.9 (m), 98.6 (dddd, *J* = 36.1, 24.0, 4.5, 3.4 Hz), 18.0 (d, *J* = 31.4 Hz), 9.0 (s); 19F NMR (367 MHz) δ –87.21 (t, 2F, *J* = 7.4 Hz), –115.43 (t, 1F, *J* = 7.1 Hz); 31P NMR (162 MHz) δ 40.51 (t, *J* = 7.9 Hz); MS (EI) *m/z* 446 (M+, 100); HRMS (EI) calcd. C12H17AuF3P: (M+), 446.0680; found: (M+), 446.0680.

[*N*,*N*-Bis(2,6-diisopropylphenyl)imidazol-2-yl](2,4,6-trifluorophenyl)gold(I) **40**

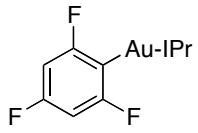

General procedure A was applied with ClAuIPr (37.3 mg, 0.06 mmol) and 1,3,5-trifluorobenzene (27 μL, 0.27 mmol) for 4 h. Column chromatography (*n*-hexanes:CH2Cl2 90:10) afforded product **40** as a white solid (41.4 mg, 96%); m.p. 249–251 ℃; R_f 0.25 (*n*-hexanes: CH_2Cl_2 70:30); IR: 1615, 1586, 1464, 1399, 1099; ^{1}H NMR (400 MHz) δ 7.44 (t, 2H, *J* = 7.8 Hz), 7.29 (d, 4H, *J* = 7.8 Hz), 7.18 (s, 2H), 6.34–6.29 (m, 2H), 2.64 (hept, 4H, *J* = 6.8 Hz), 1.38 (d, 12H, *J* = 6.9 Hz), 1.24 (d, 12H, *J* = 6.9 Hz); ^{13}C NMR (100 MHz) δ 193.7 (t, *J* = 2.8 Hz), 168.6 (ddd, *J* = 231.4, 29.1, 14.6 Hz), 163.0–158.8 (m), 145.8 (s), 134.3 (s), 130.3 (s), 123.9 (s), 122.8 (s), 97.7 (ddd, *J* = 36.0, 23.8, 4.6 Hz), 28.8 (s), 24.1 (d, *J* = 30.7 Hz); ^{19}F NMR (565 MHz, CDCl3) δ –85.13 (d, 2F, *J* = 6.2 Hz), –116.81—116.84 (m, 1F); MS (EI) *m/z* 716 (M+, 100; HRMS (EI) calcd. $C_{33}H_{38}AuF_3N_2$: (M+), 716.2639; found: (M+), 716.2639.

2,4,6-Trifluorophenyl(triphenylphosphine)gold(I) **41**

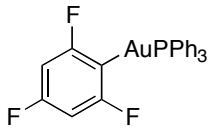

General procedure A was applied with $ClAuPPh_3$ (29.7 mg, 0.06 mmol) and 1,3,5-trifluorobenzene (27 μL, 0.27 mmol) for 4 h. Column chromatography (*n*-hexanes:CH_2Cl_2 90:10) afforded product **41** as a white solid (31.2 mg, 88%); m.p. 145–147 ℃; R_f 0.49 (*n*-hexanes: CH_2Cl_2 70:30); IR: 1588, 1437, 1403, 1103, 987; ^{1}H NMR (400 MHz) δ 7.66–7.55 (m, 6H), 7.55–7.42 (m, 9H), 6.62 (ddd, 2H, *J* = 9.4, 4.9, 1.8 Hz); ^{13}C NMR (100 MHz) δ 134.4 (d, *J* = 13.9 Hz), 131.4 (d, *J* = 2.4 Hz), 130.4 (d, *J* = 53.4 Hz), 129.2 (d, *J* = 11.0 Hz), 100.8–97.7 (m); ^{19}F NMR (367 MHz, CDCl3) δ – 86.69 (t, 2F, *J* = 7.1 Hz), –114.90 (t, 1F, *J* = 7.0 Hz); ^{31}P NMR (162 MHz, CDCl3) δ 43.18 (t, *J* = 7.9 Hz); MS (EI) *m/z* 590

(M+, 100); HRMS (EI) calcd. $C_{24}H_{17}AuF_3P$: (M+), 590.0678; found: (M+), 590.0678.

2,4,6-Trifluorophenyl(triphenylphoshite)gold(I) **42**

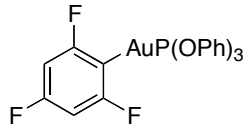

General procedure A was applied with $ClAuP(OPh)_3$ (32.6 mg, 0.06mmol) and 1,3,5-trifluorobenzene (27 µL, 0.27 mmol) for 2 h. ^1H NMR spectroscopy with addition of *p*-xylene (3.7µL, 0.03 mmol) as an external standard revealed a 37% yield.

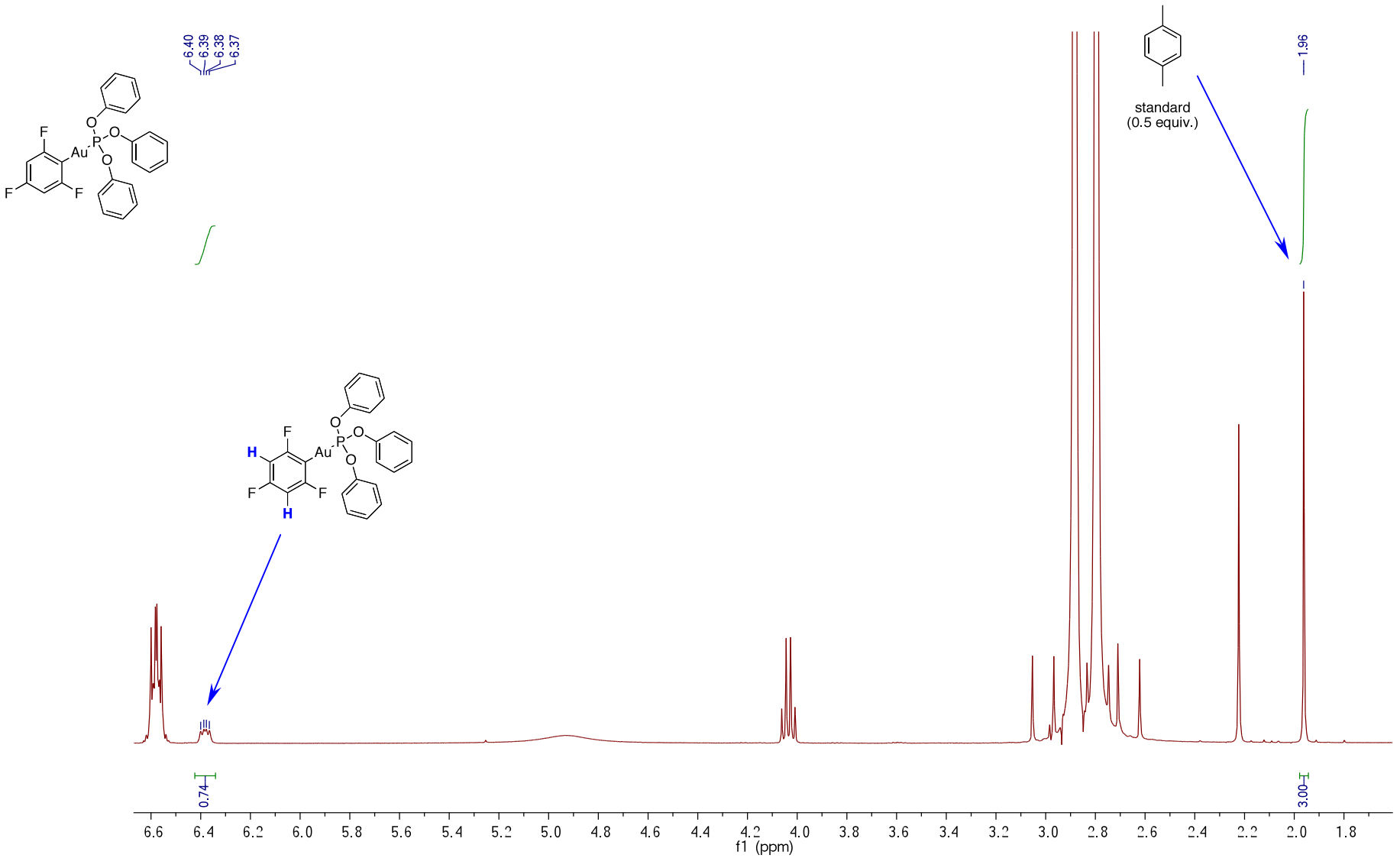
6.40
6.39
6.38
6.37
F
Au
P
O
F
F
standard
(0.5 equiv.)
1.96
H
F
Au
P
O
F
F
H
0.74
3.00
6.6
6.4
6.2
6.0
5.8
5.6
5.4
5.2
5.0
4.8
4.6
4.4
4.2
4.0
3.8
3.6
3.4
3.2
3.0
2.8
2.6
2.4
2.2
2.0
1.8
f1 (ppm)

2,3,4,5,6-Pentafluoro-phenyl(triphenylphosphine)gold(I) **43**

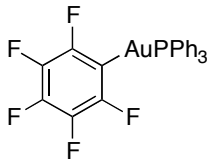

General procedure A was applied with $ClAuPPh_3$ (29.7 mg, 0.06 mmol) and pentafluorobenzene (30 μL, 0.27 mmol). Column chromatography (*n*-hexanes:EtOAc 90:10) afforded product **43** as a white solid (35.5 mg, 94%); m.p. 168–170 ˚C; R_f 0.34 (*n*-hexanes:EtOAc 85:15); IR: 1636, 1499, 1453, 1434, 1352, 1099, 1050, 953, 789, 686; ^{1}H NMR (400 MHz) δ 7.66–7.45 (m, 15H); ^{13}C NMR (101 MHz) δ 134.5 (d, J = 13.8 Hz), 131.8 (d, J = 2.4 Hz), 130.0 (d, J = 54.8), 129.4 (d, J = 11.2 Hz); ^{31}P NMR (162 MHz) δ 42.33 (apparent pent., J = 7.9 Hz); HRMS (CI) calcd. $C_{24}H_{15}AuF_5P$: (M^+) 627.0525; found: (M^+) 627.0519; spectroscopic data is in agreement with that previously reported.[88]

2,3,5,6-Tetrafluoro-phenyl(triphenylphosphine)gold(I) **44**

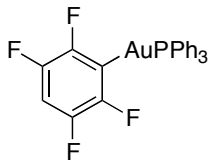

General procedure A was applied with $ClAuPPh_3$ (29.7 mg, 0.06 mmol) and 1,2,4,5-tetraflurobenzene (30 μL, 0.27 mmol). Column chromatography (*n*-hexanes:EtOAc 95:5) afforded product **44** as a white solid (33.2 mg, 91%); m.p. 154–156 ºC; R_f 0.34 (*n*-hexanes:EtOAc 90:10); IR: 1589, 1451, 1434, 1155, 1099, 887, 748, 688; ^{1}H NMR (400 MHz) δ 7.61 (dd, 6H, J = 12.4, 7.8 Hz), 7.57–7.44 (m, 9H), 6.75 (tt, 1H, J = 9.1, 7.0 Hz); ^{13}C NMR (101 MHz) δ 149.2 (dddd, J = 226.9, 21.3, 10.5, 3.0 Hz), 146.1 (dddd, J = 249.3, 24.3, 7.5, 2.6 Hz), 134.5 (d, J = 13.8 Hz), 131.7 (d, J = 2.4 Hz), 130.1 (d, J = 54.3 Hz), 129.4 (d, J = 11.2 Hz), 103.7 (t, J = 23.4 Hz); ^{31}P NMR (162 MHz) δ 42.17 (broad s); HRMS (CI) calcd. $C_{24}H_{16}AuF_4P$: (M^+) 608.0586; found: (M^+) 608.0570.

2,4-Dibromo-6-fluoro-phenyl(triphenylphosphine)gold(I) **45**

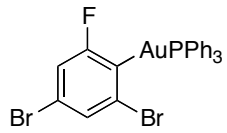

General procedure A was applied with $ClAuPPh_3$ (29.7 mg, 0.06 mmol) and 1,3-dibromo-5-fluorobenzene (34 µL, 0.27 mmol). Column chromatography (*n*-hexanes:EtOAc 95:5) afforded product **45** as a white solid (40.2 mg, 94%); m.p. 170–172 ˚C; R_f 0.54 (*n*-hexanes:EtOAc 85:15); IR: 1559, 1536, 1479, 1434, 1362, 1204, 1099, 881, 854, 745, 690; ^{1}H NMR (400 MHz) δ 7.63 (dd, 6H, *J* = 12.3, 7.7 Hz), 7.56–7.43 (m, 10H), 7.18 (d, 1H, *J* = 4.8 Hz); ^{13}C NMR (101 MHz) δ 166.3 (dd, *J* = 236.4, 3.9 Hz), 158.8 (dd, *J*, 107.8, 62.3 Hz), 134.5 (d, *J* = 13.8 Hz), 134.0 (d, *J* = 4.6 Hz), 131.6 (d, *J* = 2.4 Hz), 130.4 (d, *J* = 53.3 Hz), 129.7–129.5 (m), 129.3 (d, *J* = 11.1 Hz), 119.3 (d, *J* = 9.6 Hz), 116.3 (dd, *J* = 34.8, 3.4 Hz); ^{31}P NMR (162 MHz) δ 41.07 (d, *J* = 7.0 Hz); HRMS (CI) calcd. $C_{24}H_{17}AuBr_2FP$: (M^+) 709.9079; found: (M^+) 709.9069.

2-Fluoro-6-nitro-phenyl(triphenylphosphine)gold(I) **46**

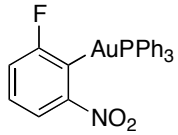

General procedure A was applied with $ClAuPPh_3$ (29.7 mg, 0.06 mmol) and 1-fluoro-3-nitrobenzene (29 µL, 0.27 mmol). Column chromatography (*n*-hexanes:EtOAc 90:10) afforded product **46** as a yellow solid (28.0 mg, 78%); m.p. 148–150 ˚C; R_f 0.21 (*n*-hexanes:EtOAc 85:15); IR: 1500, 1478, 1435, 1330, 1294, 1213, 1099, 997, 917, 808, 739; ^{1}H NMR (400 MHz) δ 8.19 (d, 1H, *J* = 7.9 Hz), 7.84 (dd, 6H, *J* = 12.4, 7.7 Hz), 7.75–7.63 (m, 9H), 7.53–7.35 (m, 2H); ^{13}C NMR (101 MHz) δ 168.0 (dd, *J* = 231.8, 4.3 Hz), 158.2 (dd, *J* = 20.3, 1.6 Hz), 151.4 (dd, *J* = 104.3, 66.9 Hz), 134.5 (d, *J* = 13.9 Hz), 131.5 (d, *J* = 2.4 Hz), 130.5 (d, *J* = 54.1 Hz), 129.3 (d, *J* = 11.2 Hz), 127.4 (d, *J* = 7.1 Hz), 119.9 (t, *J* =

3.2 Hz), 119.1 (dd, J = 32.0, 2.6 Hz); ^{31}P NMR (162 MHz) δ 41.89 (d, J = 5.1 Hz); MS (EI) *m/z* (M^+, 100); HRMS (EI) calcd. $C_{24}H_{18}AuFNO_2P$: $[M+H]^+$ 600.0797; found: $[M+H]^+$ 600.0784.

2,3,6-Trifluoro-phenyl(triphenylphosphine)gold(I) **47**

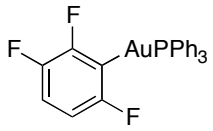

General procedure A was applied with $ClAuPPh_3$ (29.7 mg, 0.06 mmol) and 1,2,4-trifluorobenzene (28 μL, 0.27 mmol). Column chromatography (*n*-hexanes:EtOAc 90:10) afforded product **47** as a white solid (32.5 mg, 92%); m.p. 136–138 ˚C; R_f 0.26 (*n*-hexanes:EtOAc 85:15); IR: 1584, 1453, 1435, 1213, 1100, 970, 842, 800, 729, 689; ^{1}H NMR (400 MHz) δ 7.62 (ddd, 6H, J = 12.4, 7.9, 1.6 Hz), 7.57–7.42 (m, 9H), 7.91–7.74 (m, 2H); ^{13}C NMR (101 MHz) δ 134.5 (d, J = 13.8 Hz), 131.6 (d, J = 2.4 Hz), 130.4 (d, J = 53.6 Hz), 129.3 (d, J = 11.1 Hz), 114.8 (dd, J = 20.4, 9.5 Hz), 109.7 (ddd, J = 34.1, 8.8, 3.8 Hz); ^{31}P NMR (162 MHz) δ 42.17 (apparent q., J = 6.8 Hz); MS (EI) *m/z* (M^+, 100); HRMS (CI) calcd. $C_{24}H_{17}AuF_3P$: (M^+) 590.0680; found: (M^+) 590.0678.

2-thiazolyl(tri-*tert*-butylphosphine)gold(I) **49**

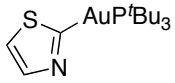

General procedure B was applied with $ClAuPPh_3$ (29.7 mg, 0.06 mmol) and thiazole (19 μL, 0.27 mmol). Column chromatography (*n*-hexanes:EtOAc 90:10) afforded product **49** as a white solid (21.9 mg, 76%); m.p. 178–183 ˚C; IR: 2951, 1393, 1170, 918; ^{1}H NMR (400 MHz) δ 8.19 (d, 1H, J = 3.1 Hz), 7.50 (dd, 1H, J = 3.1, 1.1 Hz), 1.56 (d, 27H, J = 13.1 Hz); ^{13}C NMR (101 MHz) δ 209.3 (d, J = 132.8 Hz), 143.5 (d, J = 10.3 Hz), 117.5 (s), 39.0 (d, J = 16.1 Hz), 32.4 (d, J =

4.4 Hz); ^{31}P NMR (162 MHz) δ 90.84. HRMS (EI) calcd. $C_{15}H_{29}AuNPS$: (M^+) 483.1424; found: (M^+) 483.1404.

2.7.4 Kinetic Isotope Effect Experiment

General procedure A was applied, at one third the scale, with ClAuP^{t}Bu$_3$ (8.8 mg, 0.02 mmol), 1,3-dinitrobenzene-d$_4$ (7.7 mg, 0.045 mmol) and 1,3-dinitrobenzene (7.6 mg, 0.045 mmol) for 1.5 h. The resulting mixture was filtered through a plug of cotton wool and then concentrated under reduced pressure. The crude product was analysed by EI-MS to determine the ratio of product **25** to **25-d$_3$**.

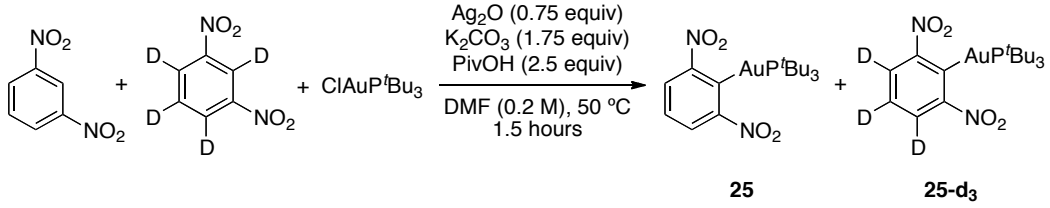

25 **25-d$_3$**

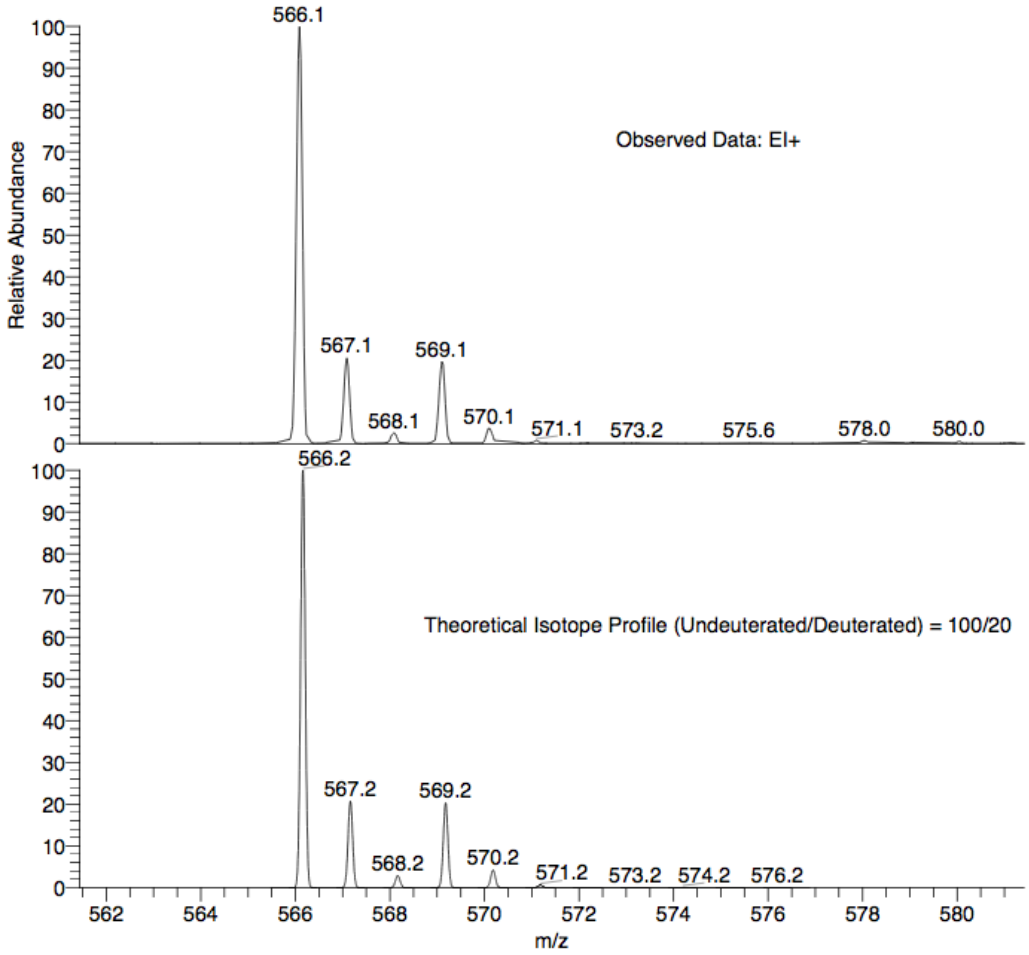

2.7.5 Other Mechanistic Experiments

Gold(I) C–H Activation with tri-tert-butylphosphine gold(I) pivalate

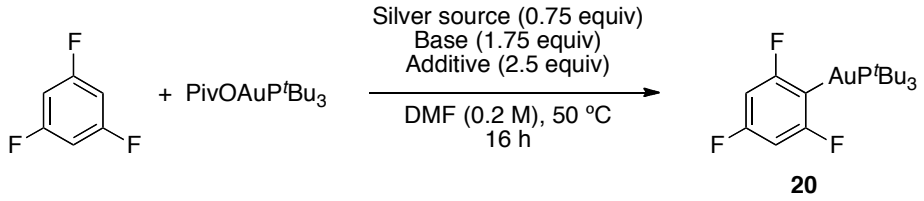

20

A mixture of PivOAuP^{t}Bu$_3$[89] (10.0 mg, 0.02 mmol), 1,3,5-trifluorobenzene (9 μL, 0.09 mmol) and the desired additives was stirred at 50 ºC for 16 h. After this time, the crude reaction mixture was filtered through a plug of cotton wool, washing with CH_2Cl_2. The filtrate was concentrated under reduced pressure and ^{1}H NMR analysis, using *p*-xylene as an internal standard, allowed detection and quantification of product **20**.

Dueteration Studies with 1,3-dinitrobenzene

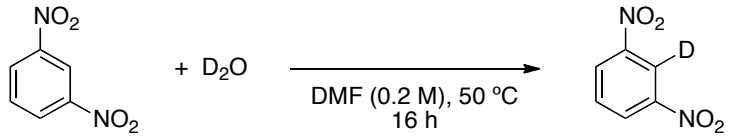

General procedure A was applied, at one third the scale and in the absence of a gold(I) salt, with 1,3-dinitrobenzene (15.1 mg, 0.09 mmol) and the desired additives. After 16 hours, the crude reaction mixture was filtered through a plug of cotton wool, washing with CH_2Cl_2. The filtrate was concentrated under reduced pressure and ^{1}H NMR analysis, using *p*-xylene as an internal standard, allowed detection and quantification of the deuterated product.

2.7.6 Crystallographic data

X-ray diffraction studies for **20** were performed at 93K using a Rigaku MM007/Saturn diffractometer (confocal optics Mo-Kα radiation) and for **21**, **22**, **23**, **24**, **25**, **40**, **41** at 93K using a Rigaku MM007/Mercury/ diffractometer (confocal optics Mo-Kα radiation) . Intensity data were collected using ω steps accumulating area detector frames spanning at least a hemisphere of reciprocal space for all structures (data were integrated using CrystalClear). All data were corrected for Lorentz, polarization and long-term intensity fluctuations. Absorption effects were corrected on the basis of multiple equivalent reflections. Structures were solved by direct methods and refined by full-matrix least-squares against *F*2 (SHELXTL). All N-H and O-H hydrogen atoms were refined isotropically subject to a distance constraint (N,O-H= 0.98 Å). All remaining hydrogen atoms were assigned riding isotropic displacement parameters and constrained to idealized geometries.

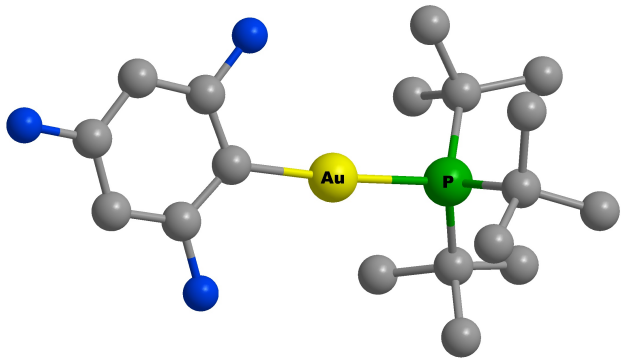

Figure E1. X-ray crystal structure of **20**.

Table E1. Crystal data and structure refinement for **20**.

Identification code	**20**
Empirical formula	C18 H29 Au F3 P
Formula weight	530.35
Temperature	93(2) K
Wavelength	0.71073 Å
Crystal system	Monoclinic
Space group	P2(1)/n

Unit cell dimensions	a = 8.5787(6) Å	a= 90°.
	b = 18.4977(13) Å	b= 90.313(3)°.
	c = 12.5721(9) Å	g = 90°.
Volume	1995.0(2) $Å^3$	
Z	4	
Density (calculated)	1.766 Mg/m^3	
Absorption coefficient	7.477 mm^{-1}	
F(000)	1032	
Crystal size	0.18 x 0.15 x 0.06 mm^3	
Theta range for data collection	5.98 to 25.35°.	
Index ranges	-10<=h<=10, -22<=k<=21, -15<=l<=15	
Reflections collected	16372	
Independent reflections	3554 [R(int) = 0.0507]	
Completeness to theta = 25.00°	97.4 %	
Absorption correction	Multiscan	
Max. and min. transmission	1.000 and 0.507	
Refinement method	Full-matrix least-squares on F^2	
Data / restraints / parameters	3554 / 0 / 208	
Goodness-of-fit on F^2	1.133	
Final R indices [I>2sigma(I)]	R1 = 0.0272, wR2 = 0.0696	
R indices (all data)	R1 = 0.0277, wR2 = 0.0699	
Largest diff. peak and hole	1.576 and -1.103 $e.Å^{-3}$	

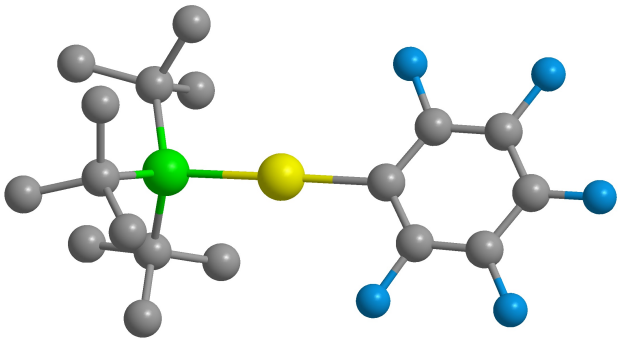

Figure E2. X-ray crystal structure of **21**.

Table E2. Crystal data and structure refinement for **21**.

Identification code	**21**	
Empirical formula	C18 H27 Au F5 P	
Formula weight	566.33	
Temperature	93(2) K	
Wavelength	0.71073 Å	
Crystal system	Monoclinic	
Space group	P2(1)/c	
Unit cell dimensions	a = 8.560(3) Å	a= 90°.
	b = 20.335(6) Å	b= 104.920(10)°.
	c = 12.155(4) Å	g = 90°.
Volume	2044.4(12) $Å^3$	
Z	4	
Density (calculated)	1.840 Mg/m^3	
Absorption coefficient	7.316 mm^{-1}	
F(000)	1096	
Crystal size	0.10 x 0.10 x 0.02 mm^3	
Theta range for data collection	2.65 to 25.32°.	
Index ranges	-10<=h<=10, -24<=k<=24, -14<=l<=10	
Reflections collected	12946	
Independent reflections	3718 [R(int) = 0.0498]	
Completeness to theta = 25.00°	99.8 %	
Absorption correction	Multiscan	

Max. and min. transmission	1.000 and 0.695
Refinement method	Full-matrix least-squares on F^2
Data / restraints / parameters	3718 / 0 / 227
Goodness-of-fit on F^2	0.786
Final R indices [I>2sigma(I)]	R1 = 0.0327, wR2 = 0.0645
R indices (all data)	R1 = 0.0448, wR2 = 0.0717
Largest diff. peak and hole	1.636 and -1.370 e.Å^{-3}

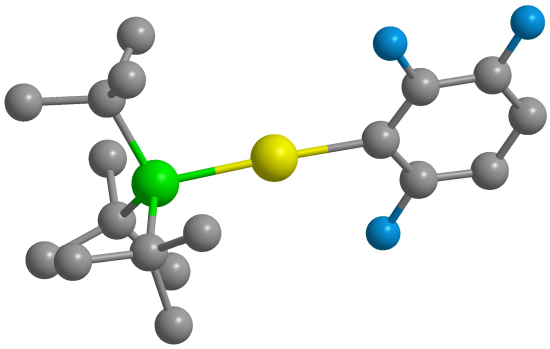

Figure E3. X-ray crystal structure of **22**.

Table E3. Crystal data and structure refinement for **22**.

Identification code	**22**	
Empirical formula	C18 H29 Au F3 P	
Formula weight	530.35	
Temperature	93(2) K	
Wavelength	0.71073 Å	
Crystal system	Monoclinic	
Space group	P2(1)/n	
Unit cell dimensions	a = 8.528(3) Å	a= 90°.
	b = 18.534(5) Å	b= 90.101(8)°.
	c = 12.578(4) Å	g = 90°.
Volume	1988.0(11) Å^3	
Z	4	
Density (calculated)	1.772 Mg/m^3	

Absorption coefficient	7.503 mm^{-1}
F(000)	1032
Crystal size	0.12 x 0.12 x 0.12 mm^3
Theta range for data collection	2.88 to 25.33°.
Index ranges	-10<=h<=7, -22<=k<=17, -13<=l<=15
Reflections collected	12201
Independent reflections	3613 [R(int) = 0.0631]
Completeness to theta = 25.00°	99.7 %
Absorption correction	Multiscan
Max. and min. transmission	1.000 and 0.393
Refinement method	Full-matrix least-squares on F^2
Data / restraints / parameters	3613 / 0 / 208
Goodness-of-fit on F^2	0.822
Final R indices [I>2sigma(I)]	R1 = 0.0330, wR2 = 0.0834
R indices (all data)	R1 = 0.0360, wR2 = 0.0868
Largest diff. peak and hole	1.519 and -1.977 $e.Å^{-3}$

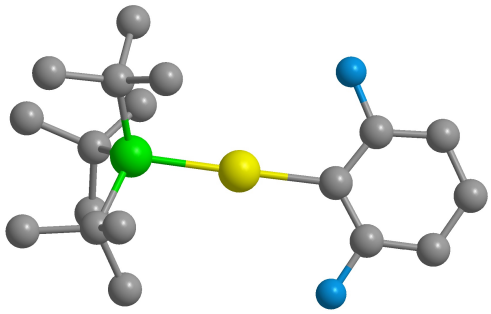

Figure E4. X-ray crystal structure of **23**.

Table E4. Crystal data and structure refinement for **23**.

Identification code	**23**	
Empirical formula	C18 H30 Au F2 P	
Formula weight	512.36	
Temperature	93(2) K	
Wavelength	0.71073 Å	
Crystal system	Monoclinic	
Space group	P2(1)/c	
Unit cell dimensions	a = 17.458(5) Å	a= 90°.
	b = 15.145(3) Å	b= 116.557(5)°.
	c = 16.548(5) Å	g = 90°.
Volume	3913.6(17) $Å^3$	
Z	8	
Density (calculated)	1.739 Mg/m^3	
Absorption coefficient	7.612 mm^{-1}	
F(000)	2000	
Crystal size	0.10 x 0.10 x 0.05 mm^3	
Theta range for data collection	2.46 to 25.37°.	
Index ranges	-21<=h<=17, -17<=k<=18, -12<=l<=19	
Reflections collected	24126	
Independent reflections	7109 [R(int) = 0.0540]	
Completeness to theta = 25.00°	99.6 %	
Absorption correction	Multiscan	
Max. and min. transmission	1.000 and 0.398	

Refinement method	Full-matrix least-squares on F^2
Data / restraints / parameters	7109 / 0 / 397
Goodness-of-fit on F^2	0.801
Final R indices [I>2sigma(I)]	R1 = 0.0326, wR2 = 0.0748
R indices (all data)	R1 = 0.0375, wR2 = 0.0788
Largest diff. peak and hole	1.330 and -1.492 e.Å^{-3}

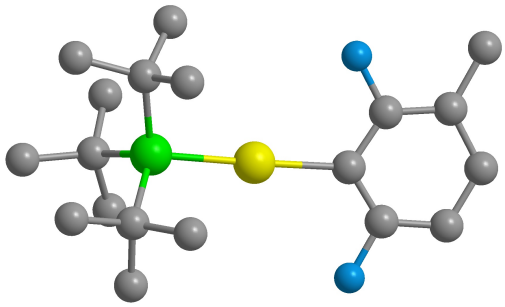

Figure E5. X-ray crystal structure of **24**.

Table E5. Crystal data and structure refinement for **24**.

Identification code	**24**	
Empirical formula	C19 H32 Au F2 P	
Formula weight	526.38	
Temperature	93(2) K	
Wavelength	0.71073 Å	
Crystal system	Monoclinic	
Space group	P2(1)/c	
Unit cell dimensions	a = 10.433(9) Å	a= 90°.
	b = 12.677(8) Å	b= 104.65(2)°.
	c = 16.210(13) Å	g = 90°.
Volume	2074(3) Å^3	
Z	4	
Density (calculated)	1.686 Mg/m^3	
Absorption coefficient	7.184 mm^{-1}	

F(000)	1032
Crystal size	0.10 x 0.10 x 0.10 mm^3
Theta range for data collection	2.02 to 25.35°.
Index ranges	-10<=h<=12, -12<=k<=15, -19<=l<=17
Reflections collected	12548
Independent reflections	3761 [R(int) = 0.0724]
Completeness to theta = 25.00°	99.1 %
Absorption correction	Multiscan
Max. and min. transmission	1.000 and 0.340
Refinement method	Full-matrix least-squares on F^2
Data / restraints / parameters	3761 / 6 / 210
Goodness-of-fit on F^2	1.241
Final R indices [I>2sigma(I)]	R1 = 0.0676, wR2 = 0.2130
R indices (all data)	R1 = 0.0978, wR2 = 0.2908
Largest diff. peak and hole	4.138 and -4.698 e.$Å^{-3}$

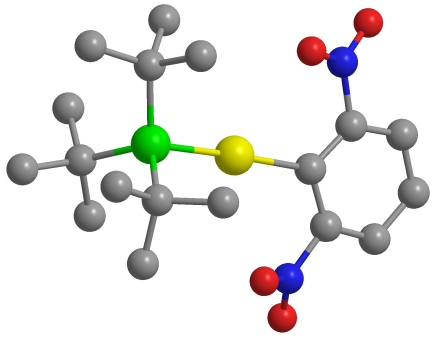

Figure E6. X-ray crystal structure of **25**.

Table E6. Crystal data and structure refinement for **25**.

Identification code	**25**
Empirical formula	C18 H30 Au N2 O4 P
Formula weight	566.38
Temperature	93(2) K
Wavelength	0.71073 Å

Crystal system	Monoclinic	
Space group	P2(1)/n	
Unit cell dimensions	a = 8.837(4) Å	a= 90°.
	b = 20.754(7) Å	b= 106.169(12)°.
	c = 11.608(5) Å	g = 90°.
Volume	2044.6(14) $Å^3$	
Z	4	
Density (calculated)	1.840 Mg/m^3	
Absorption coefficient	7.298 mm^{-1}	
F(000)	1112	
Crystal size	0.30 x 0.10 x 0.10 mm^3	
Theta range for data collection	1.96 to 25.36°.	
Index ranges	-8<=h<=10, -24<=k<=23, -13<=l<=11	
Reflections collected	12607	
Independent reflections	3686 [R(int) = 0.0916]	
Completeness to theta = 25.00°	98.8 %	
Absorption correction	Multiscan	
Max. and min. transmission	1.000 and 0.361	
Refinement method	Full-matrix least-squares on F^2	
Data / restraints / parameters	3686 / 6 / 236	
Goodness-of-fit on F^2	1.155	
Final R indices [I>2sigma(I)]	R1 = 0.0433, wR2 = 0.1234	
R indices (all data)	R1 = 0.0489, wR2 = 0.1579	
Largest diff. peak and hole	3.357 and -2.467 $e.Å^{-3}$	

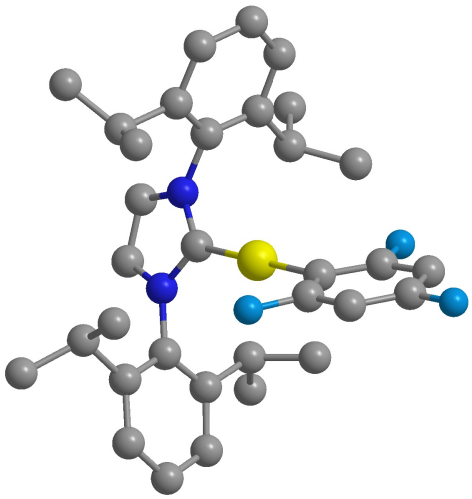

Figure E7. X-ray crystal structure of **40**.

Table E7. Crystal data and structure refinement for **40**.

Identification code	**40**	
Empirical formula	C33 H38 Au F3 N2	
Formula weight	716.62	
Temperature	93(2) K	
Wavelength	0.71073 Å	
Crystal system	Monoclinic	
Space group	P2(1)/n	
Unit cell dimensions	a = 10.905(3) Å	a= 90°.
	b = 20.102(5) Å	b= 100.793(7)°.
	c = 14.188(4) Å	g = 90°.
Volume	3055.1(14) $Å^3$	
Z	4	
Density (calculated)	1.558 Mg/m^3	
Absorption coefficient	4.857 mm^{-1}	
F(000)	1424	
Crystal size	0.20 x 0.10 x 0.02 mm^3	
Theta range for data collection	2.15 to 25.35°.	
Index ranges	-10<=h<=13, -21<=k<=24, -16<=l<=17	
Reflections collected	19176	
Independent reflections	5578 [R(int) = 0.0523]	

Completeness to theta = 25.00°	99.7 %
Absorption correction	Multiscan
Max. and min. transmission	1.000 and 0.730
Refinement method	Full-matrix least-squares on F^2
Data / restraints / parameters	5578 / 0 / 352
Goodness-of-fit on F^2	0.819
Final R indices [I>2sigma(I)]	R1 = 0.0324, wR2 = 0.0724
R indices (all data)	R1 = 0.0418, wR2 = 0.0784
Largest diff. peak and hole	1.640 and -0.988 e.$Å^{-3}$

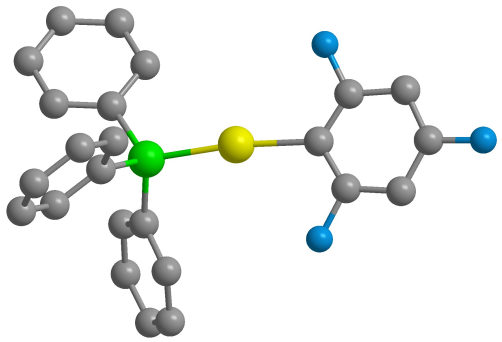

Figure E8. X-ray crystal structure of **41**.

Table E8. Crystal data and structure refinement for **41**.

Identification code	**41**	
Empirical formula	C24 H17 Au F3 P	
Formula weight	590.31	
Temperature	93(2) K	
Wavelength	0.71073 Å	
Crystal system	Monoclinic	
Space group	C2/c	
Unit cell dimensions	a = 11.677(4) Å	a= 90°.
	b = 13.180(4) Å	b= 95.868(10)°.
	c = 26.365(9) Å	g = 90°.

Volume	4037(2) $Å^3$
Z	8
Density (calculated)	1.943 Mg/m^3
Absorption coefficient	7.403 mm^{-1}
F(000)	2256
Crystal size	0.15 x 0.10 x 0.03 mm^3
Theta range for data collection	2.41 to 25.32°.
Index ranges	-14<=h<=12, -12<=k<=15, -31<=l<=26
Reflections collected	12007
Independent reflections	3617 [R(int) = 0.0597]
Completeness to theta = 25.00°	98.3 %
Absorption correction	Multiscan
Max. and min. transmission	1.0000 and 0.3531
Refinement method	Full-matrix least-squares on F^2
Data / restraints / parameters	3617 / 0 / 263
Goodness-of-fit on F^2	1.205
Final R indices [I>2sigma(I)]	R1 = 0.0524, wR2 = 0.1545
R indices (all data)	R1 = 0.0743, wR2 = 0.2302
Largest diff. peak and hole	3.892 and -5.155 $e.Å^{-3}$

Chapter Three: Gold-Mediated Double C–H Activation Cross-Coupling[ii]

3.1 Introduction

The assembly of complex organic frameworks relies on a number of transformations, not least of these being construction of the biaryl motif. Although highly effective and well studied, the traditional cross-coupling of an aryl (pseudo)halide and organometallic species (scheme 78, **A**) suffers from inherently poor step- and atom-economy. With an ever-growing drive towards the development of "greener" chemistry processes, such wasteful and convoluted synthetic pathways are increasingly disadvantageous. Consequently, the emergence of C–H activation as a progressively viable alternative to prefunctionalisation, has led to an increase in the study of coupling methodologies based on this powerful mode of reactivity.[90]

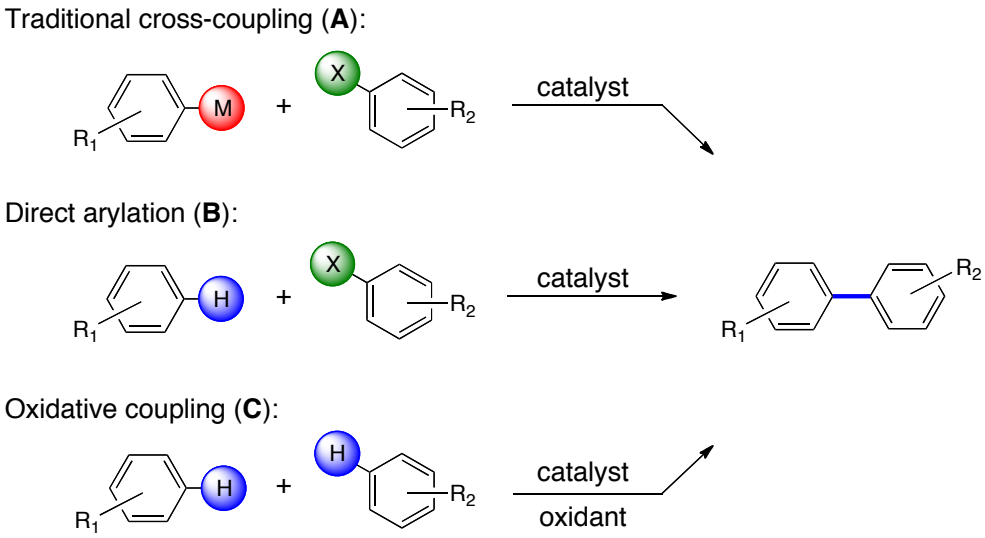

Scheme 78: Traditional and direct routes to aromatic cross-coupling. Where M and X are a metal and (pseudo)halide, respectively.

[ii] This project was conducted in collaboration with Dr X. Cambeiro and Dr P. Lu, although their contributions will not be discussed. See reference 98 for complete details of the project.

In this regard, the ultimate application of C–H activation is a cross-coupling in which neither partner is prefunctionalised (**C**, scheme 78).[91] The use of such oxidative cross-couplings would substantially streamline synthetic strategies. Additionally, the use of O_2 as the terminal oxidant would theoretically lead to the generation of only H_2O as waste, making them exceptionally environmentally friendly. However, overcoming the intrinsically low reactivity of the C–H bond, frequently necessitates the use of harsh reaction conditions, with temperatures commonly exceeding 110 ºC. The activation of only one specific C–H bond, amidst many, poses another challenge. When neither coupling partner is prefunctionalised this translates into inter- versus intra-molecular selectivity issues, as well as regioselectivity challenges. Ensuring that cross-, rather than homo-, coupling is achieved often means using a vast excess (40-100 equivalents) of one coupling partner.

Clearly, a key step towards improving these oxidative cross-coupling procedures is the development of milder C–H activation conditions. With this in mind, we considered our gold(I) C–H activation procedure to be an excellent starting point. Our conditions allow the auration of electron-deficient arenes, under remarkably mild reaction conditions, to generate the corresponding aryl gold(I) species in excellent yields.

Gold(III) salts, on the other hand, are well known for their ability to perform the C–H activation of electron-rich arenes, also under very mild reaction conditions. We envisaged the development of a procedure which would exploit the complementary selectivites of gold(I) and gold(III), in a mild and novel oxidative cross-coupling process (scheme 79). We hypothesised that the oxidation of an aryl gold(I) species (**XXII**), generated via our C–H activation procedure, would lead to the corresponding aryl gold(III) moiety (**XXIII**). This gold(III) species would then allow the potential for a second C–H activation, this time with opposite selectivity to the first. Following this second activation, of an electron-rich arene, we would obtain a gold(III) species which could then undergo reductive elimination, to yield a cross-coupled biaryl product along with the regenerated gold(I) centre.

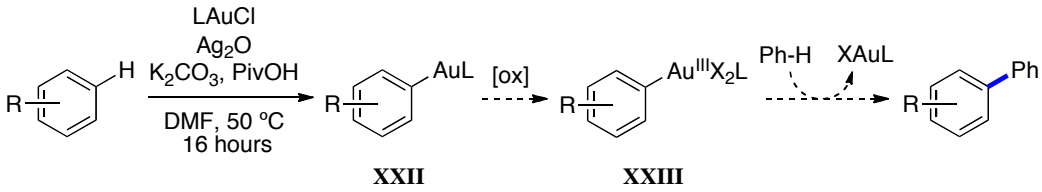

Scheme 79. Our envisaged gold(I)/(III)-mediated oxidative cross-coupling process.

Thus, we set out to explore the potential to harness the reactivity of both gold(I) and gold(III) in such a manner, to perform a mild and selective oxidative cross-coupling.

3.2 Optimisation of the reaction conditions

To assess the viability of our proposed oxidative cross-coupling, we initially explored the coupling of aryl gold(I) **43**, prepared in 99% yield under our standard C–H activation procedure, with 2-iodoanisole (table 9). Gold does not typically mediate cross-coupling procedures, as a reluctance to cycle between oxidation states has largely precluded it from this arena. However, the use of strong oxidising agents has been shown to promote the oxidation of gold(I) to gold(III).[92] A reaction temperature of 50 ºC was selected, to provide compatibility with the gold(I) C–H activation conditions.

Table 9. Optimisation of the oxidative cross-coupling with aryl gold(I) **43** with 2-iodoanisole.

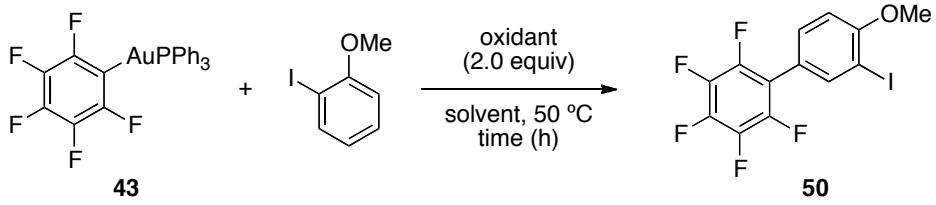

Entry	Oxidant	Solvent	Yield (%)[a]
1	-	DCE	0
2	Selectfluor	DCE	traces
3	$PhI(OAc)_2$	DCE	48
4	$PhI(OCOCF_3)_2$	DCE	51
5	$PhI(OPiv)_2$	DCE	81
6	PhI(OH)OTs	DCE	91
7[b]	PhI(OH)OTs	DCE	81
8	PhI(OH)OTs	MeCN	34
9	PhI(OH)OTs	Dioxane	52
10	PhI(OH)OTs	DMF	0
11	PhI(OH)OTs	THF	22

[a] Yields determined by ^{1}H NMR spectroscopy, using an internal standard. [b] Reaction with 1.0 equivalent of the oxidant.

Oxidant screening revealed that the use of hypervalent iodine species led to the successful formation of the desired biaryl **50** (entries 3-6, table 9), whereas no product was generated in the absence of oxidant (entry 1) or the presence of Selectfluor (entry 2). The iodosyl oxidant PhI(OH)OTs led to the greatest yield, generating the desired cross-coupling product in 91% yield (entry 6). Further optimisation demonstrated that while the use of non-polar solvents led to formation of the desired product in moderate to excellent yields (entries 6 and 9), poor product yields were observed in the presence of polar solvents (entries 8, 10 and 11).

While we were delighted to have successfully determined the viability of this process, we were disappointed to note that the necessary reaction conditions were at odds with those required for our gold(I) C–H activation. Use of DMF, the optimal solvent for the gold(I) auration, led to no formation of the desired product at all. In fact, whereas the gold(I) C–H activation requires polar solvents, this gold(III) activation demands the use of non-polar solvents. This clearly indicated that developing a procedure mediated by a sub-stoichiometric quantity of gold would pose a great challenge.

The involvement of gold in the construction of biaryl products had previously been demonstrated in the gold(III)-mediated homo-coupling of electron-rich (hetero)arenes.[33] The use of gold(I) species had also been employed stoichiometrically in palladium- and nickel-catalysed cross-couplings.[81] However, to the best of our knowledge, this process constitutes the first example of biaryl construction via a gold(I)/gold(III) oxidative cross-coupling, employing two discrete C–H activation steps.

3.3 Scope of the reaction

With our optimised reaction conditions in hand, we set out to explore the scope of the reaction. We first decided to investigate the potential of this reaction, with respect to the electron-deficient arene. Application of these reaction conditions to a number of aryl gold(I) species, all generated via our gold(I) C–H activation, led to the successful generation of a number of biaryl products (scheme 80).

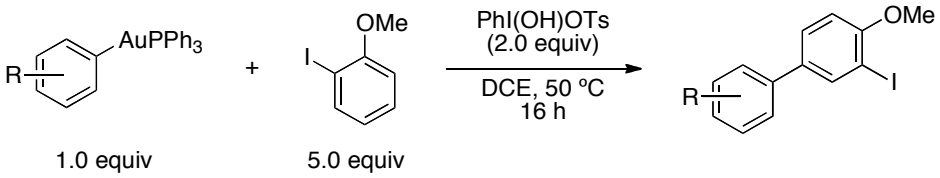

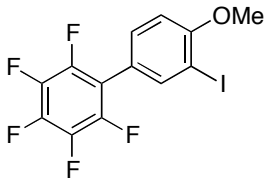

50, 84%

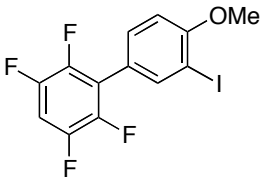

51, 76%

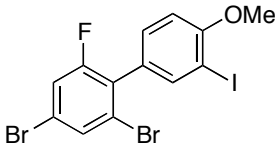

52, 58%

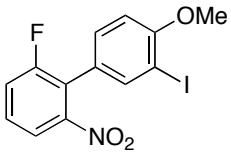

53, 86%

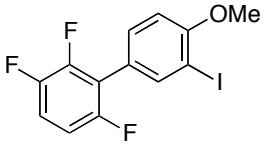

54, 70%

Scheme 80. Scope of the electron-poor arene in the gold-mediated oxidative cross-coupling. All yields are of isolated pure material.

We were pleased to observe that products **50-54** were generated in good yields. Furthermore, as we had hoped, the reaction affords excellent selectivity with cross-coupling products predominantly obtained over their homo-coupling counterparts. Only traces of biaryl products resulting from the homo-coupling of the electron-rich arene were observed by GC-MS analysis. A blank reaction, with the exclusion of the aryl gold(I) species **43** under otherwise standard oxidative cross-coupling reaction conditions, was also conducted. Under these conditions,

no homo-coupling of the electron-rich arene was observed at all. This would suggest that, where this product is observed, a gold species is mediating the formation of the homo-coupled biaryl. This process would presumably be mediated by a gold(III) species, in a process analogous to that described by Tse *et al.*[33] (scheme 24). In the presence of excess oxidant and the reasonable assumption that gold(I) is generated, via reductive elimination concurrently with the formation of our desired biaryl, it is possible that an additional gold(III) species may be formed in solution (see scheme 84). It may be that this gold(III) species mediated the formation of homo-coupled products, where they are observed. Therefore it may not be assumed that this homo-coupling takes place to the detriment of our desired cross-coupling, nor that it occurs with any preference for homo- over cross-coupling.

The lowest, yet still moderate, yield was obtained for product **52**. This biaryl is the coupling product of 2-iodoanisole and product **45**, in which the gold(I) sits between a fluorine and a bulky bromine substituent. While the excellent yield of **45** indicates that space is not an issue for the initial C–H activation, it is possible that the steric bulk about the gold(I) centre hindered subsequent access and led to a decreased yield of the cross-coupled product **52**.

Remarkably, each of the products **50**-**54** retained their iodine substituents, something not observed in palladium-mediated cross-coupling processes. This substituent not only provides a valuable handle for further transformations, but also illustrates the unique reactivity of this system.

We were delighted by the highly successful implementation of our cross-coupling strategy for a number of electron-deficient arenes and eager to explore the procedure in greater depth. Having explored the scope of the reaction, with respect to the gold(I) C–H activation process, we turned to the gold(III) activation and an investigation of the breadth of this process, beyond the auration of 2-iodoanisole.

A number of electron-rich (hetero)arenes underwent cross-coupling, generating the corresponding biaryl products in good yields. (scheme 81).

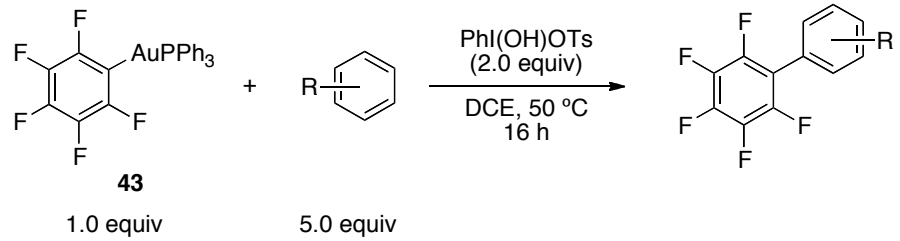

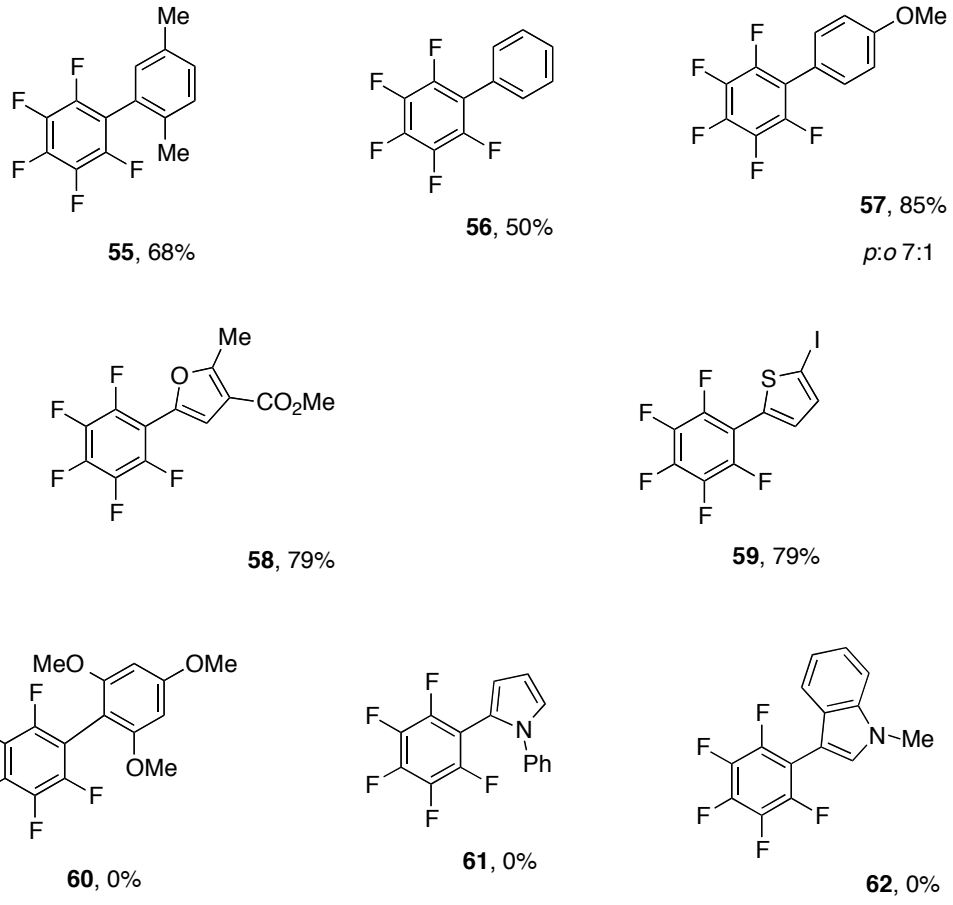

Scheme 81. Scope of the electron-rich arene in the gold-mediated oxidative cross-coupling. All yields are of isolated pure material.

We were pleased to observe the formation of cross-coupling products **55-59**, demonstrating the potential of the gold(III) C–H activation. Again, we observed excellent selectivity towards cross-coupling over homo-coupling products, affording us further support for this redox-controlled selectivity approach.

Of particular note is the activation of benzene, under these mild reaction conditions, generating biaryl product **56** in good yield and demonstrating the capability of this procedure.

Furthermore, the regioselectivity of this gold-mediated system differs from that observed for analogous palladium-catalysed procedures. This is exemplified by the coupling of aryl gold(I) **43** with anisole, generating biaryl product **57** as a mixture of *para*- and *ortho*- coupled products (7:1). Whereas palladium-mediated systems generally lead to *para*- and *meta*- couplings.[89]

When 1,3,5-trimethoxybenzene, *N*-phenylpyrole and *N*-methylindole were applied to our cross-coupling procedure with aryl gold(I) **43** their corresponding biaryl products (**60**, **61** and **62**, respectively) were not generated. The increased nucleophilicty of these (hetero)arenes most likely led to their reaction with the hypervalent iodine oxidant, rendering both reagents unavailable to perform the desired cross-coupling.[iii] This hypothesis is supported by a recent report by Nevado *et al.*, in which these (hetero)arenes were successfully employed in a similar multi-step gold-mediated cross-coupling procedure[93]. Their approach differed in isolation of the oxidised aryl gold(III) species (analogous to **XXVI** in scheme 82) before application of the electron-rich (hetero)arene, thus avoiding any deleterious side-reactions with the oxidant.

We initially selected to optimise and perform our cross-coupling reactions at 50 ºC in order to provide compatibility with our gold(I) C–H activation procedure. We are delighted that the coupling proceeds under such a mild reaction temperature and, given that the gold(I) activation proceeds to optimum product yield at this temperature, we have no immediate desire to perform this cross-coupling at any alternative reaction temperature. Nonetheless, we conducted a brief survey of reaction temperatures with the coupling of aryl gold(I) **43** and anisole, aiming to generate the biaryl product **57** (table 10).

[iii] For a detailed explanation see the supporting information of reference 98.

Table 10. Oxidative cross-coupling at alternative reaction temperatures.

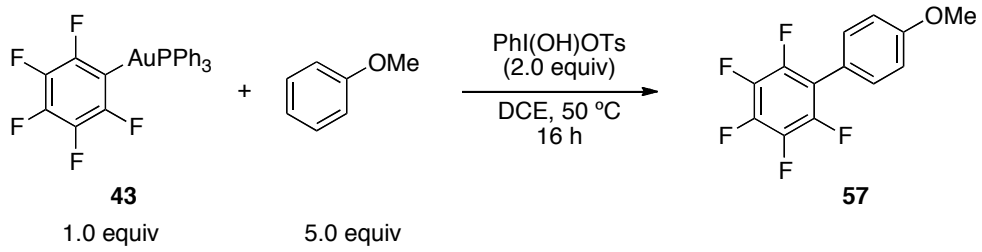

Entry	Reaction Temperature (ºC)	Yield of Product 57 (%)[a]
1	25	89
2	50	89
3	60	38

[a] Yields determined by ^{1}H NMR spectroscopy, using an internal standard.

These reactions demonstrate that a reduction in the reaction temperature has no detrimental impact on the formation of the desired cross-coupling product **57**. However, an increase in the reaction temperature does lead to a decrease in the product yield. This may be a consequence of reduced stability of a gold(I) or gold(III) species at elevated temperatures, leading to reduced generation of the biaryl product.

3.4 Mechanistic proposal

Our initial ambition was to harness the opposing reactivity of gold(I) and gold(III) in a mild and highly selective oxidative cross-coupling procedure. We had envisaged the development of a gold-mediated process such as depicted in scheme 82. Employment of our gold(I) C–H activation protocol would lead to auration of an electron-deficient arene and formation of aryl gold(I) **XXV** which, in the presence of a strong oxidant, could be oxidised to the corresponding aryl gold(III) species **XXVI**. This gold(III) centre would then be responsible for the second C–H activation, but this time being guided by the preference of the gold(III) towards activation of an electron-rich arene, to form species **XXVII**. Reductive elimination would then yield the desired cross-coupling product and regenerate the gold(I) centre, which would then be free to perform another C–H activation and restart the cycle.

The attraction of such a process lies in the remarkable reactivity of gold salts, which would endow the procedure with excellent reactivity under very mild reaction conditions.

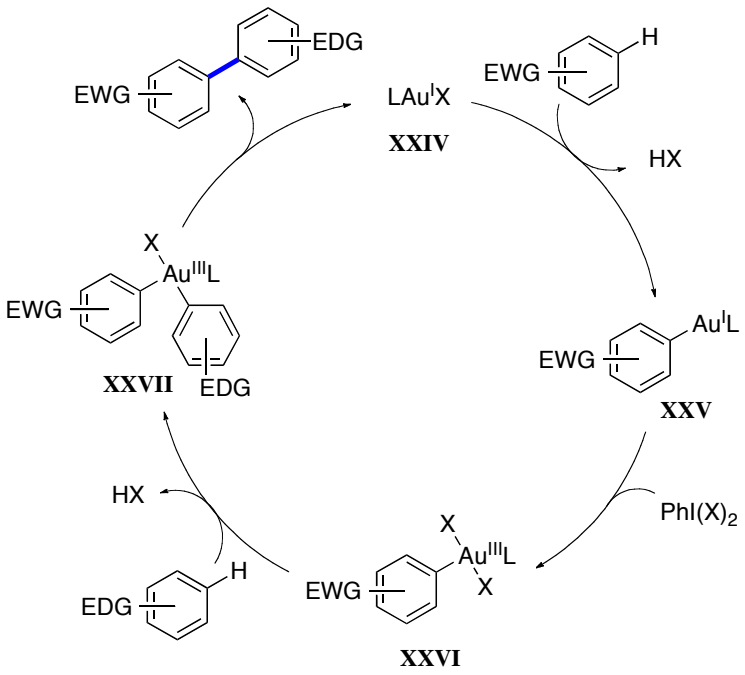

Scheme 82. Our envisaged gold-mediated oxidative cross-coupling.

However, early on in our optimisation process it became apparent that the development of such a procedure would be complicated by the disparity in the conditions demanded by the gold(I) and gold(III) C–H activations. Undeterred, we maintained our aim to assess the viability of this cross-coupling. However, this conflicting nature of the conditions, required for each consecutive activation, led us to approach this challenge in a two-step process. Aiming to gain greater insight into how this reaction operates, we conducted a series of investigations.

A kinetic isotope effect experiment was performed, with aryl gold(I) **43**, benzene and deuterated benzene (scheme 83). The ratio of products **56** and **56-d$_5$** was determined by mass spectrometric analysis to give a kinetic isotope effect (k_H/k_D) of 1.1. This value indicates that C–H bond-breaking is not involved in the rate-determining step, which would be consistent with an electrophilic aromatic substitution process for this C–H activation step.

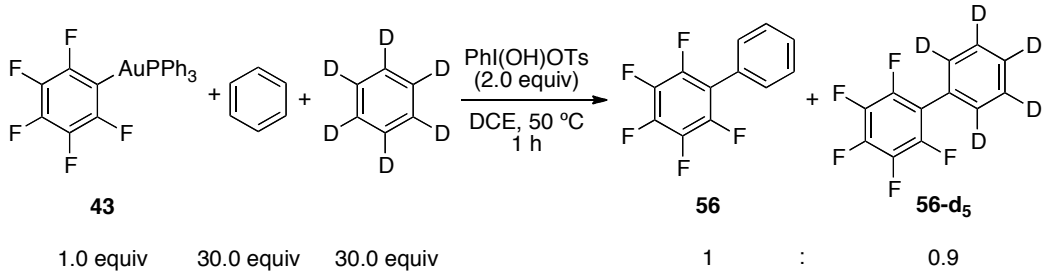

Scheme 83. Kinetic isotope effect experiment using benzene and its deuterated counterpart to couple with aryl gold(I) **43**. The results were determined by mass spectrometry.

Throughout the development of this oxidative cross-coupling we regularly analysed crude reaction mixtures by ^{1}H NMR spectroscopy in order to determine the product yield, with use of an internal standard. ^{31}P NMR analysis of the same samples revealed the presence of a peak at 37 ppm, which could not be attributed to either the aryl gold(I) species (41 ppm) nor the gold(I) chloride (33 ppm). In our initial mechanistic proposal (scheme 82) we hypothesised that a reductive elimination step would yield our desired biaryl product, with concurrent

liberation of gold(I) species **XXIV**. Given our use of the hypervalent iodine oxidant PhI(OH)OTs, we reasoned that this species may be the corresponding gold(I) tosylate. Aiming to verify this assertion, we synthesised triphenylphosphinegold(I) tosylate via transmetallation between the gold(I) chloride and silver tosylate. However, ^{31}P NMR analysis of the gold(I) tosylate revealed a peak at 27 ppm, indicating that this was not the species that we observed at the conclusion of our cross-coupling. We rationalised that this may be a consequence of the excess oxidant present in the reaction medium, liberation of the gold(I) tosylate may be followed by interaction with the oxidant to generate a gold(III) species. Indeed, treatment of our pre-prepared gold(I) tosylate with an equivalent of PhI(OH)OTs led to the appearance of a peak at 37 ppm. Therefore, under these conditions, it would appear that a pathway such as that represented in scheme 84 is followed.

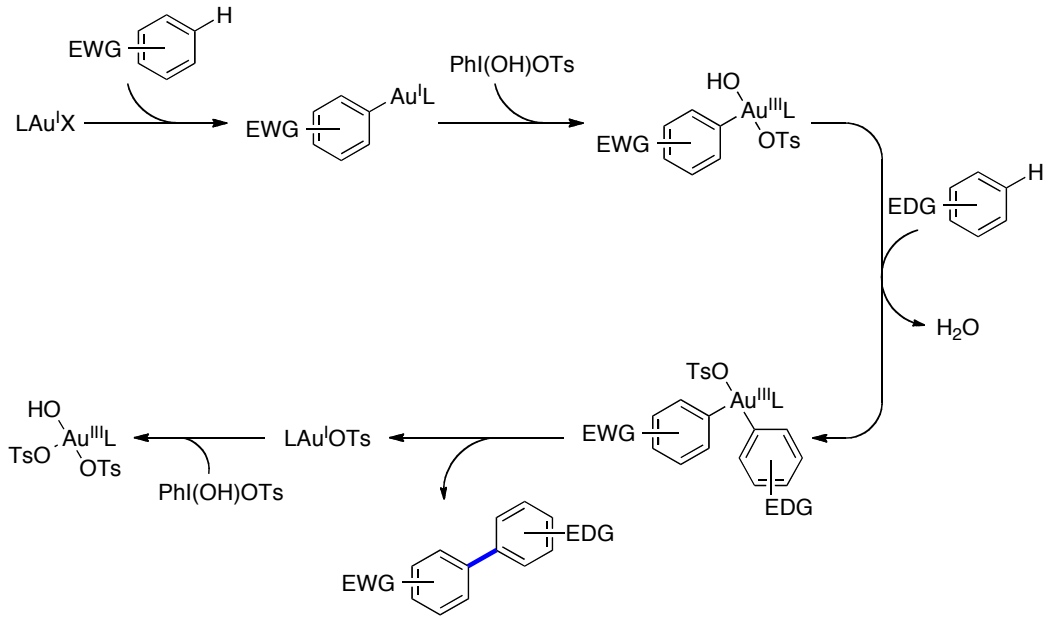

Scheme 84. Proposed reaction pathway for the oxidative cross-coupling.

Aiming to corroborate these observations, an oxidative cross-coupling was monitored intermittently by ^{31}P NMR analysis. This investigation revealed that generation of the biaryl product is accompanied by the initial formation of gold(I) tosylate (27 ppm). However, this species is short-lived and under the

oxidising reaction conditions it is quickly converted to a gold(III) species (37 ppm).

The liberation of a gold(I) tosylate, with reductive elimination from the gold(III) centre, led us to question whether this species would be able to perform the gold(I) C–H activation. Our long-term ambition would be to develop a catalytic version of this cross-coupling, in which both C–H activation steps could be performed in one-pot. Of course, the conflicting requirements of each auration step is the main barrier to such a process, but the knowledge that the liberated gold(I) species is able to restart the cycle would be an asset. With this in mind, we submitted triphenylphosphine gold(I) tosylate to the C–H activation of 1,2,4,5-tetrafluorobenzene, under our standard conditions (scheme 85).

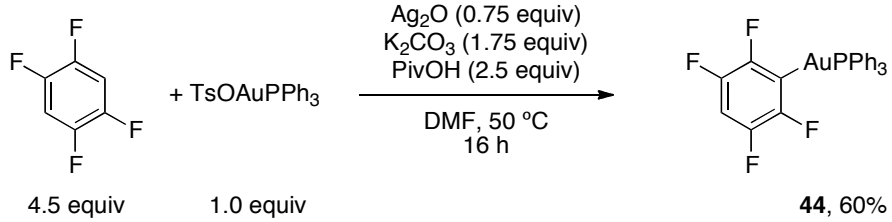

Scheme 85. Application of gold(I) tosylate to the C–H activation of 1,2,4,5-tetrafluorobenzene. The yield was determined by ^{1}H NMR analysis, using an internal standard.

We were pleased to observe that the desired aryl gold(I) product **44** was generated in 60% yield. This is somewhat lower than the 91% yield obtained with use of the corresponding gold(I) chloride. However, at this stage, the knowledge that this species is able to perform the auration of an electron-deficient arene is encouraging.

We were conscious that our development of this oxidative cross-coupling as a two-step process may undermine our assertion that it proceeds with excellent selectivity. Our ambition to harness the opposing reactivities of gold(I) and gold(III) to achieve cross- rather than homo-coupled products had indeed been achieved. However the necessary separation of the two C–H activation steps

could understandably lead to doubt over whether this selectivity stemmed from gold(I)/gold(III) control or was rather more contrived. For this reason, we performed two competition reactions (schemes 86 and 87)

The first of these competition reactions assessed the selectivity of the gold(I) C–H activation. This was achieved by submitting triphenylphosphinegold(I) chloride to the auration of 1-fluoro-3-nitrobenzene in the presence of 2-iodoanisole, under otherwise standard reaction conditions (scheme 86). The expected aryl gold(I) product **46** was generated in 64% yield, with no evidence for the C–H activation of the electron-rich arene. This demonstrated that the gold(I) C–H activation is highly selective towards electron-deficient arenes.

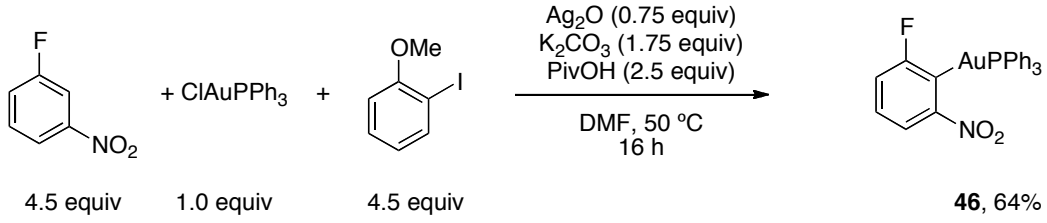

Scheme 86. Gold(I) C–H activation in the presence of an electron-rich arene.

The next competition experiment was performed to assess the selectivity of the gold(III) C–H activation step and generation of the biaryl product (scheme 87). In this case, we submitted aryl gold(I) species **46** to cross-coupling with 2-iodoanisole, in the presence of 1,2,4,5-tetrafluorobenzene.

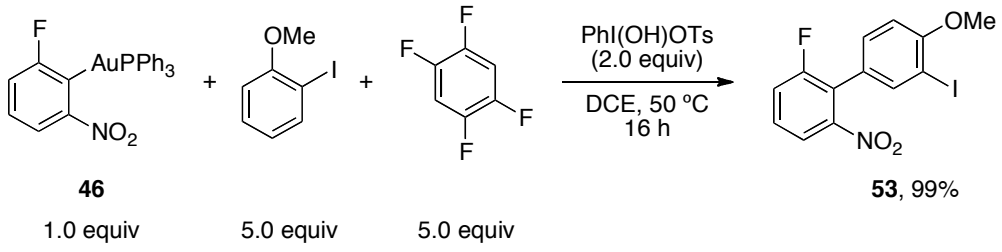

Scheme 87. Oxidative cross-coupling reaction in the presence of an electron-deficient arene.

We were pleased to observe that the desired biaryl product **53** was generated in an excellent 99% yield, as observed by ^{1}H NMR analysis. No traces of products resulting from homo-coupling of either arene were detected and no cross-coupling between the two electron-deficient arenes was observed. These results confirmed the fidelity of gold(III) for the activation of electron-rich arenes and the excellent selectivity of our cross-coupling process.

3.5 Gold-mediated decarboxylative cross-coupling

As previously mentioned, the promise of high step- and atom-economy has driven the development of transformations based around C–H activation. The construction of biaryls via a cross-coupling in which neither partner is prefunctionalised would substantially streamline synthetic strategies, with great financial and environmental benefit. Entailing two distinct C–H activations, this manner of oxidative cross-coupling poses quite a challenge. Along with the harsh reaction temperatures frequently required to break these C–H bonds, the abundance of C–H bonds in organic frameworks leads to selectivity issues.

Neither coupling partner being prefunctionalised means that the avoidance of homo-coupling poses a significant challenge. In effect, one metal centre is required to perform an activation and then undergo a reversal in selectivity in order for the second activation to yield cross-coupled products, rather than a homo-coupled species. Our strategy, to exploit the orthogonal reactivities of gold(I) and gold(III), has allowed us to achieve just this. As such, our gold-mediated oxidative coupling affords excellent selectivity, with cross-coupled products obtained almost exclusively over their homo-coupling counterparts.

This abundance of C–H bonds also leads to issues of regioselectivity, selective activation of only one bond in a molecule containing many can be challenging. As such, regioselectivity is often achieved through the use of directing groups (such as pyridine, amide, carbamate or oxazoline) or through the exploitation of the inherent electronic bias of heterocycles (such a *N*-protected indoles, pyrroles, imidazoles, benzimidazoles and benzofurans) or perfluorinated arenes. These various approaches have led to numerous procedures, with each having a rather limited substrate scope.[89, 90]

Clearly, a generally applicable approach to regioselective control is crucial. In this context, substitution of one coupling partner for readily accessible carboxylic acids provides an extremely advantageous route to cross-coupling (scheme 88).[94, 95]

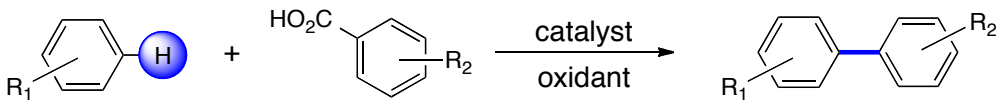

Scheme 88. Decarboxylative arylation as a route to cross-coupling.

As such, decarboxylative direct arylation has emerged as an attractive variation on oxidative cross-coupling. Activation invariably occurs at the carboxylic acid position, thus affording excellent regioselective control on one of the coupling partners. However, while possessing the potential to become a broadly applicable and "green" approach to cross-coupling, examples of decarboxylative arylation are limited, with many suffering the need for harsh reaction conditions and low substrate scope.[96]

Our group has recently reported a novel methodology, employing gold(I) salts to perform the decarboxylative activation of benzoic acids, to generate the corresponding aryl gold(I) species (scheme 89).[97]

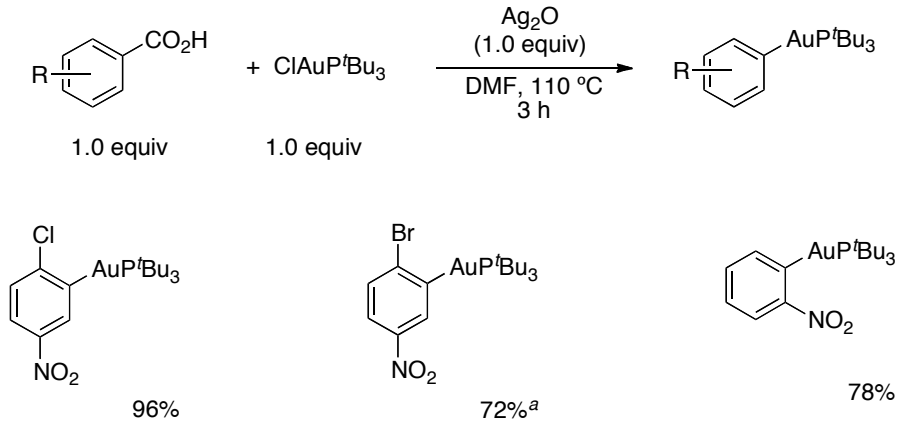

Scheme 89. Gold(I)-mediated decarboxylative activation. [a] 2 hour reaction time.

This decarboxylative activation of (hetero)aromatic carboxylic acids is a notable addition to gold(I) reactivity. The decarboxylation proceeds at markedly lower temperatures than for the other coinage metals copper(I) and silver(I). Furthermore, the resulting aryl gold(I) species are exceptionally stable towards

protodemetallation, a commonly encountered problem in copper(I)- and silver(I)-mediated procedures.

Delighted by the successful implementation of our oxidative cross-coupling strategy, for a number of electron-deficient arenes, we were eager to explore the procedure in greater depth. In particular, we were keen to discover whether application of these conditions to the aryl gold(I) species produced via decarboxylative activation would allow us to access a greater range of biaryl products.

Under these decarboxylative conditions, a range of benzoic acids were aurated to give aryl gold(I) compounds **63**-**69** in good to very good yields (scheme 90).

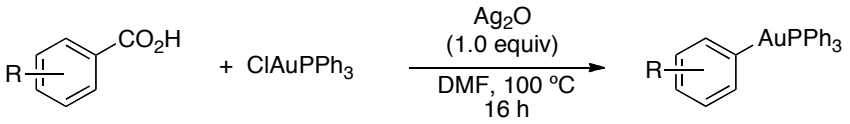

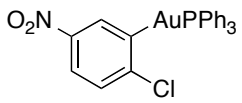

63, 68%

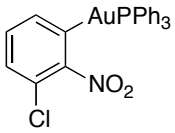

64, 70%

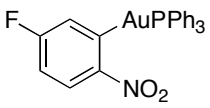

65, 78%

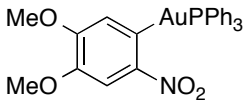

66, 82%

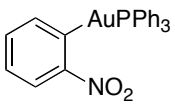

67, 52%

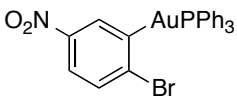

68, 54%

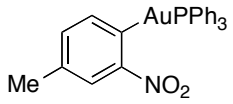

69, 77%

Scheme 90. Use of the gold(I) decarboxylation procedure to access a number of aryl gold(I) products. All yields are of isolated pure material.

Subsequent application of these aryl gold(I) species to our oxidative cross-coupling conditions, with *p*-xylene, led to the generation of biaryl products **70**-**76** in moderate to good yields (scheme 91).

The more electron-rich aryl gold(I) compounds **66** and **69** gave the poorest yields of their respective cross-coupled products (**73** and **76**). This is most likely a result of the decreased electrophilicity of their corresponding gold(III) centres.

As with our gold(I) C–H activation procedure, the reaction conditions for this decarboxylation are at odds with those required for the gold(III) C–H activation. Therefore, this cross-coupling was also performed as a two-step process. Gold(I) maintains its strong affinity for electron-deficient arenes in this decarboxylative activation, with subsequent application of the resulting aryl gold(I) species to our oxidative coupling leading to excellent selectivity for cross-coupled products.

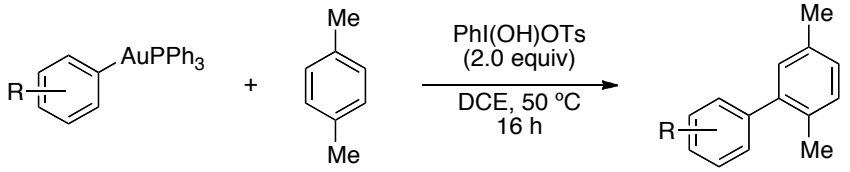

1.0 equiv 5.0 equiv

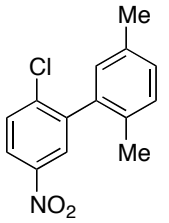

70, 75%

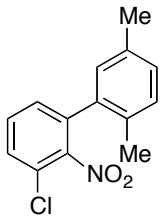

71, 72%

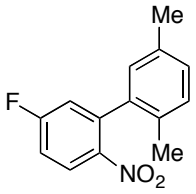

72, 66%

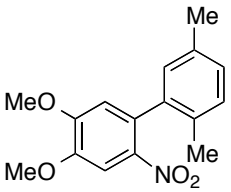

73, 57%

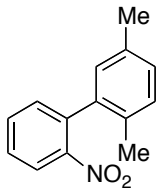

74, 73%

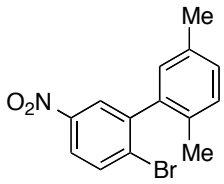

75, 73%

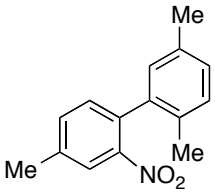

76, 58%

Scheme 91. Use of the gold(I) decarboxylation procedure to access a number of aryl gold(I) products. All yields are of isolated pure material.

Generation of the aryl gold(I) species via decarboxylation means that auration invariably occurs at the carboxylic acid site. This in turn leads to formation of the new carbon-carbon bond at this position, thus affording excellent regioselective control.

In contrast to the gold(I) C–H activation, this decarboxylation requires only one electron-withdrawing group *ortho* to the site of activation. This allows us to access a wider variety of aryl gold(I) products than with our C–H activation procedure alone. As such, a greater range of cross-coupling products are also available with use of both gold(I) activation procedures.

Having successfully explored the scope of this cross-coupling, with respect to the gold(I) activation process we then decided to look at the gold(III) activation. The cross-coupling of aryl gold(I) species **63** with *p*-xylene led to the generation of biaryl **70**, which was the highest yielding product. We therefore selected **63** to explore the gold(III) activation. As such, a number of electron-rich arenes and heteroarenes were successfully applied to our oxidative cross-coupling conditions, to form biaryl products **77**-**88** in good to very good yields (scheme 92).

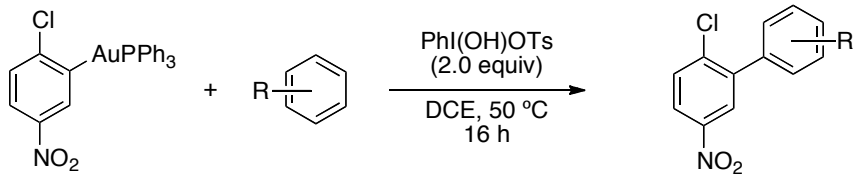

63

1.0 equiv

5.0 equiv

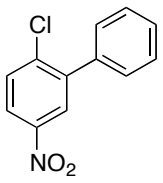

77, 65%

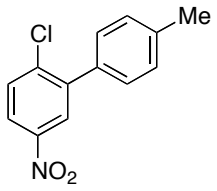

78, 83%

p:*o* 5:1

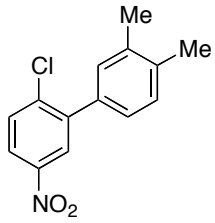

79, 83%

p:*o* 10:1

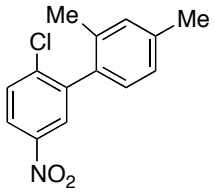

80, 81%

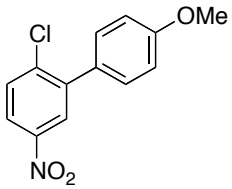

81, 74%

p:*o* 4.2:1

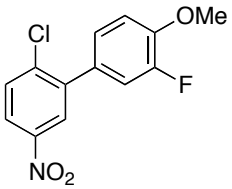

82, 75%

C5:C3 10:1

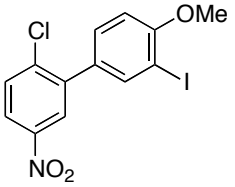

83, 74%

C5:C3 7.5:1

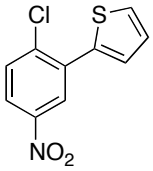

84, 85%

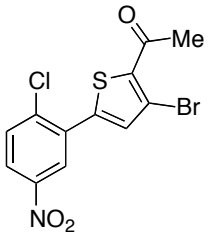

85, 74%

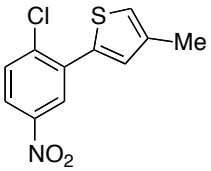

86, 87%

C5:C2 2.7:1

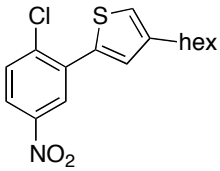

87, 85%

C5:C2 4.3:1

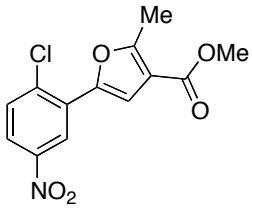

88, 62%

C5:C4 7.5:1

Scheme 92. Use of the gold(I) decarboxylation procedure to access a number of aryl gold(I) products. All yields are of isolated pure material.

The use of alternative ligands on the gold centre was also tested (table 11). Triphenylphosphine provided a superior yield of 75% for cross-coupling product **70** (entry 1, table 11), compared to 54% with tri-*tert*-butylphosphine (entry 2) and only 47% with the *N*-heterocyclic carbene IPr (entry 3).

Table 11. Alternative ligands on the gold centre with the corresponding aryl gold(I) species applied to cross-coupling with *p*-xylene, to give biaryl product **70**.

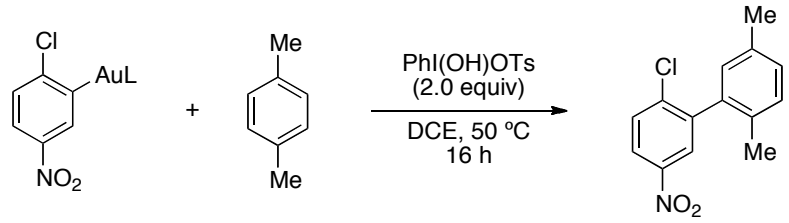

Entry	Aryl Gold(I) Species	Yield of 70 (%)
1	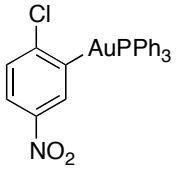 **63**	75
2	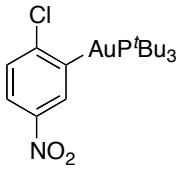 **89**	54
3	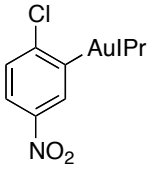 **90**	47

We rationalise that this impact of the ligand on the overall cross-coupling is likely a result of triphenylphosphine providing sufficient stabilisation, whilst not being so bulky as to limit access to the gold centre.

We also performed a kinetic isotope effect experiment for the cross-coupling of aryl gold(I) species **63** with benzene and benzene-d_6, to generate biaryl product **77** and **77-d_5**, respectively (scheme 93).

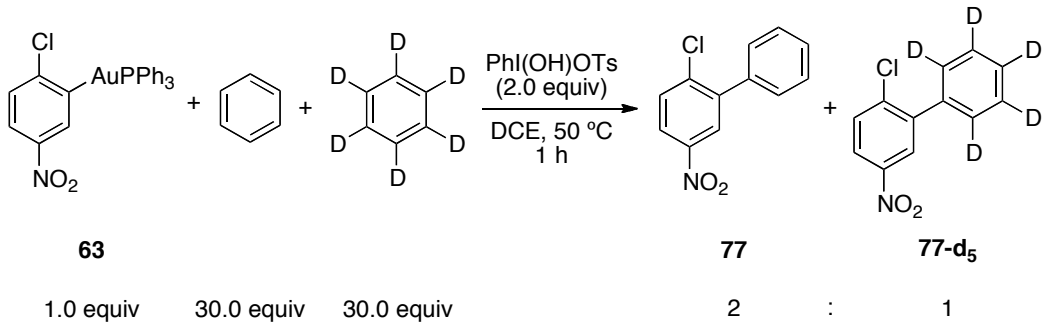

Scheme 93. Kinetic isotope effect experiment for the cross coupling of aryl gold(I) species **63** with benzene and benzene-d_6. The results were determined by mass spectrometry (k_H/k_D = 2.0).

The crude reaction mixture was analysed by mass spectrometry to determine the ratio of the two potential biaryl products **77** to **77-d_5** to be 2:1. This gives us a kinetic isotope effect (k_H/k_D) of 2.0, which is in-keeping with an electrophilic substitution as suggested earlier. The value of this KIE is higher than that determined previously, with the use of aryl gold(I) species **43**. This may be a consequence of the decarboxylative activation, requiring only one aryl *ortho*-substituent, leading to a gold(III) species with less steric hindrance. This may in turn facilitate electrophilic auration, leading to relatively faster formation of a Wheland intermediate and relatively slower cleavage of the C–H bond (scheme 94).

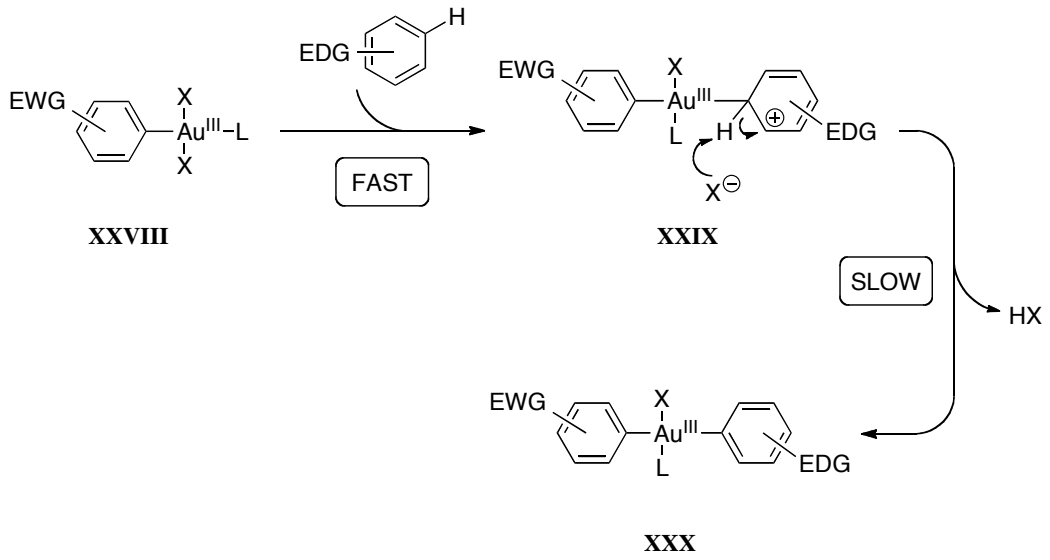

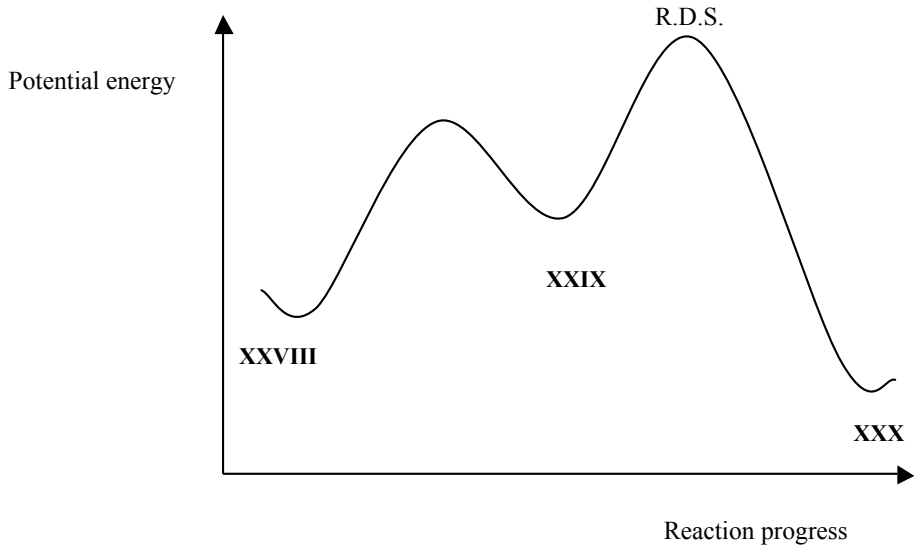

Scheme 94. Proposed rate-determining step of the reaction, proceeding through a Wheland intermediate.

Of course, the difference with this cross-coupling is that one coupling partner is a benzoic acid, undergoing gold(I) activation to liberate carbon dioxide, while the other is not at all prefunctionalised. The necessary two-step approach to this cross-coupling, as with the last, stems from the conflicting requirements of the two subsequent activations. Were it possible to uncover mutually agreeable reaction conditions, then we would expect the potential to develop a catalytic cycle much like that shown in scheme 82. However, for the time being we expect that this oxidative cross-coupling would proceed via a pathway as shown below in scheme 96.

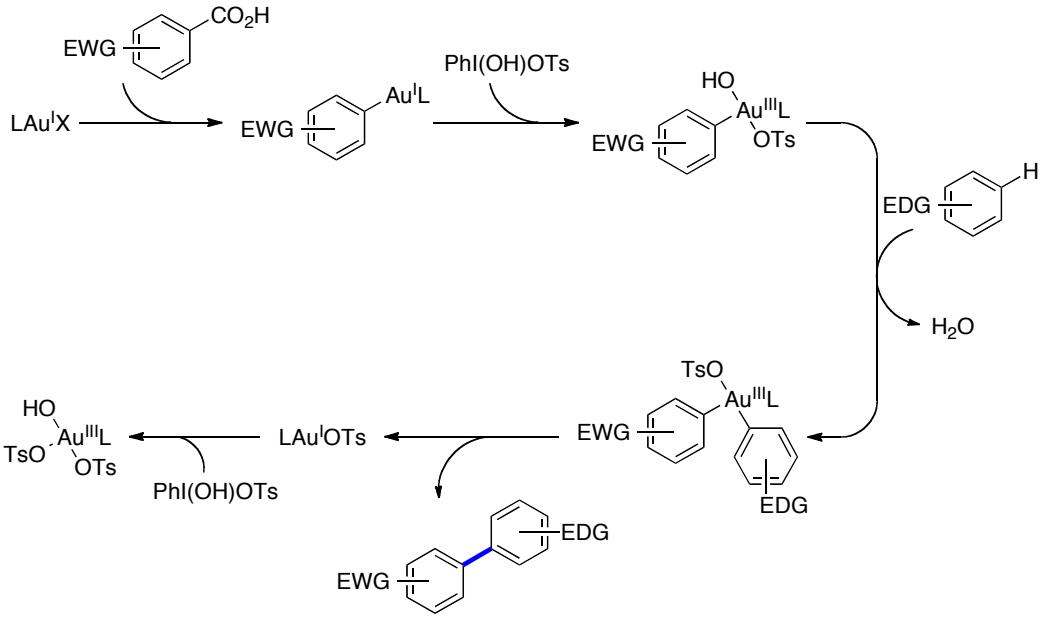

Scheme 95. Proposed pathway for the decarboxylative direct arylation.

3.6 Conclusions

At the outset of this project we had the aim of developing an oxidative cross-coupling for the formation of biaryl products, in which neither coupling partner was prefunctionalised. Our work towards developing a gold(I) C–H activation procedure had highlighted the affinity of this gold(I) for electron-deficient arenes, which was in complete contrast to the preference of the more electrophilic gold(III) for electron-rich arenes. We envisaged exploiting these two opposing modes of reactivity to achieve a highly selective cross-coupling process, which would benefit from the very mild reaction conditions generally observed for gold-mediated processes.

During our optimisation of this oxidative cross-coupling, two things became very quickly apparent. The first was that we could indeed exploit the ability of both gold(I) and gold(III) to perform the selective C–H activation of electron-poor and electron-rich arenes, respectively. We were able to generate our desired biaryl products, with excellent selectivity, in very good yields via this remarkably mild oxidative cross-coupling. However, the second was that the conflicting nature of the reaction conditions, required for each consecutive C–H activation, would necessitate a two-step procedure. Nonetheless, this process is a notable addition to the ever-increasing number of gold- mediated transformations.[98]

Furthermore, the power of gold(I) to perform the decarboxylative activation of arenes and heteroarenes was also harnessed in order to expand the scope of this cross-coupling procedure. Allowing us to access a wider variety of aryl gold(I) products, this decarboxylation was a valuable accompaniment to our C–H activation procedure.

Although we have been pleased with our achievements thus far, in the development of a gold-mediated cross-coupling, this is very much an ongoing project. Current efforts in the group are being directed towards the development of a one-pot catalytic process, which would ideally require a sub-stoichiometric quantity of gold. With this in mind, the group is undertaking a thorough kinetic and mechanistic study of the whole reaction. It is hoped that this approach will

allow an optimization of the overall process, rather than each stage individually, and identification of the ideal ligands, solvents and temperatures. With a greater understanding, it is also hoped that green principles could be applied to develop a process that is more environmentally benign. In particular, greener alternatives to the currently employed solvent and iodine(III) oxidant would go a long way towards improving the environmental impact of the cross-coupling.

Of course, before deciding to take this step back, attempts were made to perform this cross-coupling as a one-pot process (scheme C2). Solvent optimisation had revealed the conflicting nature of the requirements for gold(I) and gold(III) C–H activation. However, the gold(III) C–H activation had been performed in dioxane to generate the desired biaryl product in a reasonable 52% yield (table 9). Testing the gold(I) C–H activation, under otherwise standard reaction conditions, in dioxane revealed generation of the corresponding aryl gold(I) product in an excellent 99% yield. Therefore dioxane was selected as a suitable solvent to assess one-pot reactions. Unfortunately, combination of all reagents in one flask to not lead to the generation of either the aryl gold(I) product nor the desired biaryl. However, a reaction performed by Dr Xacobe Cambeiro determined that filtration of the reaction mixture, before addition of the iodine(III) oxidant, led to 47% of the desired biaryl **51**.

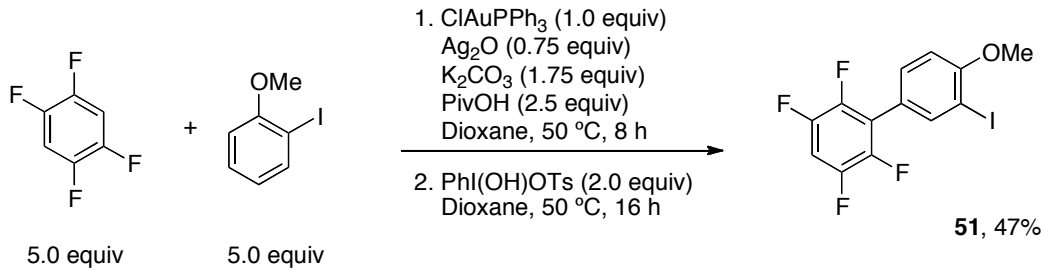

Scheme C2. Reaction as performed by co-worker. Filtration of step 1 mixture through celite before addition of oxidant led to formation of biaryl **51**.

This result serves to highlight that current incompatibility between the two sets of reaction conditions is a result of more than solvent selection alone. However, it also offers some optimism that judicious investigation of the cross-coupling process may lead to the development of a one-pot catalytic process.

3.7 Experimental

3.7.1 General Information

All reactions were carried out under nitrogen in disposable vials using reagents obtained from commercial sources and used without further purification. Column chromatography was carried out on silica gel, particle size 40–63 μm, using flash techniques. Analytical thin layer chromatography was performed on pre-coated silica gel F_{254} plates with visualisation under UV light. Melting points were obtained using a Gallenkamp hot stage apparatus and are uncorrected. IR spectra were recorded using a Bruker Tensor 37 FTIR machine and are quoted in cm^{-1}. ^{1}H NMR spectra, recorded at 400 MHz, are referenced to the residual solvent peak at 7.26 ppm ($CHCl_3$) and quoted in ppm to 2 decimal places with coupling constants (*J*) to the nearest 0.1 Hz. ^{13}C NMR spectra, recorded at 101 MHz, are referenced to the solvent peak at 77.0 ppm ($CDCl_3$) and quoted in ppm to 1 decimal place with coupling constants (*J*) to the nearest 0.1 Hz. ^{31}P NMR spectra were recorded at 162 MHz, in $CDCl_3$ and quoted in ppm to 2 decimal places and with coupling constants (*J*) to the nearest 0.1 Hz.

3.7.2 Experimental Procedures

General procedure for the optimisation of the oxidative cross-coupling

A mixture of oxidant (2.0 equiv, 0.04 mmol), arylgold(I) compound **43** (12.5 mg, 0.02 mmol) and 2-iodoanisole (13 μL, 0.10 mmol) in the desired solvent (0.10 mL, 0.20 M) was stirred at 25-50 ºC. After the selected reaction time, the resulting mixture was filtered through a plug of cotton wool, washing with CH_2Cl_2. The filtrate was concentrated under reduced pressure and ^{1}H NMR analysis, using *p*-xylene as an internal standard, allowed detection and quantification of product **50**.

General Procedure C: Biaryl synthesis via oxidative cross-coupling

A mixture of PhI(OH)OTs (118.0 mg, 0.30 mmol), arylgold(I) compound (0.15 mmol) and the aryl coupling partner (0.75 mmol) in DCE (0.75 mL, 0.20 M) was stirred at 50 ºC for 16 h. After this time, the resulting mixture was purified by column chromatography to afford the desired coupling products **50-59** and **70-88**.

General Procedure D: Synthesis of aryl gold(I) species via decarboxylative activation

A mixture of Ph_3PAuCl (50.0 mg, 0.10 mmol), Ag_2O (23.4 mg, 0.10 mmol) and the benzoic acid (0.10 mmol) in DMF (1.4 mL, 0.07 M) was stirred at 100–110 ºC for 3–16 h. After this time, the resulting mixture was filtered through a plug of cotton wool, which was washed with CH_2Cl_2 and the filtrate concentrated under reduced pressure. The crude product was purified by column chromatography with 3% Et_3N to afford products **63–69**. Thin layer chromatography was performed on silica gel plates, which were soaked in *n*-hexanes:Et_3N (95:5) and then allowed to dry before use.

3.7.3 Characterisation Data

2,3,4,5,6-Pentafluoro-3'-iodo-4'-methoxybiphenyl **50**.

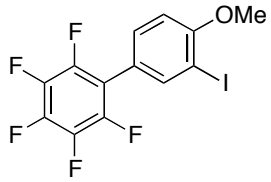

General procedure C was applied with **43** (93.9 mg, 0.15 mmol) and 2-iodoanisole (98 μL, 0.75 mmol). Column chromatography (100% *n*- hexanes) afforded product **50** as a white solid (50.4 mg, 84%); m.p.150-152 ℃; IR: 2848, 1488, 1444, 1379, 1286; ^{1}H NMR (400 MHz) δ 7.85 (dt, 1H, *J* = 2.3, 1.3 Hz), 7.39 (ddt, 1H, *J* = 8.6, 2.3, 1.3 Hz), 6.93 (d, 1H, *J* = 8.6 Hz), 3.94 (s, 3H); ^{13}C NMR (101 MHz) δ 158.9, 144.30 (dddd, *J* = 247.6, 14.7, 7.1, 3.8 Hz), 140.9, 140.5 (dm, *J* = 241.1 Hz), 138.0 (dm, *J* = 253.3 Hz), 131.6, 120.3, 114.4 (td, *J* = 17.2, 3.7 Hz), 110.8, 86.1, 56.6; MS (EI) *m/z* calcd. $C_{13}H_6F_5IO$: (M+) 400.08 found: (M+) 400.2.

2,3,5,6-Tetrafluoro-3'-iodo-4'-methoxybiphenyl **51**.

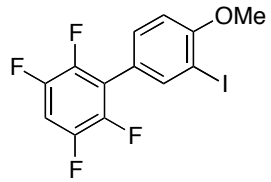

General procedure C was applied with **44** (91.2 mg, 0.15 mmol) and 2-iodoanisole (98 μL, 0.75 mmol). Column chromatography (100% *n*- hexanes) afforded product **51** as a white solid (43.5 mg, 76%); m.p. 170-172 ℃; IR: 2849, 1487, 1288, 1254, 1047; ^{1}H NMR (400 MHz) δ 7.89 (s, 1H), 7.43 (d, 1H, *J* = 8.5 Hz), 7.05 (tt, 1H, *J* = 7.4, 9.5 Hz), 6.93 (d, 1H, *J* = 8.5 Hz), 3.94 (s, 3H); ^{13}C NMR (101 MHz) δ 158.9, 146.4 (dm, *J* = 246.7 Hz), 143.9 (dm, *J* = 251.1 Hz), 140.9 (t, *J* = 2.2 Hz), 131.6 (t, *J* = 2.1 Hz), 121.5 (t, *J* = 2.4 Hz), 119.9 (t, *J* = 16.5 Hz), 110.8, 105.0 (t, *J* = 22.7 Hz), 86.0, 56.6; HRMS (EI) calcd. $C_{13}H_7F_4IO$: (M+) 381.9472; found: (M+) 381.9462.

2,4-Dibromo-6-fluoro-3'-iodo-4'-methoxybiphenyl **52**.

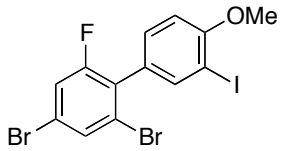

General procedure C was applied with **45** (106.8 mg, 0.15 mmol) and 2-iodoanisole (98 μL, 0.75 mmol). Column chromatography (100% *n*-hexanes) afforded product **52** as a white solid (42.3 mg, 58%); m.p. 88-90 ℃; IR: 2833, 1586, 1545, 1497; ^{1}H NMR (400 MHz) δ 7.72 (d, 1H, *J* = 1.0 Hz), 7.65 (s, 1H), 7.30 (d, 1H, *J* = 8.4 Hz), 7.26 (dd, 1H, *J* = 8.4, 1.0 Hz), 6.90 (d, 1H, *J* = 8.4 Hz), 3.94 (s, 3H); ^{13}C NMR (101 MHz) δ 159.9 (d, *J* = 253.3 Hz), 158.4, 140.8 (d, *J* = 1.0 Hz), 131.4 (d, *J* = 3.9 Hz), 131.3 (d, *J* = 1.0 Hz), 128.5 (d, *J* = 19.0 Hz), 127.6, 125.4 (d, *J* = 3.4 Hz), 121.8 (d, *J* = 10.9 Hz), 118.8 (d, *J* = 26.7 Hz), 110.4, 85.6, 56.5; HRMS (EI) calcd. $C_{13}H_8Br_2FIO$: (M+) 485.9129; found: (M+) 485.79209.

2-Fluoro-3'-iodo-4'-methoxy-6-nitrobiphenyl **53**.

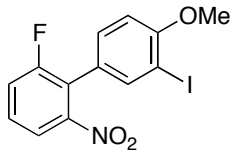

General procedure C was applied with **46** (89.9 mg, 0.15 mmol) and 2-iodoanisole (98 μL, 0.75 mmol). Column chromatography (100% *n*- hexanes) afforded product **53** as a white solid (48.1 mg, 86%); m.p. 126-128 ℃; IR: 2849, 1525, 1462, 1353, 1283, 1247; ^{1}H NMR (400 MHz) δ 7.73 (d, 1H, *J* = 1.0 Hz), 7.67 (d, 1H, *J* = 8.2 Hz), 7.47 (td, 1H, *J* = 8.2, 5.3 Hz), 7.38 (t, 1H, *J* = 8.4 Hz), 7.25 (dd, 1H, *J* = 8.5, 1.0 Hz), 6.88 (d, 1H, *J* = 8.5 Hz), 3.92 (s, 3H); ^{13}C NMR (101 MHz) δ 160.0 (d, *J* = 250.1 Hz), 158.7, 150.5 (d, *J* = 2.9 Hz), 139.8 (d, *J* = 1.9 Hz), 130.4 (d, *J* = 1.5 Hz), 129.5 (d, *J* = 8.9 Hz), 124.0, 123.2 (d, *J* = 20.5 Hz), 120.1 (d, *J* = 23.6 Hz), 119.8 (d, *J* = 3.7 Hz), 110.8, 86.1, 56.5; MS (EI) *m/z* calcd. $C_{13}H_9FINO_3$: (M+) 373.12; found: (M+) 373.7.

2,3,6-Trifluoro-3'-iodo-4'-methoxybiphenyl **54**.

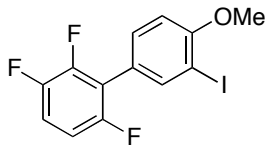

A modification of general procedure C was applied, using **47** (88.5 mg, 0.15 mmol) and 2-iodoanisole (196 μL, 1.5 mmol) at 70 ºC. Column chromatography (100% *n*-hexanes) afforded product **54** as a white solid (38.2 mg, 70%); m.p. 130-132 ℃; IR: 2842, 1482, 1381, 1285, 1251; ^{1}H NMR (400 MHz) δ 7.89 (app. dt, *J* = 2.2, 1.2 Hz, 1H), 7.43 (app. ddt, *J* = 8.6, 1.9, 1.4 Hz, 1H), 7.11 (app. qd, *J* = 9.1, 4.9 Hz, 1H), 6.92 (d, 8.6 Hz, 1H), 6.91 (app. tdd, *J* = 9.0, 3.8, 2.3 Hz, 1H), 3.94 (s, 3H); ^{13}C NMR (101 MHz) δ 158.5, 155.4 (dm, *J* = 246.6 Hz), 147.9 (ddd, *J* = 249.9, 14.3, 7.3 Hz), 147.6 (ddd, *J* = 244.9, 13.7, 3.7 Hz), 141.0 (app. t, *J* = 2.2 Hz), 131.6 (app. t, *J* = 2.1 Hz), 122.5 (d, *J* = 2.4 Hz), 118.7 (dd, *J* = 20.6, 5.0 Hz), 115.8 (dd, *J* = 19.3, 9.9 Hz), 111.0 (ddd, *J* = 25.5, 6.8, 4.2 Hz), 110.7, 85.9, 56.6; HRMS (EI) calcd. $C_{13}H_8F_3IO$: (M+) 363.9566; found: (M+) 363.9557.

2,3,4,5,6-Pentafluoro-2',5'-dimethylbiphenyl **55**.

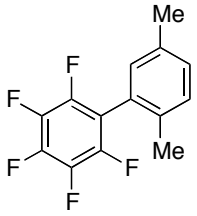

General procedure C was applied with **43** (93.9 mg, 0.15 mmol) and *p*- xylene (93 μL, 0.75 mmol). Column chromatography (100% *n*-hexanes) afforded product **55** as a white solid (27.7 mg, 68%); m.p. 64–66 ℃; IR: 1654, 1525, 1480, 1375, 1135; ^{1}H NMR (400 MHz) δ 7.23 (d, 1H, *J* = 7.8), 7.19 (d, 1H, *J* = 7.8 Hz), 7.00 (s, 1H), 2.36 (s, 3H), 2.13 (s, 3H); ^{13}C NMR (101 Hz), 7.19 (d, MHz) δ 144.2 (dddd, *J* = 247.2, 11.3, 7.4, 3.9 Hz), 140.7 (dm, *J* = 253.3 Hz), 137.8 (dm, *J* = 253.2 Hz), 135.7, 134.3, 131.2, 130.6, 130.5, 125.8, 115.8 (td, *J* =

19.9, 4.2 Hz), 21.0, 19.3. MS (EI) *m/z* calcd. $C_{14}H_9F_5$: (M+) 272.06; found: (M+) 272.0; spectroscopic data is in agreement with that previously reported.[99]

2,3,4,5,6-Pentafluorobiphenyl **56**.

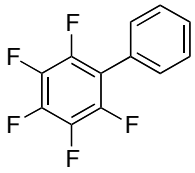

General procedure C was applied with **43** (93.9 mg, 0.15 mmol) and benzene (67 μL, 0.75 mmol). Column chromatography (100% *n*-hexanes) afforded product **56** as a white solid (18.3 mg, 50%); m.p. 48-52 ℃; IR: 1653, 1488, 1439, 1319, 1199; ^{1}H NMR (400 MHz) δ 7.49-7.39 (m, 6H); ^{13}C NMR (101 MHz) δ 144.3 (dddd, *J* = 247.8, 14.8, 7.4, 3.8 Hz), 140.5 (dm, *J* = 253.8 Hz), 138.0 (dm, *J* =250.1 Hz), 130.3, 129.5, 128.9, 126.6, 116.1 (td, *J* = 17.1, 4.1 Hz); MS (EI) *m/z* calcd. $C_{12}H_5F_5$: (M+) 244.16; found: (M+) 244.2; spectroscopic data is in agreement with that previously reported.[96]

2,3,4,5,6-Pentafluoro-4'-methoxybiphenyl **57**.

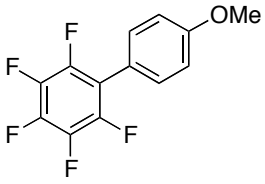

General procedure C was applied with **43** (93.9 mg, 0.15 mmol) and anisole (82 μL, 0.75 mmol). Regioisomers ratio was determined by ^{1}H NMR analysis of the crude product (6.6:1 *p*:*o*). Column chromatography (100% *n*-hexanes) afforded product **57** as a white solid (34.9 mg, 85%); m.p. 108-110 ℃; IR: 3026, 2943, 2847, 1577, 1481, 977, 826; ^{1}H NMR (400 MHz) δ 7.36 (d, 2H, *J* = 8.7 Hz), 7.02 (d, 2H, *J* = 8.8 Hz), 3.87 (s, 3H);^{13}C NMR (101 MHz) δ 160.4, 144.3 (dm, *J* = 246.5 Hz), 140.1 (dm, *J* = 254.7 Hz), 138.0 (dm, *J* = 251.0 Hz), 131.6, 118.5, 115.8 (td, *J* = 17.1, 3.9 Hz), 114.4, 55.5; MS (EI) *m/z* calcd. $C_{13}H_7F_5O$: (M+)

274.04; found: (M+) 274.6; spectroscopic data is in agreement with that previously reported.[96]

Methyl 2-methyl-5-(pentafluorophenyl)furan-3-carboxylate **58**.

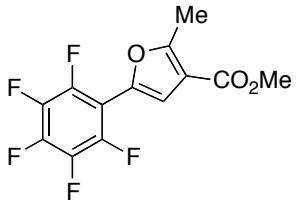

General procedure C was applied with **43** (93.9 mg, 0.15 mmol) and methyl 2-methylfuroate (94 μL, 0.75 mmol). Column chromatography (100% *n*-hexanes) afforded product **58** as a white waxy solid (33.9 mg, 74%); IR: 3030, 2851, 1657, 1611, 1516, 1483, 1415; ^{1}H NMR (400 MHz) δ 7.10 (s, 1H), 3.87 (s, 3H), 2.67 (s, 3H); ^{13}C NMR (101 MHz) δ 163.9, 160.7, 143.6 (dm, J = 249.6 Hz), 140.5 (dm, J = 241.7 Hz), 139.0 (d, J = 2.8 Hz), 138.2 (dm, J = 247.8 Hz), 115.3, 114.5 (t, J = 5.6 Hz), 106.2 (td, J = 14.2, 4.2 Hz), 51.8, 14.1; MS (EI) *m/z* calcd. $C_{13}H_7F_5O_3$: (M+) 306.18; found: (M+) 306.0.

5-Iodo-2-(pentafluorophenyl)thiophene **59**.

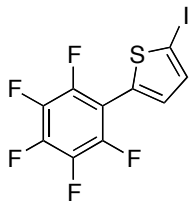

General procedure C was applied with **43** (93.9 mg, 0.15 mmol) and 2-iodothiophene (83 μL, 0.75 mmol). Column chromatography (100% *n*-hexanes) afforded product **59** as a white solid (44.6 mg, 79%); m.p. 62-64 ℃; IR: 3136, 2921, 1652, 1510, 800; ^{1}H NMR (400 MHz) δ 7.33 (d, 1H, J = 3.9 Hz), 7.19 (t, 1H, J = 3.9 Hz); ^{13}C NMR (101 MHz) δ 144.0 (dm, J = 256.8 Hz), 140.3 (dm, J = 256.8 Hz), 138.1 (dm, J = 256.8), 137.4, 132.5, 131.7 (t, J = 6.0 Hz), 77.6. (EI) *m/z* calcd. $C_{10}H_2F_5IS$: (M+) 375.88; found: (M+) 376.0.

2-Chloro-5-nitro-phenyl(triphenylphosphine)gold(I) **63**.

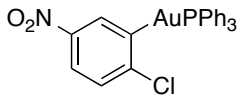

General procedure D was applied, at five times the scale, with 2-chloro-5-nitrobenzoic acid (100.8 mg, 0.50 mmol) at 100 ºC for 16 h. Column chromatography (*n*-hexanes:EtOAc:Et_3N 82:15:3) afforded product **63** as a yellow solid (209.4 mg, 68%); m.p. 126–128 ˚C; R_f 0.31 (*n*-hexanes:EtOAc:Et_3N 77:20:3); IR: 3053, 1589, 1506, 1479, 1435, 1339, 1277, 1100, 870, 750, 737, 709, 687; ^{1}H NMR (400 MHz) δ 8.38 (dd, 1H, *J* = 5.8, 2.7 Hz,), 7.85 (dd, 1H, *J* = 8.7, 2.6 Hz), 7.61 (dd, 6H, *J* = 12.2, 7.7 Hz), 7.56–7.43 (m, 10H); ^{13}C NMR (101 MHz) δ 174.5 (d, *J* = 115.4 Hz), 151.1 (d, *J* = 2.6 Hz), 146.2 (d, *J* = 6.7 Hz), 134.7, 134.5 (d, *J* = 13.7 Hz), 131.6 (d, *J* = 2.2 Hz), 130.3 (d, *J* = 52.7 Hz), 129.4 (d, *J* = 11.0 Hz), 128.1 (d, *J* = 4.8 Hz), 122.0; ^{31}P NMR (162 MHz) δ 41.59 (s); MS (CI) *m/z* 616 $[M+H]^+$; HRMS (CI) calcd. $C_{24}H_{18}AuClNO_2P$: $[M+H]^+$ 616.0502; found: $[M+H]^+$ 616.0500.

3-Chloro-2-nitro-phenyl(triphenylphosphine)gold(I) **64**.

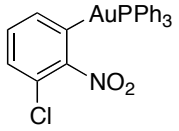

General procedure D was applied with 3-chloro-2-nitrobenzoic acid (20.2 mg, 0.10 mmol) at 110 ºC for 3 h. Column chromatography (*n*-hexanes:EtOAc:Et_3N 87:10:3) afforded product **64** as a white solid (43.1 mg, 70%); m.p. 162–164 ˚C; R_f 0.17 (*n*-hexanes:EtOAc:Et_3N 86:10:4); IR: 1517, 1479, 1433, 1364, 1100, 995, 851, 780; ^{1}H NMR (400 MHz) δ 7.64–7.41 (m, 16H), 7.31 (t, 1H, *J* = 7.6 Hz), 7.21 (dd, 1H, *J* = 7.9, 1.2 Hz); ^{13}C NMR (101 MHz) δ 158.1, 138.5, 134.5 (d, *J* = 13.8 Hz), 131.6 (d, *J* = 2.3 Hz), 130.2 (d, *J* = 52.6 Hz), 130.3, 129.3 (d, *J* = 11.1 Hz), 127.5, 124.2; ^{31}P NMR (162 MHz) δ 42.07 (s); MS (EI) *m/z* 182,

262, 459, 615 (M^+); HRMS (EI) calcd. $C_{24}H_{18}AuClNO_2P$: (M^+) 615.0424; found: (M^+) 615.0427.

5-Fluoro-2-nitro-phenyl(triphenylphosphine)gold(I) **65**.

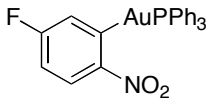

General procedure D was applied with 5-fluoro-2-nitrobenzoic acid (18.5 mg, 0.10 mmol) at 110 ºC for 3 h. Column chromatography (*n*-hexanes:EtOAc:Et_3N 87:10:3) afforded product **65** as a yellow solid (46.8 mg, 78%); m.p. 108–110 ˚C; R_f 0.27 (*n*-hexanes:EtOAc:Et_3N 81:15:4); IR: 1594, 1562, 1499, 1434, 1325, 1203, 1097, 873, 707, 687; ^{1}H NMR (400 MHz) δ 8.21 (dd, 1H, *J* = 9.0, 4.8 Hz), 7.61 (ddd, 6H, *J* = 12.2, 7.7, 1.7 Hz), 7.56–7.39 (m, 10H), 6.85 (ddd, 1H, *J* = 9.0, 7.8, 2.9 Hz); ^{13}C NMR (101 MHz) δ 171.6 (d, *J* = 5.8 Hz), 165.3 (d, *J* = 257.8 Hz), 153.6 (d, *J* = 1.5 Hz), 134.5 (d, *J* = 14.0 Hz), 131.4 (d, *J* = 2.3 Hz), 130.7 (d, *J* = 51.0 Hz), 129.3 (d, *J* = 10.9 Hz), 126.5 (dd, *J* = 13.6, 4.5 Hz), 113.0 (d, *J* = 24.1 Hz); ^{31}P NMR (162 MHz) δ 41.09 (s); MS (EI) *m/z* 182, 262, 459, 599 (M^+); HRMS (EI) calcd. $C_{24}H_{18}AuFNO_2P$: (M^+) 599.0725; found: (M^+) 599.0727.

4,5-Dimethoxy-2-nitro-phenyl(triphenylphosphine)gold(I) **66**.

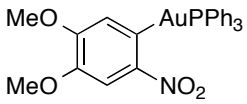

General procedure D was applied with 4,5-dimethoxy-2-nitrobenzoic acid (22.7 mg, 0.10 mmol) at 110 ºC for 3 h. Column chromatography (*n*-hexanes:EtOAc:Et_3N 82:15:3) afforded product **66** as a yellow solid (52.6 mg, 82%); m.p. 134–136 ˚C; R_f 0.15 (*n*-hexanes:EtOAc:Et_3N 81:15:4); IR: 1557, 1500, 1478, 1434, 1309, 1261, 1244, 1208, 1099, 1027, 997, 750, 692; ^{1}H NMR (400 MHz) δ 7.84 (s, 1H), 7.63 (ddd, 6H, *J* = 12.0, 7.4, 1.8 Hz), 7.55–7.39 (m, 9H) 7.19 (s, 1H), 3.97 (s, 3H), 3.92 (s, 3H); ^{13}C NMR (101 MHz) δ 152.9, 150.3,

146.8, 134.5 (d, 14.0 Hz), 131.4, 129.2 (d, J = 10.9 Hz), 120.9, 107.8, 56.2, 56.1; ^{31}P NMR (162 MHz) δ 40.92 (s); MS (EI) *m/z* 183, 262, 641 (M^+); HRMS (EI) calcd. $C_{26}H_{23}AuNO_4P$: (M^+) 641.1025; found: (M^+) 641.1021.

2-Nitro-phenyl(triphenylphosphine)gold(I) **67**.

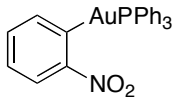

General procedure D was applied with 2-nitrobenzoic acid (16.7 mg, 0.10 mmol) at 110 ºC for 3 h. Column chromatography (*n*-hexanes:EtOAc:Et_3N 87:10:3) afforded product **67** as a yellow solid (30.3 mg, 52%); m.p. 120–122 ˚C; R_f 0.28 (*n*-hexanes:EtOAc:Et_3N 81:15:4); IR: 1585, 1498, 1433, 1323, 1297, 1242, 1099, 718, 686; ^{1}H NMR (400 MHz) δ 8.12 (dd, 1H, J = 8.3, 1.0 Hz), 7.76 (dd, 1H, J = 7.2, 1.5 Hz), 7.61 (ddd, 6H, J = 11.9, 7.6, 1.9 Hz), 7.54–7.42 (m, 10H), 7.22 (ddd, 1H, J = 8.6, 7.2, 1.5 Hz); ^{13}C NMR (101 MHz) δ 167.4, 157.8, 141.0, 134.5 (d, J = 14.3 Hz), 132.4, 131.3 (d, J = 47.0 Hz), 131.2 (d, J = 2.0 Hz), 129.2 (d, J = 10.7 Hz), 125.9, 123.9; ^{31}P NMR (162 MHz) δ 38.71 (s) ; MS (EI) *m/z* 183, 262, 581 (M^+); HRMS (EI) calcd. $C_{24}H_{19}AuNO_2P$: (M^+) 581.0813; found: (M^+) 581.0813; spectroscopic data is in agreement with that previously reported.[100]

2-Bromo-5-nitro-phenyl(triphenylphosphine)gold(I) **68**.

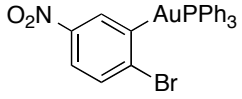

General procedure D was applied with 2-bromo-5-nitrobenzoic acid (24.6 mg, 0.10 mmol) at 110 ºC for 3 h. Column chromatography (*n*-hexanes:EtOAc:Et_3N 82:15:3) afforded product **68** as a yellow solid (35.7 mg, 54%); m.p. 136–138 ˚C; R_f 0.32 (*n*-hexanes:EtOAc:Et_3N 77:20:3); IR: 1584, 1506, 1478, 1435, 1334, 1273, 1099, 866, 735, 688; ^{1}H NMR (400 MHz) δ 8.27 (dd, 1H, J = 5.9, 2.9 Hz), 7.75 (dd, 1H, J = 8.7, 2.9 Hz), 7.72–7.58 (m, 7H), 7.58–7.42 (m, 9H); ^{13}C NMR (101 MHz) δ 178.6 (d, J = 116.1 Hz), 146.6 (d, J = 6.7 Hz), 142.5 (d, J = 3.2

Hz), 135.1, 134.5 (d, J = 13.8 Hz), 131.6 (d, J = 2.3 Hz), 131.2 (d, J = 5.1 Hz), 130.4 (d, J = 52.6 Hz), 129.3 (d, J = 11.0 Hz), 122.1; ^{31}P NMR (162 MHz) δ 40.77 (s); MS (EI) *m/z* 182, 262, 401, 659 (M^+); HRMS (EI) calcd. $C_{24}H_{18}AuBrNO_2P$: (M^+) 658.9924; found: (M^+) 658.9929.

4-Methyl-2-nitro-phenyl(triphenylphosphine)gold(I) **69**.

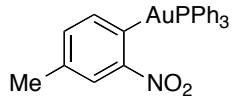

General procedure D was applied with 4-methyl-2-nitrobenzoic acid (18.1 mg, 0.10 mmol) at 110 ºC for 3 h. Column chromatography (*n*-hexanes:EtOAc:Et_3N 87:10:3) afforded product **69** as a yellow solid (45.8 mg, 77%); m.p. 184–186 ˚C; R_f 0.23 (*n*-hexanes:EtOAc:Et_3N 82:15:3); IR: 1503, 1479, 1433, 1333, 1099, 827, 746, 689; ^{1}H NMR (400 MHz) δ 7.96 (s, 1H), 7.63 (ddd, 6H, J = 12.1, 7.5, 1.9 Hz), 7.54–7.42 (m, 10H), 7.34 (dd, 1H, J = 7.4, 1.6 Hz), 2.38 (s, 3H); ^{13}C NMR (101 MHz) δ 163.8, 157.9, 140.6, 135.8, 134.5 (d, J = 14.1 Hz), 133.5, 131.3 (d, J = 2.2 Hz), 131.1 (d, J = 49.2 Hz), 129.2 (d, J = 10.8), 124.2, 21.1; ^{31}P NMR (162 MHz) δ 40.70; MS (EI) *m/z* 182, 262, 459, 595 (M^+); HRMS (EI) calcd. $C_{25}H_{21}AuNO_2P$: (M^+) 595.0970; found: (M^+) 595.0980.

2-Chloro-2',5'-dimethyl-5-nitrobiphenyl **70**.

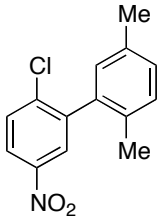

General procedure C was applied with **63** (92.4 mg, 0.15 mmol) and *p*-xylene (93 µL, 0.75 mmol). Column chromatography (*n*-hexanes:EtOAc 99:1) afforded product **70** as a white solid (29.4 mg, 75%); m.p. 68–70 ˚C; R_f 0.31 (*n*-hexanes:EtOAc 97:3); IR: 2923, 1569, 1538, 1503, 1340, 1085, 1031, 919, 814, 737; ^{1}H NMR (400 MHz) δ 8.17 (dd, 1H, J = 8.7, 2.5 Hz), 8.13 (d, 1H, J = 2.5

Hz), 7.63 (d, 1H, J = 8.7 Hz), 7.20 (d, 1H, J = 8.0 Hz), 7.19 (d, 1H, J = 8.0 Hz), 6.95 (s, 1H), 2.36 (s, 3H), 2.08 (s, 3H); ^{13}C NMR (101 MHz) δ 146.5, 142.5, 140.8, 137.1, 135.6, 132.9, 130.4, 130.2, 129.8, 129.7, 126.2, 123.5, 21.0, 19.3; HRMS (CI) calcd. $C_{14}H_{12}ClNO_2$: $[M+H]^+$ 262.0629; found: $[M+H]^+$ 262.0631.

3-Chloro-2',5'-dimethyl-2-nitrobiphenyl **71**.

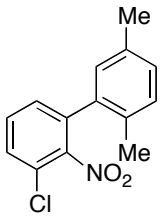

General procedure C was applied with **64** (92.3 mg, 0.15 mmol) and *p*-xylene (93 μL, 0.75 mmol). Column chromatography (*n*-hexanes:EtOAc 98:2) afforded product **71** as a white solid (28.2 mg, 72%); m.p. 124–126 ˚C; R_f 0.35 (*n*-hexanes:EtOAc 95:5); IR: 1597, 1527, 1458, 1365, 1276, 850, 796, 782, 649; ^{1}H NMR (400 MHz) δ 7.51 (dd, 1H, J = 8.1, 1.3 Hz), 7.45 (t, 1H, J = 7.9 Hz), 7.23 (dd, 1H, J = 7.6, 1.3 Hz), 7.14 (d, 1H, J = 7.9 Hz), 7.10 (d, 1H, J = 7.9 Hz), 6.94 (s, 1H), 2.31 (s, 3H), 2.09 (s, 3H); ^{13}C NMR (101 MHz) δ 149.4, 136.4, 135.3, 134.5, 133.2, 130.5, 130.3, 130.0, 129.7, 129.6, 129.4, 125.0, 21.0, 19.6; HRMS (CI) calcd. $C_{14}H_{12}ClNO_2$: $[M+H]^+$ 262.0629; found: $[M+H]^+$ 262.0629.

5-Fluoro-2',5'-dimethyl-2-nitrobiphenyl **72**.

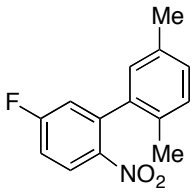

General procedure C was applied with **65** (89.9 mg, 0.15 mmol) and *p*-xylene (93 μL, 0.75 mmol). Column chromatography (*n*-hexanes:EtOAc 98:2) afforded product **72** as an oil (24.4 mg, 66%); R_f 0.53 (*n*-hexanes:EtOAc 90:10); IR: 1619, 1581, 1523, 1474, 1346, 1208, 849, 812, 765, 624; ^{1}H NMR (400 MHz) δ

8.07 (dd, 1H, *J* = 9.0, 5.1 Hz), 7.22–7.17 (m, 1H), 7.16 (d, 1H, *J* = 8.6 Hz), 7.12 (d, 1H, *J* = 8.0), 7.02 (dd, 1H, *J*= 8.6, 2.8 Hz), 6.90 (s, 1H), 2.33 (s, 3H), 2.06 (s, 3H); ^{13}C NMR (101 MHz) δ 164.2 (d, *J* = 257.1 Hz), 140.2 (d, *J* = 9.3 Hz), 136.6 (d, *J* = 0.9 Hz), 135.5, 132.3, 130.1, 129.4, 128.6, 127.1 (d, *J* = 10.0 Hz), 119.3 (d, *J* = 22.9 Hz), 115.3 (d, *J* = 23.2 Hz), 21.0, 19.4; HRMS (CI) calcd. $C_{14}H_{12}FNO_2$: $[M+H]^+$ 246.0919; found: $[M+H]^+$ 246.0925.

4,5-Dimethoxy-2',5'-dimethyl-2-nitrobiphenyl **73**.

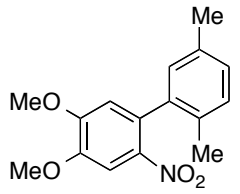

General procedure C was applied with **66** (96.2 mg, 0.15 mmol) and *p*-xylene (93 µL, 0.75 mmol). Column chromatography (*n*-hexanes:EtOAc 90:10) afforded product **73** as an oil (28.5 mg, 66%); R_f 0.33 (*n*-hexanes:EtOAc 80:20); IR: 1575, 1517, 1461, 1334, 1274, 1216, 1089, 1034, 910, 869, 729; ^{1}H NMR (400 MHz) δ 7.67 (s, 1H), 7.15 (d, 1H, *J* = 7.8 Hz), 7.11 (d, 1H, *J* = 7.8 Hz), 6.92 (s, 1H), 6.68 (s, 1H), 4.00 (s, 3H), 3.93 (s, 3H), 2.34 (s, 3H), 2.04 (s, 3H); ^{13}C NMR (101 MHz) δ 152.7, 148.0, 141.0, 138.4, 135.3, 132.7, 131.7, 129.9, 128.9, 128.8, 113.5, 107.6, 56.6, 56.5, 21.1, 19.5; HRMS (CI) calcd. $C_{16}H_{17}NO_4$: $[M+H]^+$ 288.1230; found: $[M+H]^+$ 288.1232.

2,5-Dimethyl-2'-nitrobiphenyl **74**.

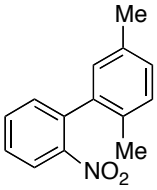

General procedure C was applied with **67** (87.2 mg, 0.15 mmol) and *p*-xylene (93 μL, 0.75 mmol). Column chromatography (*n*-hexanes:EtOAc 98:2) afforded product **74** (24.9 mg, 73%); R_f 0.33 (*n*-hexanes:EtOAc 95:5); IR: 1527, 1476, 1339, 1018, 929, 811, 735; ^{1}H NMR (400 MHz) δ 7.98 (dd, 1H, *J* = 8.0, 1.2 Hz), 7.63 (td, 1H, *J* = 7.5, 1.2 Hz), 7.51 (td, 1H, *J* = 8.0, 1.4 Hz), 7.33 (dd, 1H, *J* = 7.5, 1.4 Hz), 7.16 (d, 1H, *J* = 7.8 Hz), 7.11 (dd, 1H, *J* = 7.8, 1.1 Hz), 6.92 (s, 1H), 2.33 (s, 3H), 2.06 (s, 3H); ^{13}C NMR (101 MHz) δ 149.2, 137.3, 136.7, 135.2, 132.5, 132.2, 129.9, 128.94, 128.91, 128.1, 124.1, 20.9, 19.4; spectroscopic data is in agreement with that previously reported.[101]

2-Bromo-2',5'-dimethyl-5-nitrobiphenyl **75**.

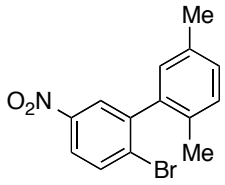

General procedure C was applied with **68** (98.8 mg, 0.15 mmol) and *p*-xylene (93 μL, 0.75 mmol). Column chromatography (*n*-hexanes:EtOAc 98:2) afforded product **75** as a white solid (33.5 mg, 73%); m.p. 90–92 ˚C; R_f 0.47 (*n*-hexanes:EtOAc 95:5); IR: 1562, 1515, 1456, 1337, 1022, 901, 813, 737; ^{1}H NMR (400 MHz) δ 8.10 (d, 1H, *J* = 2.6 Hz), 8.07 (dd, 1H, *J* = 8.6, 2.6 Hz), 7.84 (d, 1H, *J* = 8.6 Hz), 7.22–7.15 (m, 2H), 6.93 (s, 1H), 2.37 (s, 3H), 2.07 (s, 3H); ^{13}C NMR (101 MHz) δ 147.2 144.7, 139.0, 135.6, 133.7, 132.7, 131.6, 130.2, 129.7, 129.6, 125.8, 123.4, 21.1, 19.4; HRMS (CI) calcd. $C_{14}H_{12}BrNO_2$: $[M+H]^+$ 306.0214; found: $[M+H]^+$ 306.0219.

2',4,5'-Trimethyl-2-nitrobiphenyl **76**.

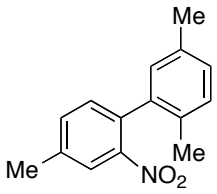

General procedure C was applied with **69** (89.3 mg, 0.15 mmol) and *p*-xylene (93 μL, 0.75 mmol). Column chromatography (*n*-hexanes:EtOAc 98:2) afforded product **76** as an oil (21.1 mg, 58%); m.p. ˚C; R_f 0.41 (*n*-hexanes:EtOAc 95:5); IR: 1525, 1466, 1350, 1011, 921, 818, 735; ^{1}H NMR (400 MHz) δ 7.79 (s, 1H), 7.42 (d, 1H, *J* = 7.7 Hz), 7.20 (d, 1H, *J* = 7.7 Hz), 7.14 (d, 1H, *J* = 7.8 Hz), 7.09 (d, 1H, *J* = 7.8 Hz), 6.90 (s, 1H), 2.49 (s, 3H), 2.32 (s, 3H), 2.05 (s, 3H); ^{13}C NMR (101 MHz) δ 149.1, 138.7, 137.5, 135.3, 134.0, 133.4, 132.8, 132.1, 129.9, 129.2, 128.9, 124.5, 21.1, 21.0, 19.5; HRMS (CI) calcd. $C_{15}H_{15}NO_2$: $[M+H]^+$ 242.1176; found: $[M+H]^+$ 242.1172.

2-Chloro-5-nitrobiphenyl **77**.

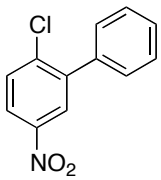

General procedure C was applied with **63** (92.4 mg, 0.15 mmol) and benzene (67 μL, 0.75 mmol). Column chromatography (*n*-hexanes:EtOAc 99:1) afforded product **77** as a white solid (22.8 mg, 65%); m.p. 52–54 ˚C; R_f 0.31 (*n*-hexanes:EtOAc 97:3); IR: 3091, 1566, 1510, 1353, 1241, 1076, 1035, 903, 825, 740; ^{1}H NMR (400 MHz) δ 8.24 (d, 1H, *J* = 2.6 Hz), 8.15 (dd, 1H, *J* = 8.7, 2.6 Hz), 7.65 (d, 1H, *J* = 8.7 Hz), 7.54–7.41 (m, 5H); ^{13}C NMR (101 MHz) δ 146.7, 142.1, 139.7, 137.3, 131.1, 129.4, 128.8, 128.6, 126.3, 123.3; spectroscopic data is in agreement with that previously reported.[102]

2-Chloro-4'-methyl-5-nitrobiphenyl **78**.

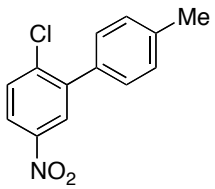

General procedure C was applied with **63** (92.4 mg, 0.15 mmol) and toluene (80 μL, 0.75 mmol). Column chromatography (*n*-hexanes:EtOAc 99:1) afforded product **78** (30.8 mg, 83%) with a regioisomeric ratio of 5.0:1; R_f 0.34 (*n*-hexanes:EtOAc 97:3); IR: 1520, 1507, 1460, 1348, 1312, 1238, 1079, 913, 882, 823, 813, 740, 727, 676; ^{1}H NMR (400 MHz) δ 8.23 (d, 1H, *J* = 2.7 Hz), 8.18 (minor isomer, dd, 1H, *J* = 8.8, 2.7 Hz), 8.13 (dd, 1H, *J* = 8.7, 2.7 Hz), 7.64 (d, 1H, *J* = 8.7 Hz), 7.36 (d, 2H, *J* = 8.1 Hz), 7.30 (d, 2H, *J* = 8.1 Hz), 2.44 (s, 3H); ^{13}C NMR (101 MHz) δ 146.7, 142.1, 139.8, 138.8, 134.4, 131.0, 129.3, 129.2, 126.3, 123.1, 21.5; MS (EI) *m/z* 247 (M^+, 100); HRMS (EI) calcd. $C_{13}H_{10}ClNO_2$: (M^+) 247.0395; found: (M^+) 247.0399.

2-Chloro-3',4'-dimethyl-5-nitrobiphenyl **79**.

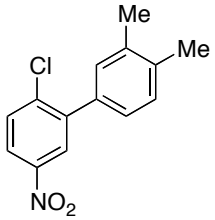

General procedure C was applied with **63** (92.4 mg, 0.15 mmol) and *o*-xylene (91 μL, 0.75 mmol). Column chromatography (*n*-hexanes:EtOAc 99:1) afforded product **79** (32.5 mg, 83%) with a regioisomeric ratio of 10:1; R_f 0.31 (*n*-hexanes:EtOAc 97:3); IR: 1519, 1504, 1462, 1345, 1083, 880, 852, 812, 740; ^{1}H NMR (400 MHz) δ 8.24 (dd, 1H, *J* = 2.7, 0.5 Hz), 8.14 (ddd, 1H, *J* = 8.8, 2.7, 0.8 Hz), 7.65 (dd, 1H, J = 8.8, 0.5 Hz), 7.30–7.20 (m, 3H), 2.36 (s, 6H); ^{13}C NMR (101 MHz) δ 146.6, 142.2, 139.7, 137.5, 137.0, 134.9, 131.0, 130.4, 129.8, 126.8, 126.3, 123.0, 20.0, 19.8; MS (CI) *m/z* 262 $[M+H]^+$; HRMS (CI) calcd. $C_{14}H_{12}ClNO_2$: $[M+H]^+$ 262.0629; found: $[M+H]^+$ 262.0632.

2'-Chloro-2,4-dimethyl-5'-nitrobiphenyl **80**.

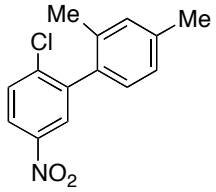

General procedure C was applied with **63** (92.4 mg, 0.15 mmol) and *m*-xylene (91 μL, 0.75 mmol). Column chromatography (*n*-hexanes:EtOAc 99:1) afforded product **80** (31.7 mg, 81%); R_f 0.34 (*n*-hexanes:EtOAc 97:3); IR: 1526, 1461, 1345, 1071, 872, 828, 768, 741; ^{1}H NMR (400 MHz) δ 8.16 (dd, 1H, *J* = 8.7, 2.8 Hz), 8.13 (d, 1H, *J* = 2.8 Hz), 7.63 (d, 1H, *J* = 8.7 Hz), 7.14 (s, 1H), 7.10 (d, 1H, *J* = 7.8 Hz), 7.03 (d, 1H, *J* = 7.8 Hz), 2.40 (s, 3H), 2.09 (s, 3H); ^{13}C NMR (101 MHz) δ 146.5, 142.3, 141.0, 138.9, 135.9, 134.4, 131.1, 130.4, 129.2, 126.8, 126.4, 123.5, 21.4, 19.8; MS (CI) *m/z* 262 $[M+H]^+$; HRMS (CI) calcd. $C_{14}H_{12}ClNO_2$: $[M+H]^+$ 262.0629; found: $[M+H]^+$ 262.0630.

2-Chloro-4'-methoxy-5-nitrobiphenyl **81**.

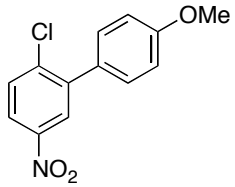

General procedure C was applied with **63** (92.4 mg, 0.15 mmol) and anisole (82 μL, 0.75 mmol). Column chromatography (*n*-hexanes:EtOAc 98:2) afforded product **81** (29.2 mg, 74%) with a regioisomeric ratio of 4.2:1; R_f 0.19 (*n*-hexanes:EtOAc 97:3); IR: 2935, 1608, 1566, 1525, 1460, 1343, 1246, 1178, 1080, 881, 740; ^{1}H NMR (400 MHz) δ 8.22 (d, 1H, *J* = 2.7), 8.11 (dd, 1H, *J* = 8.7, 2.7 Hz), 7.62 (d, 1H, *J* = 8.7 Hz), 7.41 (d, 2H, *J* = 8.6 Hz), 7.01 (d, 2H, *J* = 8.6 Hz), 3.88 (s, 3H), 3.79 (minor isomer, s, 3H); ^{13}C NMR (101 MHz) δ 160.1, 157.7 (minor isomer), 146.7, 141.8, 141.4 (minor isomer), 139.8, 139.4 (minor isomer), 131.0, 130.8 (minor isomer), 130.7, 130.6 (minor isomer), 130.3 (minor isomer), 129.7, 126.9 (minor isomer), 126.2, 123.4 (minor isomer), 122.9, 120.7 (minor isomer), 114.1, 111.2 (minor isomer), 55.7 (minor isomer), 55.5; MS (CI)

m/z 264 $[M+H]^+$; HRMS (EI) calcd. $C_{13}H_{10}ClNO_3$: $[M+H]^+$ 264.0422; found: $[M+H]^+$ 264.0424.

2-Chloro-3'-fluoro-4'-methoxy-5-nitrobiphenyl **82**.

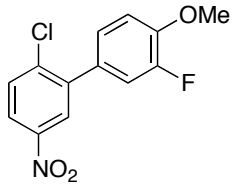

General procedure C was applied with **63** (92.4 mg, 0.15 mmol) and 1-fluoro-2-methoxybenzene (84 µL, 0.75 mmol). Column chromatography (*n*-hexanes:EtOAc 98:2) afforded product **82** (31.5 mg, 75%) with a regioisomeric ratio of 10:1; R_f 0.13 (*n*-hexanes:EtOAc 97:3); IR: 2970, 1738, 1522, 1439, 1365, 1229; ^{1}H NMR (400 MHz) δ 8.30 (minor isomer, dd, 1H, *J* = 8.8, 2.7 Hz), 8.21 (d, 1H, *J* = 2.7 Hz), 8.17 (dd, 1H, *J* = 8.8, 2.7 Hz), 7.73 (minor isomer, d, 1H, *J* = 8.8 Hz), 7.64 (d, 1H, *J* = 8.8 Hz), 7.24 (dd, 1H, *J* = 11.8, 2.2 Hz), 7.18 (ddd, 1H, *J* = 8.4, 2.1, 1.2 Hz), 7.07 (t, 1H, *J* = 8.5 Hz), 3.97 (s, 3H); ^{13}C NMR (101 MHz) δ 152.0 (d, *J* = 247.0 Hz), 148.2 (d, *J* = 10.6 Hz), 146.7, 140.6, 139.7, 131.2, 129.9 (d, *J* = 6.9 Hz), 126.2, 125.6 (d, *J* = 3.7 Hz), 133.4, 117.4 (d, *J* = 19.6 Hz), 113.3, 56.5; MS (EI) *m/z* 281 (M^+, 100); HRMS (EI) calcd. $C_{13}H_9ClFNO_3$: (M^+) 281.0250; found: (M^+) 281.0253.

2-Chloro-3'-iodo-4'-methoxy-5-nitrobiphenyl **83**.

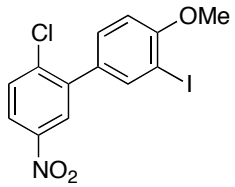

General procedure C was applied with **63** (92.4 mg, 0.15 mmol) and 1-iodo-2-methoxybenzene (98 µL, 0.75 mmol). Column chromatography (*n*-hexanes:EtOAc 98:2) afforded product **83** (43.2 mg, 74%) with a regioisomeric ratio of 7.5:1; m.p. ˚C; R_f 0.13 (*n*-hexanes:EtOAc 97:3); IR: 1568, 1510, 1494,

1341, 1253, 1047, 822, 809, 740, 663; ^{1}H NMR (400 MHz) δ 8.30 (minor isomer, dd, 1H, *J* = 8.8, 2.6 Hz), 8.20 (d, 1H, *J* = 2.6 Hz), 8.13 (dd, 1H, *J* = 8.8, 2.6 Hz), 7.88 (d, 1H, *J* = 2.0 Hz), 7.73 (minor isomer, d, 1H, *J* = 8.8 Hz), 7.63 (d, 1H, *J* = 8.8 Hz), 7.43 (dd, 1H, *J* = 8.5, 2.0 Hz), 6.92 (d, 1H, *J* = 8.5 Hz), 3.95 (s, 3H); ^{13}C NMR (101 MHz) δ 158.6, 146.7, 140.2, 140.1, 139.8, 131.4, 131.1, 130.7, 126.2, 123.4, 110.6, 85.9, 56.7; MS (EI) *m/z* 389 (M^+, 100), 391; HRMS (EI) calcd. $C_{13}H_9ClINO_3$: (M^+) 388.9313; found: $(M)^+$ 388.9310.

2-(2-Chloro-5-nitrophenyl)thiophene **84**.

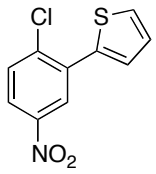

General procedure C was applied with **63** (92.4 mg, 0.15 mmol) and thiophene (60 μL, 0.75 mmol). Column chromatography (*n*-hexanes:EtOAc 99:1) afforded product **84** as a white solid (30.5 mg, 85%); m.p. 44–46 ˚C; R_f 0.53 (*n*-hexanes:EtOAc 90:10); IR: 1514, 1464, 1290, 1258, 1244, 1066, 900, 867, 848, 824, 760, 739, 697, 632; ^{1}H NMR (400 MHz) δ 8.42 (d, 1H, *J* = 2.5 Hz), 8.09 (dd, 1H, *J* = 8.8, 2.5 Hz), 7.65 (d, 1H, *J* = 8.8 Hz), 7.50 (d, 1H, *J* = 5.1 Hz), 7.47 (d, 1H, *J* = 3.7 Hz), 7.17 (t, 1H, *J* = 3.7 Hz); ^{13}C NMR (101 MHz) δ 146.8, 139.2, 137.9, 135.0, 131.7, 129.2, 128.0, 127.7, 126.2, 123.1; MS (EI) *m/z* 158, 218, 239 (M^+, 100), 241; HRMS (EI) calcd. $C_{10}H_6ClNO_2S$: (M^+) 238.9806; found: (M^+) 238.9802.

1-(3-Bromo-5-(2-chloro-5-nitrophenyl)thiophen-2-yl)ethanone **85**.

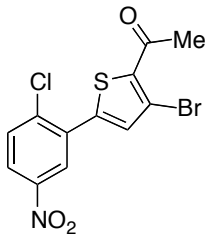

General procedure C was applied with **63** (92.4 mg, 0.15 mmol) and 2-acetyl-3-bromothiophene (153.8 mg, 0.75 mmol). Column chromatography (*n*-hexanes:EtOAc 95:5) afforded product **85** (39.7 mg, 74%); R_f 0.26 (*n*-hexanes:EtOAc 90:10); IR: 1680, 1523, 1421, 1390, 1347, 1226, 869, 851, 828, 738, 658; ^{1}H NMR (400 MHz) δ 8.40 (d, 1H, *J* = 2.5 Hz), 8.19 (dd, 1H, *J* = 8.8, 2.5 Hz), 7.70 (d, 1H, *J* = 8.8 Hz), 7.44 (s, 1H), 2.75 (s, 3H); ^{13}C NMR (101 MHz) δ 190.2, 146.8, 143.7, 140.7, 139.4, 134.5, 132.7, 132.0, 125.9, 124.7, 114.1, 29.9; MS (EI) *m/z* 300, 344, 346, 359 (M^+), 360; HRMS (EI) calcd. $C_{12}H_7BrClNO_3S$: (M^+) 358.9013; found: (M^+) 358.9009.

2-(2-Chloro-5-nitrophenyl)-4-methylthiophene **86**.

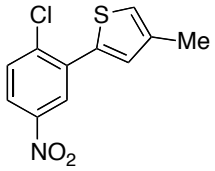

General procedure C was applied with **63** (92.4 mg, 0.15 mmol) and 3-methylthiophene (73 µL, 0.75 mmol). Column chromatography (*n*-hexanes:EtOAc 99:1) afforded product **86** (29.2 mg, 87%) with a regioisomeric ratio of 2.7:1; R_f 0.58 (*n*-hexanes:EtOAc 90:10); IR: 3092, 1563, 1510, 1472, 1344, 1293, 1262, 1226, 1133, 959, 903, 738, 646; ^{1}H NMR (400 MHz) δ 8.40 (d, 1H, *J* = 2.5 Hz), 8.26 (minor isomer, d, 1H, *J* = 2.6 Hz), 8.18 (minor isomer, dd, 1H, *J* = 8.8, 2.6 Hz), 8.07 (dd, 1H, *J* = 8.8, 2.5 Hz), 7.66 (minor isomer, d, 1H, *J* = 8.8 Hz), 7.63 (d, 1H, *J* = 8.8 Hz), 7.37 (minor isomer, d, 1H, *J* = 5.1 Hz), 7.28 (s, 1H), 7.07 (s, 1H), 6.97 (minor isomer, d, 1H, *J* = 5.1 Hz), 2.34 (s, 3H), 2.13 (minor isomer, s, 3H); ^{13}C NMR (101 MHz) δ major isomer: 146.7, 138.9,

138.3, 137.5, 135.0, 131.6, 131.3, 125.9, 123.4, 122.8, 15.9; minor isomer: 146.3, 142.0, 137.1, 135.3, 131.7, 130.8, 130.1, 127.8, 125.8, 124.1, 14.7; MS (EI) *m/z* 127, 171, 253 (M^+); HRMS (EI) calcd. $C_{11}H_8ClNO_2S$: (M^+) 252.9959; found: (M^+) 252.9960.

2-(2-Chloro-5-nitrophenyl)-4-hexylthiophene **87**.

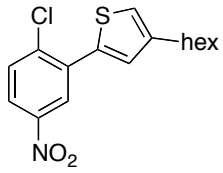

General procedure C was applied with **63** (92.4 mg, 0.15 mmol) and 3-hexylthiophene (135 µL, 0.75 mmol). Column chromatography (*n*-hexanes:EtOAc 99:1) afforded product **87** (41.0 mg, 85%) with a regioisomeric ratio of 4.3:1; R_f 0.71 (*n*-hexanes:EtOAc 90:10); IR: 2925, 2855, 1567, 1522, 1467, 1345, 904, 858, 739; ^{1}H NMR (400 MHz) δ 8.41 (d, 1H, *J* = 2.5 Hz), 8.24 (minor isomer, d, 1H, *J* = 2.5 Hz), 8.18 (minor isomer, dd, 1H, *J* = 8.8, 2.5 Hz), 8.07 (dd, 1H, *J* = 8.8, 2.5 Hz), 7.66 (minor isomer, d, *J* not observed but expected to be 8.8 Hz), 7.64 (s, 1 H), 7.38 (minor isomer, d, 1H, *J* = 5.1 Hz), 7.31 (s, 1H), 7.08 (s, 1H), 7.01 (minor isomer, d, 1H, *J* = 5.1 Hz), 2.65 (t, 2H, *J* = 7.7 Hz), 2.41 (minor isomer, t, 2H, *J* = 7.7 Hz), 1.70–0.80 (both isomers, m, 11H); ^{13}C NMR (101 MHz) δ major isomer: 146.7, 144.0, 138.9, 137.3, 135.1, 131.6, 130.4, 125.9, 122.7, 122.6, 31.8, 30.7, 30.6, 29.1, 22.8, 14.2; minor isomer: 146.3, 142.3, 142.1, 135.4, 131.4, 130.8, 128.7, 127.9, 126.0, 124.2, 31.7, 30.4, 29.1, 28.9, 22.7, 14.1; MS (EI) *m/z* 171, 206, 253, 323 (M^+); HRMS (EI) calcd. $C_{16}H_{18}ClNO_2S$: (M^+) 323.0741; found: (M^+) 323.0739.

Methyl 5-(2-chloro-5-nitrophenyl)-2-methylfuran-3-carboxylate **88**.

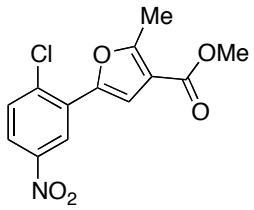

General procedure C was applied with **63** (92.4 mg, 0.15 mmol) and methyl 2-methyl-3-furan carboxylate (94 mg, 0.75 mmol). Column chromatography (*n*-hexanes:EtOAc) afforded product **88** (27.5 mg, 62%) with a regioisomeric ratio of 7.5:1; R_f 0.24 (*n*-hexanes:EtOAc 90:10); IR: 1704, 1602, 1516, 1469, 1433, 1400, 1345, 1289, 1245, 1199, 1168, 1106, 1090, 950, 911, 833, 765, 742, 619; ^{1}H NMR (400 MHz) δ 8.81 (d, 1H, *J* = 2.5 Hz), 8.20 (minor isomer, dd, 1H, *J* = 8.8, 2.4 Hz), 8.16 (minor isomer, d, 1H, *J* = 2.4 Hz), 8.10 (dd, 1H, *J* = 8.8, 2.5 Hz), 7.68 (minor isomer, 1H, *J* = 8.8 Hz), 7.61 (d, 1H, *J* = 8.8 Hz), 7.19 (s, 1H), 3.95 (s, 3H), 2.43 (s, 3H); ^{13}C NMR (101 MHz) δ 159.8, 149.3, 147.0, 143.5 (minor isomer), 140.4, 137.2, 132.7, 132.0, 131.0 (minor isomer), 129.6, 126.9 (minor isomer), 124.4 (minor isomer), 123.7, 123.5, 117.5, 52.0, 11.8, 10.4 (minor isomer); MS (CI) *m/z* 296 [$(M+H)^+$, 100]; HRMS (CI) calcd. $C_{13}H_{10}ClNO_5$: $[M+H]^+$ 296.0320; found: $[M+H]^+$ 296.0324.

2-Chloro-5-nitrophenyl(tri-tert-butylphosphine)gold(I) **89**.

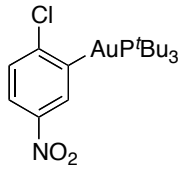

A mixture of ClAuP^{t}Bu$_3$ (26.1 mg, 0.06 mmol), 2-chloro-5-nitrobenzoic acid (12.1 mg, 0.06 mmol) and Ag_2O (13.9 mg, 0.06 mmol) in 0.9 mL of DMF was stirred at 110 ºC for 3 h. After this time the reaction mixture was filtered through cotton wool, washed with CH_2Cl_2 and evaporated to dryness. Column chromatography on deactivated (2% Et3N) silica gel (hexanes:EtOAc 9:1) afforded product **89** as a white solid (29.5 mg, 96%); m.p. 152–154 ºC; R_f 0.60 (*n*-hexanes:EtOAc 9:1); IR: 1513, 1337, 1277, 1024; ^{1}H NMR (400 MHz) δ 8.31

(dd, 1H, J = 5.0, 2.9 Hz), 7.81 (dd, 1H, J = 8.7, 2.9 Hz), 7.43 (dd, 1H, J = 8.7, 1.72 Hz), 1.58 (d, 27H, J = 13.0 Hz); ^{13}C NMR (101 MHz) δ 177.7 (d, J = 104.4 Hz), 151.2 (d, J = 2.8 Hz), 146.1, 134.3, 127.8 (d, J = 4.1 Hz), 121.4, 39.1 (d, J = 15.6 Hz), 32.4 (d, J = 4.5 Hz); ^{31}P NMR (162 MHz) δ 91.34 (s, 1P); HRMS (ESI) calcd. $C_{18}H_{31}AuClNO_2P$: ([M+H]+), 556.1441; found: ([M+H]+), 556.1434.

2-Chloro-5-nitro-phenyl[*N*,*N*-Bis(2,6-diisopropylphenyl)imidazol-2-yl](2,4,6 trifluorophenyl)gold(I) **90**.

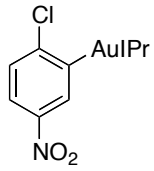

A mixture of IPrAuCl (74.3 mg, 0.10 mmol), Ag_2O (23.4 mg, 0.10 mmol) and 2-chloro-5-nitrobenzoic acid (0.10 mmol) in DMF (1.4 mL, 0.07 M) was stirred at 110 ºC for 5 h. After this time, the resulting mixture was filtered through a plug of cotton wool, which was washed with CH_2Cl_2 and the filtrate concentrated under reduced pressure. The crude product was purified by column chromatography (*n*-hexanes:EtOAc:Et_3N 87:10:3) to afford product **90** (57.2 mg, 77%); R_f 0.19 (*n*-hexanes:EtOAc:Et_3N 86:10:4); IR: 2954, 1514, 1463, 1370, 1337, 1216, 1028, 873, 803, 761; ^{1}H NMR (400 MHz) δ 7.78 (d, 1H, *J* = 2.8 Hz), 7.58 (dd, 1H, *J* = 8.7, 2.8 Hz), 7.51 (t, 2H, *J* = 7.8 Hz), 7.31 (d, 4H, *J* = 7.8 Hz), 7.19 (s, 2H), 7.14 (d, 1H, *J* = 8.7 Hz), 2.64 (sept., 1H, *J* = 6.8 Hz), 1.38 (d, 12H, *J* = 6.8 Hz), 1.24 (d, 12H, *J* = 6.8 Hz); ^{13}C NMR (101 MHz) δ 193.2, 171.4, 151.9, 145.8, 135.0, 134.4, 130.4, 127.1, 124.0, 123.0, 120.6, 28.8, 24.5; HRMS (CI) calcd. $C_{33}H_{40}AuClN_3O_2$: (M^+) 742.2469; found: (M^+) 742.2460.

3.7.4 Kinetic Isotope Effect Experiments

Procedure for the dual C–H activation coupling kinetic isotope effect experiment

A mixture of PhI(OH)OTs (0.04 mmol, 15.6 mg) and aryl gold(I) compound **43** (12.5 mg, 0.02 mmol), benzene (54 μL, 0.60 mmol) and benzene-d_6 (53 μL, 0.60 mmol) in DCE (0.1 mL) was stirred at 50 ºC for 1 h. After this time, the mixture was filtered through a plug of silica washing with hexane and the filtrate was concentrated under reduced pressure. The crude product was analysed by EI-MS to determine the ratio of products (**56**:**56-d_5** = 1:0.9).

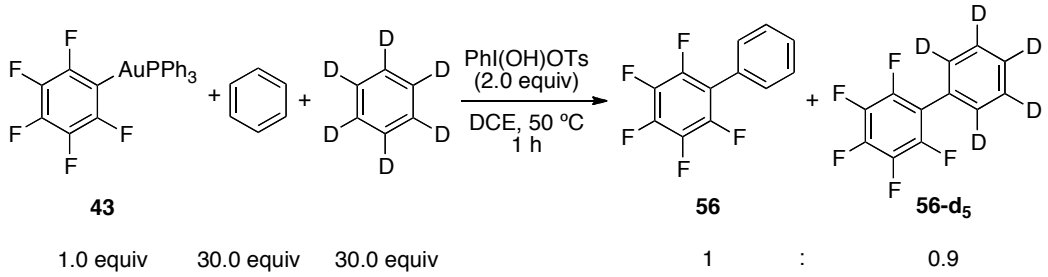

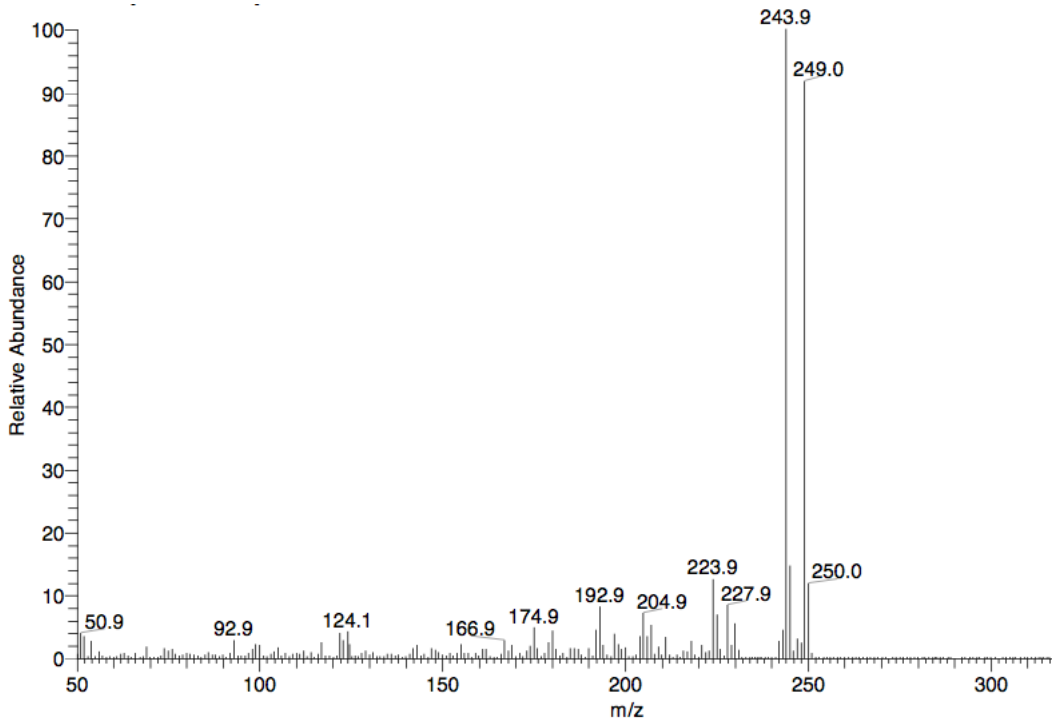

m/z= 239.5-254.4

m/z	Intensity	Relative
240.0	16190.2	0.10
241.0	21022.1	0.13
241.9	433054.2	2.62
242.9	738410.2	4.47
243.9	16533666.0	100.00
244.9	2412590.2	14.59
245.9	171777.7	1.04
246.9	485686.0	2.94
248.0	380951.8	2.30
249.0	15179932.3	91.81
250.0	1952939.6	11.81
251.0	117576.2	0.71
252.0	4885.4	0.03
253.0	1159.2	0.01
254.2	1208.9	0.01

Procedure for the decarboxylative arylation kinetic isotope effect experiment

A mixture of PhI(OH)OTs (0.04 mmol, 15.6 mg), aryl gold(I) compound **43** (0.02 mmol, 12.3 mg), benzene (54 µL, 0.60 mmol) and d_6-benzene (53 µL, 0.60 mmol) in DCE (0.1 mL) was stirred at 50 ºC for 1 hour. After this time the mixture was filtered through a plug of cotton wool, which was washed with EtOAc and the filtrate concentrated under reduced pressure. The crude product was analysed by EI-MS to determine the ratio of product **77** to **77- d_5**.

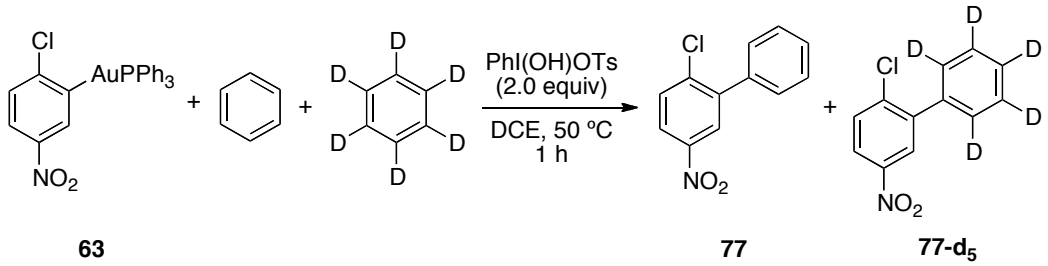

63				**77**		**77-d_5**
1.0 equiv	30.0 equiv	30.0 equiv		2	:	1

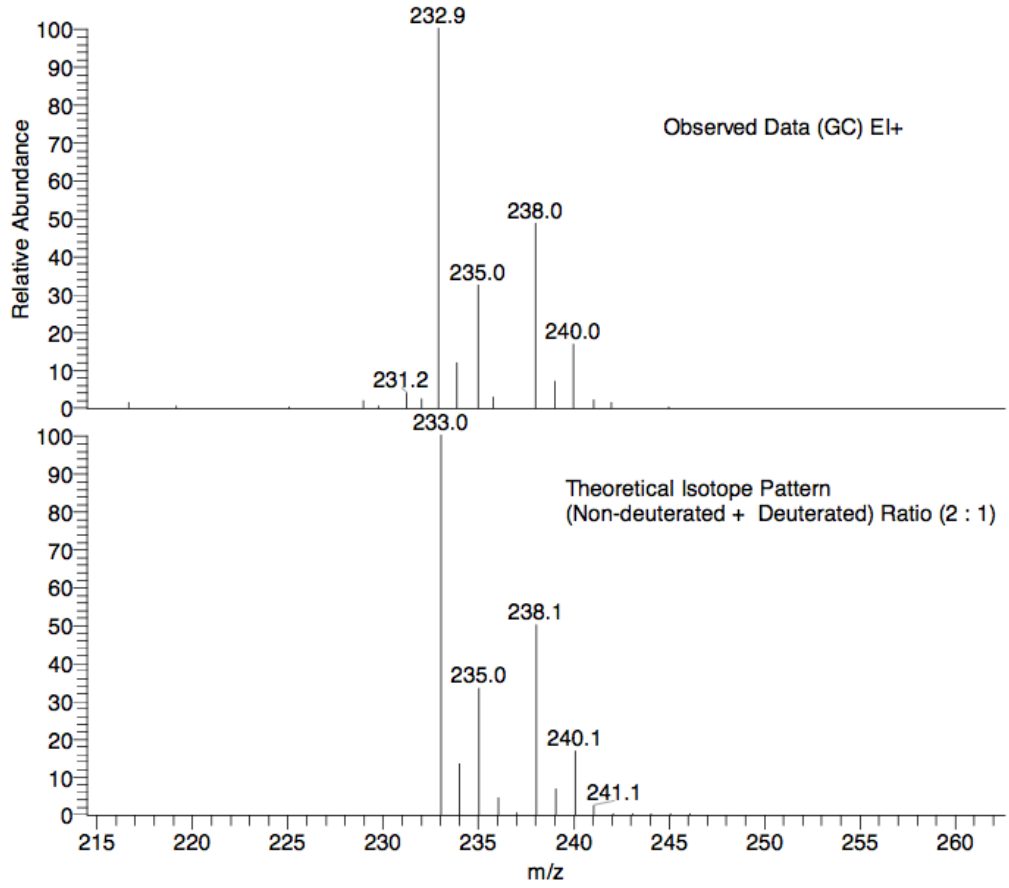

3.7.5 Other Mechanistic Experiments

Gold(I) C–H Activation with triphenylphosphine gold(I) tosylate

General procedure A was applied, at one third the scale, with $TsOAuP^tBu_3$[103] (12.6 mg, 0.02 mmol) and 1,2,4,5-tetrafluorobenzene (10 μL, 0.09 mmol) for 16 h. After this time, the crude reaction mixture was filtered through a plug of cotton wool, washing with CH_2Cl_2 and the filtrate concentrated under reduced pressure. ^1H NMR analysis, using *p*-xylene as an internal standard, revealed product **44** in 60% yield.

Gold(I) Selectivity Competition Experiment

General procedure A was applied, at one third the scale, with $ClAuPPh_3$ (9.9 mg, 0.02 mmol), 1-fluoro-3-nitrobenzene (10 μL, 0.09 mmol) and 2-iodoanisole (12 μL, 0.09 mmol) for 16 h. After this time, the crude reaction mixture was filtered though a plug of cotton wool, washing with CH_2Cl_2 and the filtrate concentrated under reduced pressure. ^1H NMR analysis, using *p*-xylene as an internal standard, revealed product **46** in 64% yield.

Gold(III) Selectivity Competition Experiment

General procedure C was applied, at one third the scale, with **46** (30 mg, 0.05 mmol), 2-iodoanisole (33 μL, 0.25 mmol) and 1,2,4,5-tetrafluorobenzene (28 μL, 0.25 mmol). After 16 hours, the crude reaction mixture was filtered though a plug of cotton wool, washing with CH_2Cl_2 and the filtrate concentrated under reduced pressure. ^1H NMR analysis, using *p*-xylene as an internal standard, revealed product **53** in 99% yield.

References

1. N. Winterton, *Green Chem.*, 2001, **3**, G73.
2. J. A. Labinger and J. E. Bercaw, *Nature*, 2002, **417**, 507.
3. This review focuses on gold–mediated C–H functionalisation, for alternative recent reviews covering the use of other transition metals see: (a) C–H activation, *Topics in Current Chemistry*, ed. J.-Q. Yu and Z. Shi, Springer, 2010, vol. 292. (b) D. Balcells, E. Clot and O. Eisenstein, *Chem. Rev.*, 2010, **110**, 749. (c) D. A. Colby, R. G. Bergman and J. Ellman, *Chem. Rev.,* 2010, **110**, 624. (d) P. Sehnal, R. J. K. Taylor and I. J. S. Fairlamb, *Chem. Rev.*, 2010, **110**, 824. (e) H. M. L. Davies and J. R. Denton, *Chem. Soc. Rev.*, 2009, **38**, 3061. (f) L. Ackermann, R. Vicente and A. R. Kapdi, *Angew. Chem. Int. Ed.,* 2009, **48**, 9792. (g) F. Bellina and R. Rossi, *Tetrahedron,* 2009, **65**, 10269.
4. For recent reviews on homogeneous gold catalysis see: (a) A. Fürstner, *Chem. Soc. Rev.*, 2010, **38**, 3208. (b) A. S. K. Hashmi and M. Rudolph, *Chem. Soc. Rev.,* 2008, **37**, 1766. (c) A. Arcadi, *Chem. Rev.*, 2008, **108**, 3266. (d) Z. Li, C. Brouwer and C. He, *Chem. Rev.*, 2008, **108**, 3239.
5. M. S. Kharasch and H. S. Isbell, *J. Am. Chem. Soc.*, 1931, **53**, 3053.
6. M. S. Kharasch and T. M. Beck, *J. Am. Chem. Soc.*, 1934, **56**, 2057.
7. K. S. Liddle and C. Parkin, *J. Chem. Soc., Chem Commun.*, 1972, 26.
8. P. W. J. de Graaf, J. Boersma and G. J. M. van der Kerk, *J. Organomet. Chem.*, 1976, **105**, 399.
9. A. S. K. Hashmi, L. Schwarz, J.-H. Choi and T. M. Frost, *Angew. Chem. Int. Ed.*, 2000, **39**, 2285.
10. G. Dyker, E. Muth, A. S. K. Hashmi and L. Ding, *Adv. Synth. Catal*., 2003, **345**, 1247.
11. D. Aguilar, M. Contel, R. Navarro and E. P. Urriolabeitia, *Organometallics*, 2007, **26**, 4604.
12. D. Aguilar, M. Contel, R. Navarro, T. Soler and E. P. Urriolabeitia, *J. Organomet. Chem.*, 2009, **694**, 486.
13. A. Arcadi, G. Bianchi, M. Chiarini, G. D'Anniballe and F. Marinelli, *Synlett*, 2004, **6**, 944.
14. M. Alfonsi, A. Arcadi, G. Bianchi, F. Marinelli and A. Nardini, *Eur. J. Org. Chem.*, 2006, 2393.
15. Y. Liu, J. Zhu, J. Qian, B. Jiang and Z. Xu, *J. Org. Chem.*, 2011, **76**, 9096.
16. C. Ferrer and A. M. Echavarren, *Angew. Chem. Int. Ed.*, 2006, **45**, 1105.

17. C. Nevado and A. M. Echavarren, *Chem. Eur. J.*, 2005, **11**, 3155.
18. (a) Z. Shi and C. He. *J. Org. Chem*., 2004, **69**, 3669. (b) Z. Li, Z. Shi and C. He, *J. Organomet. Chem*., 2005, **690**, 5049.
19. M. T. Reetz and K. Sommer, *Eur. J. Org. Chem.*, 2003, 3485.
20. Y.-P. Xiao, X.-Y. Lui and C.-M. Che, *J. Organomet. Chem.*, 2009, **694**, 494.
21. Z. Shi and C. He, *J. Am. Chem. Soc.*, 2004, **126**, 5964.
22. Y. Lui, X. Li, G. Lin, Z. Xiang, J. Xiang, M. Zhao, J. Chen and Z. Yang, *J. Org. Chem.*, 2008, **73**, 4625.
23. R. Marcos, C. Rodríguez-Escrich, C. I. Herrerías and M. A. Pericàs, *J. Am. Chem. Soc.*, 2008, **130**, 16838.
24. X. Sun, W. Sun, R. Fan and J. Wu, *Adv. Synth. Catal*., 2007, **349**, 2151.
25. R. Skouta and C.-J. Li, *Angew. Chem. Int. Ed.*, 2007, **46**, 1117.
26. Z. Shi and C. He, *J. Am. Chem. Soc.*, 2004, **126**, 13596.
27. Y. Luo and C.-J. Li, *Chem. Commun.*, 2004, 1930.
28. K. Mertins, I. Iovel, J. Kischel, A. Zapf and M. Beller, *Adv. Synth. Catal.*, 2006, **348**, 691.
29. W. Rao and P. W. H. Chen, *Org. Biomol. Chem.*, 2008, **6**, 2426.
30. P. Rubenbauer and T. Bach, *Adv. Synth. Catal.*, 2008, **350**, 1125.
31. C.-F. Xu, M. Xu, L.-Q. Yang and C.-Y. Li, *J. Org. Chem.*, 2012, **77**, 3010.
32. Y. Liu, J. Zhu, J. Qian and Z. Xu, *J. Org. Chem.*, 2012, **77**, 5411.
33. (a) A. Kar, N. Mangu, H. M. Kaiser, M. Beller and M. K. Tse, *Chem. Commun.*, 2008, 386. (b) A. Kar, N. Mangu, H. M. Kaiser and M. K. Tse, *J. Organomet. Chem.*, 2009, **694**, 524.
34. Y. Fuchita, Y. Utsunomiya and M. Yasutake, *J. Chem. Soc., Dalton Trans*., 2001, 2330.
35. J. P. Brand, J. Charpentier and J. Waser, *Angew. Chem. Int. Ed.*, 2009, **48**, 9346.
36. J. P. Brand and J. Waser, *Angew. Chem. Int. Ed.*, 2010, **49**, 7304.
37. T. de Haro and C. Nevado, *J. Am. Chem. Soc*., 2010, **132**, 1512.
38. Z. Li, D. A. Capretto, R. O. Rahaman and C. He, *J. Am. Chem. Soc.*, 2007, **129**, 12058.
39. F. Mo, J. M. Yan, D. Qui, F. Li, Y. Zhang and J. Wang, *Angew. Chem. Int. Ed.*, 2010, **49**, 2028.
40. A. Pradal, P. Y. Toullec and V. Michelet, *Org. Lett.*, 2011, **13**, 6086.
41. P. Lu, T. C. Boorman, A. M. Z. Slawin and I. Larrosa, *J. Am. Chem. Soc.*, 2010, **132**, 5580.

42. S. Gaillard, A. M. Z. Slawin and S. P. Nolan, *Chem. Commun.*, 2010, **46**, 2742.

43. I. I. F. Boogaerts and S. P. Nolan, *J. Am. Chem. Soc.*, 2010, **132**, 8858.

44. P. Y. Toullec, E. Genin, L. Leseure, J.-P. Genêt and V. Michelet, *Angew. Chem. Int. Ed.*, 2006, **45**, 7427.

45. C.-M. Chao, M. R. Vitale, P. Y. Toullec, J.-P. Genêt and V. Michelet, *Chem. Eur. J.*, 2009, **15**, 1319.

46. C. H. M. Amijs, C. Ferrer and A. M. Echavarren, *Chem. Commun.*, 2007, 698.

47. N. D. Shapiro and D. Toste, *J. Am. Chem. Soc*., 2007, **129**, 4160.

48. N. Kern, A. Blanc, J.-M. Weibel and P. Pale, *Chem. Commun.*, 2011, **47**, 6665.

49. D. Qian abd J. Zhang, *Chem. Commun.*, 2012, **48**, 7082.

50. (a) K. Sonogashira, Y. Tohda and N. Hagihara, *Tetrahedron Lett*., 1975, **16**, 4467. (b) P. Siemsen, R. C. Livingston and F. Diederich, *Angew. Chem. Int. Ed*., 2000, **39**, 2632. (b) R. Chinchilla and C. Nájera, *Chem. Rev.*, 2007, **107**, 874.

51. L. A. Jones, S. Sanz and M. Laguna, *Catalysis Today*, 2007, **122**, 403.

52. (a) A. S. K. Hashmi, C. Lothschütz, R. Döpp, M. Rudolph, T. D. Ramamurthi and F. Rominger, *Angew. Chem. Int. Ed.*, 2009, **48**, 8243. (b) Y. Shi, K. A. Roth, S. D. Ramgren and S. A. Blum, *J. Am. Chem. Soc.*, 2009, **131**, 18022.

53. C. González-Arellano, A. Abad, A. Corma, H. García, M. Iglesias and F. Sánchez, *Angew. Chem. Int. Ed.*, 2007, **46**, 1536.

54. C. González-Arellano, A. Corma, M. Iglesias and F. Sánchez, *J. Catal*., 2006, **238**, 497.

55. R. O. M. A. de Souza, M. S. Bittar, L. V. P. Mendes, C. M. F. da Silva, V. T. da Silva and O. A. C. Antunes, *Synlett*, 2008, **12**, 1777.

56. P. Li, L. Wang, M. Wang and F. You, *Eur. J. Org. Chem*., 2008, 5946.

57. T. Lauterbach, M. Livendahl, A. Rosellón, P. Espinet and A. M. Echavarren, *Org. Lett.,* 2010, **12**, 3006.

58. A. Corma, R. Juárez, M. Boronat, F. Sánchez, M. Inglesias and H. García, *Chem. Commun.*, 2011, **47**, 1446.

59. X. Yao and C.-J. Li, *Org. Lett.*, 2006, **8**, 1953.

60. C. Li, W. Li and J. Wang, *Tetrahedron Lett.*, 2009, **50**, 2533.

61. C. Wei and C.-J. Li, *J. Am. Chem. Soc*., 2003, **125**, 9584.

62. F. Xiao, Y. Chen, Y. Liu and J. Wang, *Tetrahedron*, 2008, 2755.

63. V. K.-Y. Lo, Y. Liu, M.-K. Wong and C.-M. Che, *Org. Lett.*, 2006, **8**, 1529.

64. B. Huang, X. Yao and C.J. Li, *Adv. Synth. Catal.*, 2006, **348**, 1528.

65. C. Li, F. Mo, W. Li and J. Wang, *Tetrahedron*, 2009, 6053.

66. B. Yan and Y. Liu, *Org. Lett.*, 2007, **9**, 4323.

67. C. J. Jones, D. Taube, V. R. Ziatdinov, R. A. Periana, R. J. Nielsen, J. Oxgaard and W. A. Goddard III, *Angew. Chem. Int. Ed.*, 2004, **43**, 4626.

68. A. S. K. Hashmi, S. Schäfer, M. Wölfle, C. Diez Gil, P. Fischer, A. Laguna, M. C. Blanco and M. C. Gimeno, *Angew. Chem. Int. Ed.*, 2007, **46,** 6184.

69. M. R. Fructos, P. de Frémont, S. P. Nolan, M. M. Díaz-Requejo and P. J. Pérez, *Organometallics*, 2006, **25**, 2237.

70. M. R. Fructos, T. R. Belderrain, P. de Frémont, N. M. Scott, S. P. Nolan, M. M. Díaz-Requejo and P. J. Pérez, *Angew. Chem. Int. Ed*., 2005, **44,** 5284.

71. Y. Horino, T. Yamamoto, K. Ueda, S. Kuroda and D. Toste, *J. Am. Chem. Soc*., 2009, **131**, 2809.

72. Y. Liu, D. Zhang, J. Zhou and C. Liu, *J. Phys. Chem. A*, 2010, **114**, 6164.

73. A. Escribano-Cuesta, V. López-Carillo, D. Janssen and A. M. Echavarren, *Chem. Eur. J.*, 2009, **15**, 5646.

74. S. Bhunia and R.-S. Liu, *J. Am. Chem. Soc*., 2008, **130**, 16488.

75. I. D. Jurberg, Y. Odabachian and F. Gagosz, *J. Am. Chem. Soc*., 2010, **132**, 3543.

76. J. Xie, H. Li, J. Zhou, Y. Cheng and C. Zhu, *Angew. Chem. Int. Ed.*, 2012, **51**, 1252.

77. J. Xie, H. Li, Q. Xue, Y. Cheng and C. Zhu, *Adv. Synth. Catal.*, 2012, **354**, 1646.

78. Y. Zhang, B. Feng and C. Zhu, *Org. Biomol. Chem.*, 2012, **10**, 9137.

79. (a) N. Lebrasseur and I. Larrosa, *J. Am. Chem. Soc.*, 2008, **130**, 2926. (b) J. Cornella, P. Lu and I. Larrosa *Org. Lett.* 2009, **11**, 5506. (c) J. Cornella, H. Lalhali and I. Larrosa, *Chem. Comm.,* 2010, **46**, 8276. (d) J. Cornella, M. Righi and I. Larrosa, *Angew. Chem. Int. Ed.*, 2011, **50**, 9429.

80. K. A. Porter, A. Schier and H. Schmidbaur, *Organometallics*, 2009, **22**, 4922.

81. D. V. Partyka, M. Zeller, A. D. Hunter and T. G. *Gray*, *Angew. Chem. Int. Ed*., 2006, **45**, 8188.

82. (a) M. Peña-López, M. Ayán-Varela, L. A. Sarandeses and J. P. Sestelo, *Chem. Eur. J.*, 2010, **16**, 9905. (b) J. J. Hirner and S. A. Blum, *Organometallics*, 2011, **30**, 1299.

83. M. M. Rahman, H.-Y. Liu, K. Eriks, A. Prock and W. P. Giering, *Organometallics,* 1989, **8**, 1.

84. (a) M. Lafrance, C. N. Rowley, T. K. Woo and K. Fagnou, *J. Am. Chem. Soc.*, 2006, **128**, 8754. (b) D. Garcia-Cuadrado, A. A. C. Braga, F. Maseras, A. M. Echavarren, *J. Am. Chem. Soc.*, 2006, **128**, 1066.

85. S. Dupuy, F. Lazreg, A. M. Z. Slawin, C. S. J. Cazin and S. P. Nolan, *Chem. Commun.*, **2011**, *47*, 5455.

86. N. Ahlsten, G. J. P. Perry, X. C. Cambeiro, T. C. Boorman and I. Larrosa, *Catal. Sci. Technol.*, 2013, **DOI:** 10.1039/C3CY00240C.

87. Gold(I) chloride species were either obtained from commercial sources or prepared via procedure as detailed in T. E. Müller, J. C. Green, D. M. P. Mingos, C. M. McPartlin, C. Whittingham, G. J. Williams and T. M. Woodroffe, *J. Organomet. Chem.,* 1998, **551**, 313, using the corresponding phosphine from commercial sources.

88. P. Byabartta, *Transition Metal Chemistry*, 2007, **32**, 716.

89. Prepared via procedure as detailed in P. Römbke, A. Schier and H. Schmidbaur, *Verlag der Zeitschrift für Naturforschung, Tübingen*, 2002, 605, using silver pivalate prepared via procedure as detailed in T. A. Stromnova, D. V. Paschenko, L. I. Boganova, M. V. Daineko, S. B. Katser, A. V. Churakov, L. G. Kuz'mina and J. A. K. Howard, *Inorganica Chimica Acta*, 2003, **350**, 283.

90. For a recent review on dual C–H activation see: C. S. Yeung and V. M. Dong, *Chem. Rev.,* 2011, **111**, 1215 and references therein.

91. For examples of dual C–H activation procedures see: (a) R. Li, L. Jiang and W. Lu, *Organometallics*, 2006, **25**, 5973. (b) J. B. Xia and S.-L. You, *Organometallics*, 2007, **26**, 4869. (c) T. A. Dwight, N. R. Rue, D. Charyk, R. Josselyn and B. DeBoef, *Org. Lett*., 2007, **9**, 3137. (d) D. R. Stuart and K. Fagnou, *Science*, 2007, **316**, 1172. (e) K. L. Hull and M. S. Sanford, *J. Am. Chem. Soc.*, 2007, **129**, 11904. (f) D. R. Stuart, E. Villemure and K. Fagnou, *J. Am. Chem. Soc.*, 2007, **129**, 12072. (g) S. Potavathri, A. S. Dumas, T. A. Dwight, G. R. Naumiec, J. M. Hammann and B. DeBoef, *Tetrahedron Lett.*, 2008, **49**, 4050. (h) B.-J. Li, S.-L. Tian, Z. Fang and Z.-J. Shi, *Angew.Chem., Int. Ed. Engl.*, 2008, **47**, 1115. (i) G. Brasche, J. Garcia-Fortanet and S. L. Buchwald, *Org.Lett.*, 2008, **10**, 2207. (j) S. H. Cho, S. J. Hwang and S. Chang, *J. Am. Chem. Soc.*, 2008, **130**, 9254. (k) K. L. Hull and M. S. Sanford, *J. Am. Chem. Soc.*, 2009, **131**, 9651. (l) X. Zhao, C. S. Yeung, V. M. Dong, *J. Am. Chem. Soc.*, 2010, **132**, 5837. (m) Y. Wei and W. Su, *J. Am. Chem. Soc.*, 2010, **132**, 16377. (n) C. S. Yeung, X. Zhao, N. Borduas and V. M. Dong *Chem. Sci.*, 2010, **1**, 331. (o) H. Li, J. Liu, C.-L. Sun, B.-J. Li and Z.-J. Shi, *Org. Lett.*, 2011, **13**, 276.

92. (a) H. A. Wegner, S. Ahles and M. Neuburger, *Chem.–Eur. J.,* 2008, **14**, 11310. (b) G. Zhang, Y. Peng, L. Cui and L. Zhang, *Angew. Chem., Int. Ed. Engl.*, 2009, **48**, 3112. (c) P. Yu, L. Cui, G. Zhang and L. Zhang, *J. Am. Chem. Soc.*, 2009, **131**, 5062. (d) T. D. Haro and C. Nevado, *Angew. Chem., Int. Ed. Engl.*, 2011, **50**, 906. (e) G. Zhang, Y. Luo, Y. Wang and L. Zhang, *Angew. Chem. Int. Ed.* 2011, **50**, 4450.

93. M. Hofer and C. Nevado, *Tetrahedron*, 2013, **69**, 5751.

94. For selected reviews see: (a) D. Tanaka, A. S. P. Romeril, A. G. Myers, *J. Am. Chem. Soc.*, 2005, **127**, 10323. (b) P. Forgione, M.-C. Brochu, M. St-Onge, K. H. Thesen, M. D. Bailey and F. Bilodeau, *J. Am. Chem. Soc.*, 2006, **128**, 11350. (c) L. J. Goossen, N. Rodriguez, K. Goossen, *Angew. Chem., Int. Ed. Engl.*, 2008, **47**, 3100. (d) J.-M. Becht, C. Le Drian, *Org. Lett.*, 2008, **10**, 3161. (e) R. Shang, Y. Fu, Y. Wang, Q. Xu, H.-Z. Yu and L. Liu, *Angew. Chem., Int. Ed. Engl.*, 2009, **48**, 9350. (f) M.Miyasaka, A. Fukushima, T. Satoh, K. Hirano and M. Miura, *Chem.–Eur. J.*, 2009, **15**, 3674. (g) Z. Fu, S. Huang, W. Su and M. Hong, *Org. Lett.*, 2010, **12**, 4992. (h) L. J. Goossen, N. Rodriguez, P. P. Lange and C. Linder, *Angew. Chem., Int. Ed. Engl.*, 2010, **49**, 1111.

95. L. J. Goossen, G. Deng, L. M. Levy, *Science* 2006, **313**, 662.

96. (a) A. Voutchkova, A. Coplin, N. E. Leadbeater and R. H. Crabtree, *Chem. Commun.*, 2008, 6312. (b) C. Wang, I. Piel and F. Glorius, *J. Am. Chem. Soc.*, 2009, **131**, 4194. (c) W.-Y. Yu, W. N. Sit, Z. Zhou and A. S.-C. Chan, *Org. Lett.*, 2009, **11**, 3174. (d) C. Wang, R. Souvik and F. Glorius, *J. Am. Chem. Soc.*, 2010, **132**, 14006. (e) F. Zhang and M.F. Greaney, *Angew. Chem. Int. Ed.*, 2010, **49**, 2768. (f) J. Zhou, P. Hu, M. Zhang, S. Huang, M. Wang and W. Su, *Chem. Eur. J.*, 2010, **16**, 5876. (g) K. Xie, Y. Yang, X. Zhou, X. Li, S. Wang, Z. Tan, X. An and C.-C. Guo, *Org. Lett.*, 2010, **12**, 1564. (h) H. Zhao, Y. Wei, J. Xu, J. Kan, W. Su, and M. Hong, *J. Org. Chem.*, 2011, **76**, 882.

97. J. Cornella, M. Rosillo-Lopez and I. Larrosa, *Adv. Synth. Catal.*, 2011, **353**, 1359.

98. X. C. Cambeiro, T. C. Boorman, P. Lu and I. Larrosa, *Angew. Chem. Int. Ed.*, 2013, **52**, 1781-1784.

99. Q.-Y. Chen and Z. T. Li, *J. Org. Chem.,* 1993, **58**, 2599.

100. J. Vicente, A. Arcas and M. T. Chicote, *J. Organomet. Chem.*, 1983, **252**, 257.

101. A. Dari, L. E. Christaens and M. J. Renson, *Acta Chemica Scandinavica*, 1993, **47**, 208.

102. (a) P. K. Suryadevara, S. Olepu, J. W. Lockman, J. Ohkanda, M. Karimi, C. L. M. J. Verlinde, J. M. Kraus, J. Schoepe, W. C. Van Voorhis, A. D. Hamilton, F. S. Buckner and M. H. Gelb, *J. Med. Chem.*, 2009, **52**, 3703. (b) M. A. Kotharé, J. Ohkanda, J. W. Lockman, Y. Qian, M. A. Blaskovich, S. M. Sebti and A. D. Hamilton, *Tetrahedron*, 2000, **56**, 9833.

103. Prepared via procedure as detailed in P. Römbke, A. Schier and H. Schmidbaur, *J. Chem. Soc., Dalton Trans.*, 2001, 2482, using silver tosylate prepared via procedure as detailed in P. Teo and R. Grubbs, *Organometallics*, 2010, **29**, 6045.